FOREWORD

This report was prepared by Battelle Memorial Institute under Contract No. AF 33(616)-6888. This contract was initiated under Project No. 7381, "Materials Application", Task No. 738103, "Data Collection and Correlation". The work was administered under the direction of the Directorate of Materials and Processes, Aeronautical Systems Division, with Mr. Marvin Knight acting as project engineer.

This report covers work performed during the period from February 1, 1961, to March 15, 1962.

The guidance and cooperation of many people and organizations contributed substantially to the successful execution of this program. First of all, the contributions of the following people to the technical direction of the program are gratefully acknowledged: Captain James P. Cooper of AFBMD; Messrs. Sherwin Lewis, Glen Howell, and William McGrath (now at Aerospace Corporation) of STL; Mr. Alton Brisbane and Mr. Marvin Knight of ASD; and Mr. R. M. McClintock and Mr. Thomas Durham of the Cryogenic Engineering Laboratory, NBS.

Materials and technical data were supplied to the project gratis through the assistance and cooperation of the following: Messrs. J. L. Shaw and W. S. Mounce of the International Nickel Company; Mr. L. Looby of Armco Steel Corporation; Mr. L. G. Haines of Washington Steel Company; Messrs. M. D. Scott and F. Ireland of the Beryllium Corporation; Messrs. D. Keniston and H. Simmonds of American Brass Company; Mr. V. H. Hall of Wallace Barnes Company; and Mr. W. Minkler of Titanium Metals Corporation of America.

Finally, the competent and painstaking efforts of Mr. Wayne Belton and Mr. Omar Deel of Battelle in determining theoretical stress concentration factors and in reducing and plotting data are also gratefully acknowledged.

ABSTRACT

The notched fatigue behavior of 13 alloys has been investigated in the temperature range room temperature to -423 F and in the lifetime range 10^4 to 10^6 cycles. The alloys studied were chosen on the basis of actual or potential application in missile and spacecraft cryogenic systems. The materials were in sheet form and were fatigued in fully reversed bending experiments. V-notches in the edges of the specimens had theoretical stress concentration factors of about 3.1 and 6.4. The results are presented as S-N plots and comparisons with unnotched fatigue strengths are made in tables of notch sensitivity values. S-N plots of the unnotched fatigue data obtained in the previous year are included for convenience.

PUBLICATION REVIEW

This technical documentary report has been reviewed and is approved.

FOR THE COMMANDER:

W. P. Conrardy

W. P. CONRARDY
Chief, Materials Engineering Branch
Applications Laboratory
Directorate of Materials and Processes

TABLE OF CONTENTS

	Page
INTRODUCTION	1
MATERIALS	2
EXPERIMENTAL WORK	6
Design of the Notched Fatigue Specimens	6
Discussion of Theoretical Stress Concentration Factors (K_T) for Bending	6
Fabrication of Specimens	24
Procedure for Determining the Values of K_T	26
Description of Experimental Equipment	26
Procedure in Fatigue Experiments	30
RESULTS	34
DISCUSSION	34
Behavior of Metals at Cryogenic Temperatures	34
Effect of Notches and Low Temperatures on Fatigue Behavior	69
CONCLUSIONS	76
RECOMMENDATIONS FOR FUTURE WORK	77
REFERENCES	78

LIST OF FIGURES

		Page
Figure 1.	Stress-Strain Curve for Annealed 6Al-4V Titanium at Room Temperature	8
Figure 2.	Stress-Strain Curve for Normalized and Aged 2800 Steel at Room Temperature	9
Figure 3.	Stress-Strain Curves for Annealed 347 Stainless Steel at Room Temperature and -423 F	10
Figure 4.	Stress-Strain Curve for Cold-Rolled 301 Stainless Steel at Room Temperature	11
Figure 5.	Stress-Strain Curve for Annealed "A" Nickel at Room Temperature	12
Figure 6.	Stress-Strain Curves for Cold-Rolled and Age-Hardened "K" Monel Nickel at Room Temperature and -423 F	13
Figure 7.	Stress-Strain Curve for Cold-Rolled Inconel Nickel Alloy at Room Temperature	14
Figure 8.	Stress-Strain Curve for Annealed and Age-Hardened Berylco 25 Beryllium-Copper at Room Temperature	15
Figure 9.	Stress-Strain Curves for Cold-Rolled and Age-Hardened Berylco 25 Beryllium Copper at Room Temperature and -423 F	16
Figure 10.	Stress-Strain Curves for Cold-Rolled and Stress-Relieved 70/30 Brass at Room Temperature and -423 F	17
Figure 11.	Stress-Strain Curve for Annealed and Age-Hardened Ni-Span C Iron-Nickel Alloy at Room Temperature	18
Figure 12.	Stress-Strain Curve for Quenched and Tempered 1075 Carbon Steel at Room Temperature	19
Figure 13.	Stress-Strain Curve for 17-7PH (TH 1050) Stainless Steel at Room Temperature	20
Figure 14.	Stress-Strain Curve for 17-7PH (RH 950) Stainless Steel at Room Temperature	21
Figure 15.	Stress-Strain Curve for Annealed and Age-Hardened Inconel "X" Nickel at Room Temperature	22
Figure 16.	Geometrical Designs of Notched and Unnotched Fatigue Specimens	23
Figure 17.	Effect of r/d and n/d Ratios on Theoretical Stress-Concentration Factor Based on Net Section	25

LIST OF FIGURES
(Continued)

Page

Figure 18. Notch Roots of Three Typical 301 Stainless Steel Fatigue Specimens 27

Figure 19. Close-Up View of Machine for Use to -320 F 28

Figure 20. Cross Section of Liquid-Hydrogen Dewar and Contents 29

Figure 21. Arrangement for Measuring Deflection of Specimens Under Dead-Weight Loading 32

Figure 22. Typical Notched Fatigue Specimen Before and After Fatigue Experiment 33

Figure 23. Unnotched (K_T = 1) Fatigue Behavior of Annealed 6Al-4V Titanium . 35

Figure 24. Unnotched (K_T = 1) Fatigue Behavior of Normalized and Aged 2800 Steel 36

Figure 25. Unnotched (K_T = 1) Fatigue Behavior of Annealed 347 Stainless Steel 37

Figure 26. Unnotched (K_T = 1) Fatigue Behavior of Cold-Rolled 301 Stainless Steel 38

Figure 27. Unnotched (K_T = 1) Fatigue Behavior of Annealed "A" Nickel . . . 39

Figure 28. Unnotched (K_T = 1) Fatigue Behavior of Cold-Rolled and Age-Hardened "K" Monel Nickel 40

Figure 29. Unnotched (K_T = 1) Fatigue Behavior of Cold-Rolled Inconel Nickel . 41

Figure 30. Unnotched (K_T = 1) Fatigue Behavior of Annealed and Age-Hardened Berylco 25 Beryllium-Copper 42

Figure 31. Unnotched (K_T = 1) Fatigue Behavior of Cold-Rolled and Age-Hardened Berylco 25 Beryllium-Copper 43

Figure 32. Unnotched (K_T = 1) Fatigue Behavior of Cold-Rolled and Stress-Relieved 70/30 Brass 44

Figure 33. Unnotched (K_T = 1) Fatigue Behavior of Annealed and Age-Hardened Ni-Span C Iron-Nickel Alloy 45

Figure 34. Unnotched (K_T = 1) Fatigue Behavior of Quenched and Tempered 1075 Carbon Steel 46

Figure 35. Unnotched (K_T = 1) Fatigue Behavior of 17-7PH (TH 1050) Stainless Steel 47

LIST OF FIGURES
(Continued)

		Page
Figure 36.	Unnotched (K_T = 1) Fatigue Behavior of 17-7PH (RH 950) Stainless Steel	48
Figure 37.	Unnotched (K_T = 1) Fatigue Behavior of Annealed and Age-Hardened Inconel "X" Nickel	49
Figure 38.	Notched (K_T = 3.1) Fatigue Behavior of Annealed 6Al-4V Titanium	50
Figure 39.	Notched (K_T = 3.1) Fatigue Behavior of Normalized and Aged 2800 Steel	51
Figure 40.	Notched (K_T = 3.2) Fatigue Behavior of Annealed 347 Stainless Steel	52
Figure 41.	Notched (K_T = 3.1) Fatigue Behavior of Cold-Rolled 301 Stainless Steel	53
Figure 42.	Notched (K_T = 3.0) Fatigue Behavior of Annealed "A" Nickel	54
Figure 43.	Notched (K_T = 3.2) Fatigue Behavior of Cold-Rolled and Age-Hardened "K" Monel Nickel	55
Figure 44.	Notched (K_T = 3.2) Fatigue Behavior of Cold-Rolled Inconel Nickel	56
Figure 45.	Notched (K_T = 3.2) Fatigue Behavior of Annealed and Age-Hardened Berylco 25 Beryllium-Copper	57
Figure 46.	Notched (K_T = 3.1) Fatigue Behavior of Cold-Rolled and Age-Hardened Berylco 25 Beryllium-Copper	58
Figure 47.	Notched (K_T = 3.2) Fatigue Behavior of Cold-Rolled and Stress-Relieved 70/30 Brass	59
Figure 48.	Notched (K_T = 3.1) Fatigue Behavior of Annealed and Age-Hardened Ni-Span C Iron-Nickel Alloy	60
Figure 49.	Notched (K_T = 3.2) Fatigue Behavior of Quenched and Tempered 1075 Carbon Steel	61
Figure 50.	Notched (K_T = 3.0) Fatigue Behavior of 17-7PH (RH 950) Stainless Steel	62
Figure 51.	Notched (K_T = 3.2) Fatigue Behavior of Annealed and Age-Hardened Inconel "X" Nickel	63
Figure 52.	Notched (K_T = 6.4) Fatigue Behavior of Annealed 6Al-4V Titanium	64

LIST OF FIGURES
(Continued)

Page

Figure 53. Notched (K_T = 6.4) Fatigue Behavior of Annealed 347 Stainless Steel 65

Figure 54. Notched (K_T = 6.6) Fatigue Behavior of Cold-Rolled and Age-Hardened Berylco 25 Beryllium-Copper 66

Figure 55. Notched (K_T = 6.4) Fatigue Behavior of Cold-Rolled and Stress-Relieved 70/30 Brass 67

Figure 56. Notched (K_T = 6.4) Fatigue Behavior of Annealed and Age-Hardened Inconel "X" Nickel 68

LIST OF TABLES

		Page
Table 1.	Chemical Analysis of Materials	3
Table 2.	Materials Tested in As-Received Condition	4
Table 3.	Materials Heat Treated Before Testing	5
Table 4.	Properties of 15 Material-Condition Combinations at Room Temperature and -423 F	7
Table 5.	Notch Sensitivities With $K_T = 3.1$	71
Table 6.	Summary of Fatigue Results at Room Temperature for $K_T = 1$, $K_T = 3.1$, and $K_T = 6.4$	72
Table 7.	Summary of Fatigue Results at -110 F for $K_T = 1$, $K_T = 3.1$, and $K_T = 6.4$	73
Table 8.	Summary of Fatigue Results at -320 F for $K_T = 1$, $K_T = 3.1$, and $K_T = 6.4$	74
Table 9.	Summary of Fatigue Results at -423 F for $K_T = 1$, $K_T = 3.1$, and $K_T = 6.4$	75
Table 10.	Fatigue Strength/Density Comparison of 6Al-4V Titanium With Other Alloys	76

LIST OF SYMBOLS

CPM - cycles per minute

RPM - revolutions per minute

KSI - thousand pounds per square inch

PSI, psi - pounds per square inch

F_{TU} - ultimate tensile strength

K_T = theoretical stress-concentration factor

K_N = fatigue-notch factor = $\frac{\text{unnotched fatigue strength at N cycles}}{\text{notched fatigue strength at N cycles}}$

R = stress ratio = algebraic ratio of minimum stress to maximum stress in one cycle

(1) means Reference 1 in List of References

● - data obtained at room temperature

▲ - data obtained at temperature of solid CO_2

■ - data obtained at temperature of liquid nitrogen

× - data obtained at temperature of liquid hydrogen

→ - means that the specimen did not fail after the indicated number of cycles

INTRODUCTION

The primary objective of the work reported here has been the investigation of the fatigue behavior of certain alloys in the temperature range room temperature to -423 F.

The development of intercontinental missiles and other spacecraft using cryogenic liquids as fuels or coolants precipitated an urgent need for data on the mechanical properties of engineering materials. In response to this need, a program was initiated by the Air Force at the Cryogenic Engineering Laboratory of NBS and at Battelle to generate such data and to incorporate them in a loose-leaf Cryogenic Materials Data Handbook.* The work being reported here on the investigation of the fatigue behavior of 13 alloys was conducted under Contract No. AF 33(616)-6888. In the first year of this contract, the unnotched fatigue behavior of these alloys was studied and reported in WADD TR 61-132.(1)** In the second year, the notched fatigue behavior of the same alloys has been studied using medium and sharp notches. All of the data included in the two reports has been submitted to Aeronautical Systems Division for inclusion in the Cryogenic Materials Data Handbook. During the first year of the fatigue program, a survey of the literature on cryogenic fatigue was made; the very limited data found in that survey were also included in the Handbook.

The effort in this investigation of cryogenic fatigue behavior of engineering materials has concentrated on 13 metallic alloys. The choice of alloys and conditions for study in this program was based mainly on experience in the development of the Atlas and Titan missiles, and in particular involved component parts such as valves, diaphragms, and switches. Although fatigue problems had also been encountered in cryogenic pressure vessels (tanks and piping), the special aspects of these problems were not investigated in this program.

The experimental program was carried out on sheet specimens with medium and with sharp edge notches. The specimens were fatigued in fully reversed bending experiments in which the specimens were driven by means of a cam and connecting rod (constant deflection experiments). The experiments were conducted at room temperature, -110 F, -320 F, and -423 F, with the specimens in contact with the coolants. It was recognized that experiments in which specimens and coolants were in contact might give results different from experiments in which such contact was prevented. However, in many of the applications of current interest, contact between the metal part and the cryogenic liquid would often be a condition of operation.

The results are presented as stress-lifetime and strain-lifetime plots in the lifetime range 10^4 to 10^6 cycles. Comparisons of the notched fatigue strengths with unnotched fatigue strengths obtained in the previous work are made in terms of notch sensitivity values. S-N plots of the unnotched data are included for convenience.

*Quarterly or semiannual additions to the Handbook are available from the Office of Technical Services (OTS), United States Department of Commerce, Washington 25, D. C.

**Numbers in parentheses refer to the references listed at the end of the report.

Manuscript released by authors March 14, 1962, for publication as an ASD Technical Report.

MATERIALS

The materials and material conditions selected for investigation in the program were based on specific applications such as valves, diaphragms, and switches in missile applications which were subjected to cyclic stresses. The choices were modified to some extent to include a broader range of materials and material conditions. Thus, in addition to providing engineering data for specific applications the program has been useful in examining the general area of cryogenic behavior of engineering materials.

The material-condition combinations evaluated in this program included:

(1) 6Al-4V titanium alloy – annealed

(2) 2800 (9 per cent Ni) steel – normalized and aged

(3) 347 austenitic stainless steel – annealed

(4) 301 austenitic stainless steel – cold rolled

(5) "A" Nickel – annealed

(6) "K" Monel nickel alloy – cold rolled and age hardened

(7) Inconel nickel alloy – cold rolled

(8) Berylco 25 beryllium copper – annealed and age hardened

(9) Berylco 25 beryllium copper – cold rolled and age hardened

(10) 70/30 brass cold rolled and stress relieved

(11) Ni-Span C iron – nickel alloy – annealed and age hardened

(12) 1075 plain carbon steel – quenched and tempered

(13) 17-7PH precipitation hardenable stainless steel – TH 1050 Condition

(14) 17-7PH precipitation hardenable stainless steel – RH 950 Condition

(15) Inconel "X" nickel alloy – annealed and age hardened.

It was desired to obtain as complete a metallurgical processing history as possible for the materials; therefore the materials were ordered from the suppliers with this in mind. In several cases chemical analysis, tensile yield strength, and ultimate tensile strength were furnished, and the condition of the materials as shipped was also specified. Chemical analyses and tensile tests at room temperature were conducted on those materials for which this information was not supplied. Table 1 shows the chemical analyses of the materials and Tables 2 and 3 show the condition and room-temperature properties of the materials in the condition in which they were tested. In the second year of the contract it appeared desirable to identify the tensile properties of the materials at -423 F. For some of the materials, reliable data from the literature were already available. Some additional tests were conducted at Battelle.

TABLE 1. CHEMICAL ANALYSIS OF MATERIALS

	C	Fe	Al	Mn	S	Si	Ni	Cr	Cu	Mo	Be	Co	Sn	Pb	Zn	Other
Ti-6Al-4V	0.010	0.08	6.2	--												3.9 V, 0.013 N_2, 0.006 H_2, Bal. Ti
2800 steel	0.10	Bal.		0.75	0.024	0.23	8.6									0.01 P
Type 347 SS	0.06	Bal.		1.67	0.018	0.38	10.82	18.62								
Type 301 SS	0.09	Bal.		0.71	0.012	0.43	6.80	17.57	0.14	0.23						0.019 P
"A" Nickel	0.05	0.19		0.23	0.006	0.05	Bal.		0.04							
"K" Monel	0.10	1.22	2.37	0.42	0.008	0.19	Bal.		28.99							
Inconel	0.05	6.70		0.20	0.008	0.22	Bal.	15.56	0.03							
Berylco 25, AT		0.15	0.06	0.005		0.13	0.010	0.006	Bal.		1.89	0.29	0.010	0.002	0.03	0.02 Ag
Berylco 25, 1/2 HT		0.14	0.09	0.004		0.12	0.015	0.001	Bal.		1.94	0.27	0.020	0.002	0.03	0.02 Ag
70/30 brass		0.01[a]							70.36					0.01	29.27	
Ni-Span C	0.03	Bal.	0.54	0.45		0.22	41.65	5.33								2.18 Ti
1075 steel	0.71	Bal.		0.57	0.030											
17-7PH SS	0.05	Bal.	1.25	0.73	0.010	0.36	7.41	17.03								
Inconel "X"	0.05	6.53	0.75	0.53	0.008	0.40	Bal.	14.76	0.12							2.45 Ti

(a) The iron content is corrected from 0.08 (reported in WADDTR 61-132) to 0.01.

TABLE 2. MATERIALS TESTED IN AS-RECEIVED CONDITION

Material	Source	Condition and Thickness	Mechanical Properties			
			Ultimate Tensile Strength, psi	Tensile Yield Strength (0.2% Offset), psi	Elongation, per cent	Hardness, Vickers Diamond, 5-Kg Load
Ti-6Al-4V	Titanium Metals Corp. of America	Annealed, 0.072 inch	136,000	130,000	11.4	313
2800 steel	International Nickel Company	Normalized and aged[a], 0.040 inch	128,000	81,000	17.3	246
Type 347 SS	Armco Steel Corporation	Annealed, 0.029 inch	92,500	37,000	55.2	146
Type 301 SS	Washington Steel Company	Extra full hard, 0.039 inch	240,000	222,000	4.3	460
"A" Nickel	International Nickel Company	Annealed, 0.021 inch	61,600[b]	13,500[b]	43.4	77
"K" Monel	International Nickel Company	Cold rolled half-hard and age hardened, 0.051 inch	182,000	163,000	8.5	353
Inconel	International Nickel Company	Hard cold rolled, 0.035 inch	132,000	128,000	3.8	293

(a) The 2800 steel was heat treated according to ASTM Method A-353 by Inco, as follows: normalized from 1650 and 1450 F, and reheated at 1050 F for 2 hours - all treatments in nonoxidizing atmosphere.

(b) Strength data taken from Cryogenic Materials Data Handbook.

TABLE 3. MATERIALS HEAT TREATED BEFORE TESTING

Material	Source	Condition As Received and Thickness	Heat Treatment (Final Condition)	Mechanical Properties in Final Condition: Ultimate Tensile Strength, psi	Tensile Yield Strength (0.2% Offset), psi	Elongation, per cent	Hardness, Vickers Diamond, 5-Kg Load
Berylco 25	Beryllium Corporation	Annealed, 0.021 inch	600 F for 3 hours, air cooled (AT)	178,000	146,000	9	362
Berylco 25	Beryllium Corporation	Cold rolled half-hard, 0.078 inch	600 F for 2 hours, air cooled (1/2 HT)	191,000	166,000	2.8	368
70/30 Brass	American Brass Co.	No. 8 spring temper, 0.040 inch	Stress relief 400 F for 1 hour	95,000	88,000	2.8	191
Ni-Span C	International Nickel Co.	Cold rolled, annealed, 0.021 inch	Age hardened 5 hours at 1200 F, air cooled	152,000	100,000	20.7	265
1075 steel	Wallace Barnes Co.	Annealed, 0.052 inch	Heated 1-1/2 hours at 1500 F, oil quenched; tempered 1-1/2 hours at 950 F, air cooled	151,000	133,000	8.9	353
17-7PH SS	Armco Steel Corp.	0.063 inch	Solution annealed at 1950 F, air cooled; heated to 1400 F, held 1-1/2 hours, cooled to 60 F within 1 hour, held 1/2 hour; heated to 1050 F, held 1-1/2 hour, air cooled (TH 1050)	196,000	175,000	12.6	331
Inconel "X"	International Nickel Co.	Cold rolled, annealed, 0.020 inch	Aged 20 hours at 1300 F, air cooled	177,000	122,000	26	362
17-7PH SS	Armco Steel Corp.	0.063 inch	Solution annealed at 1950 F, cool to 1750 F, held for 10 minutes, air cool, -100 F for 8 hours, 950 F for 1 hour, air cool	210,000(a)	188,000(a)	--	--

(a) Strength data taken from Armco Technical Data Manual.

Table 4 summarizes available properties of the 15 material-condition combinations investigated in this program.

Figures 1 through 15 are the stress-strain characteristics obtained at room temperature and at -423 F where available for the tested materials.

EXPERIMENTAL WORK

The equipment and the procedures used in this notch fatigue program were essentially the same as were used in the unnotched program. However, for completeness, a full description of the specimens, the equipment, and the procedures for both notched and unnotched experiments is detailed in the following sections.

Design of the Notched Fatigue Specimens

The notched fatigue specimens used in this program were similar in size and shape to the unnotched specimens used earlier. The unnotched and the notched specimens were designed with small over-all dimensions in order that the cryostats could be small, thus minimizing the volume requirements of liquid hydrogen.

The unnotched and notched specimen geometries are shown in Figure 16. In the notched specimens a 60-degree V-notch has been imposed on a continuous radius which approximates the constant stress section of the unnotched specimens. The nearly-constant stress section minimizes the longitudinal stress gradient near the notch. The same basic notch was used for both the medium and the sharp notches, with the root radii for the medium notches ($K_T = 3$) being approximately 0.005 inch and for the sharp notches ($K_T = 6$) being nearly 0.0025 inch. The dimensions and the shapes of the notched specimens were chosen so that the notches could be fabricated reproducibly without unusual difficulties. Since the notched and unnotched fatigue specimens were made from the same lots of sheet materials, the thicknesses were the same, ranging from approximately 0.02 to 0.08 inch for all of the materials. The exact thicknesses of all materials are indicated in Tables 2 and 3.

Discussion of Theoretical Stress Concentration Factors (K_T) for Bending[3]

Probably the most widely used theoretical stress concentration factors for notched plates in transverse bending are based on a solution by Lee[4] and are presented by Petersen[5] as plots of K_T versus the ratio of notch root radius r to net width d. Lee's solution was derived for hyperbolic notches in an infinitely wide plate using classical thin-plate theory. The notched specimens used in this fatigue program do not satisfy the assumptions inherent in Lee's solution because of their finite width (finite notch depth) and finite thickness. Determination of the effects of finite width and finite thickness on the value of K_T would require experimental measurement using possibly a photoelastic model or mathematical analysis for a notched plate of finite width and thickness, a large task.

TABLE 4. PROPERTIES OF 15 MATERIAL-CONDITION COMBINATIONS AT ROOM TEMPERATURE AND -423 F

	Crystal Structure	Density, lb/in.^{3}	Modulus of Elasticity in Tension, 10^6 psi		Tensile Strength, 1000 psi		Yield Strength, 1000 psi		Elongation, per cent	
			RT	-423 F	RT	-423 F	RT	-423 F	RT	-423 F
1075	Bcc	0.282	28	33[a]	151[b]	233[b]	133	--	8.9	--
301	Fcc[c]	0.290	25[d]	30[d]	240[b]	367[e]	222	331[e]	4.3	1.5[e]
347	Fcc	0.290	29	31[b]	92.5	210[f]	37	46[f]	55.2	41[f]
17-7PH (TH 1050)	Fcc	0.282	30	33[b]	196	--	175	--	12.6	--
17-7PH (RH 950)	Fcc	0.282	30	33[b]	169	217[b]	132	--	19.0	--
2800	Bct and Fcc	--	28	30[g]	128	218[b]	81	159[b]	17.3	11.5[b]
Ni-Span C	Fcc	0.294	28	37[a]	152	224[b]	100	123[b]	20.7	31.0[b]
"A" Nickel	Fcc	0.321	29[a]	33[a]	62	107[b]	14	33[b]	43.4	36.0[b]
Inconel	Fcc	0.307	31		132	176[b]	128	161[b]	3.8	22.0[b]
"K" Monel	Fcc	0.306	26	30[b]	182	238[b]	163	208[b]	8.5	15.0[b]
Inconel "X"	Fcc	0.300	31	36[b]	177	216[b]	122	136[b]	26.0	34.5[b]
Berylco 25-AT	Fcc	0.297	17	18[b]	178	--	146	--	9.0	--
Berylco 25-1/2 HT	Fcc	0.297	19	21[b]	191	238[b]	166	178[b]	2.8	3.5[b]
70/30 brass	Fcc	0.308	16	21[b]	95	120[b]	88	100[b]	2.8	28.0[b]
6Al-4V	Hcp and Bcc	0.160	16	20[b]	136	247[b]	130	188[b]	11.4	3.5[b]

(a) Data from Campbell, Battelle (SR-4 strain gage).
(b) Data from Campbell, Battelle (Extensometer).
(c) Partially transforms to Bcc as a result of certain combinations of low temperature and straining.
(d) Data from Christian, Convair, Third Quarterly Progress Report, Contract AF 33(616)-7719, pp 16-17.
(e) Data from Hanson, NASA, NASA TN D592, p 16.
(f) Data from McConnel and Brady, USS, DMIC 148, p 48.
(g) Data from Cryogenic Materials Data Handbook (extrapolated value).

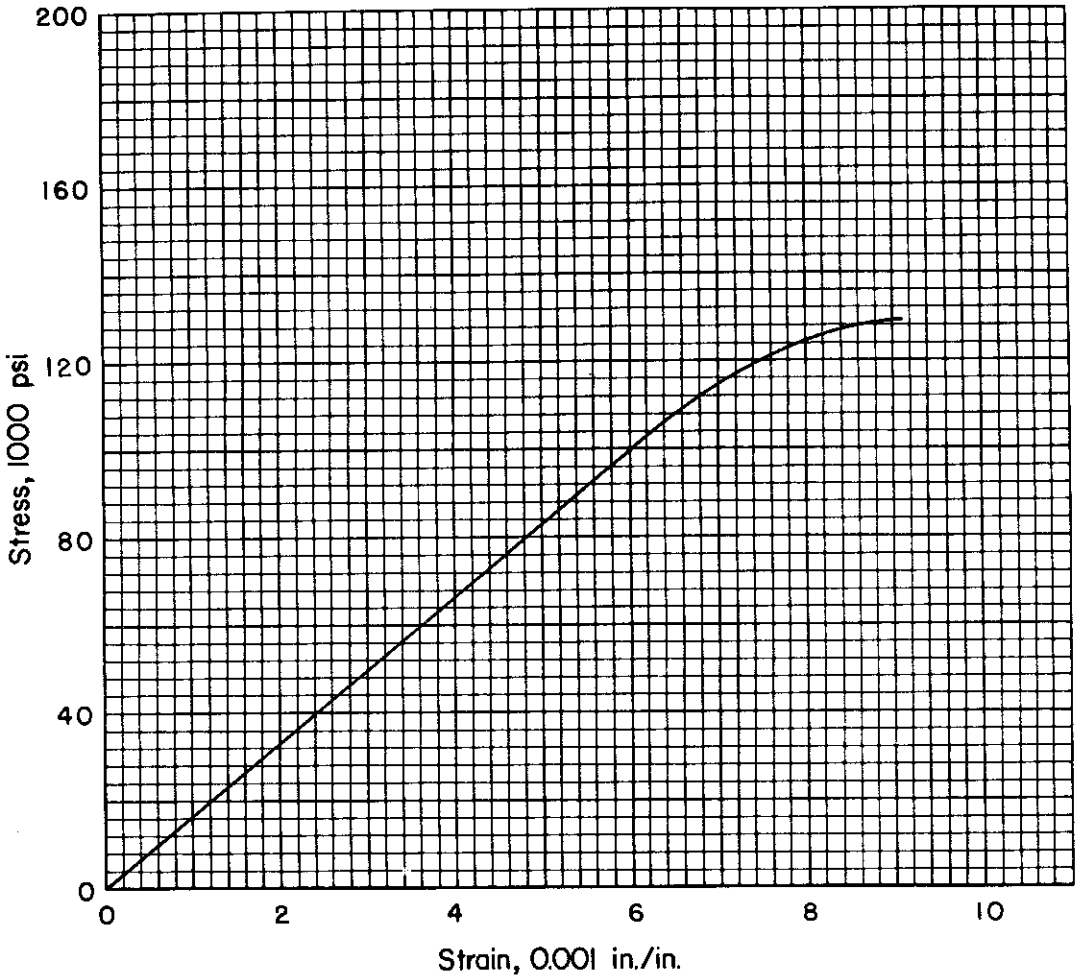

FIGURE 1. STRESS-STRAIN CURVE FOR ANNEALED 6Al-4V TITANIUM AT ROOM TEMPERATURE

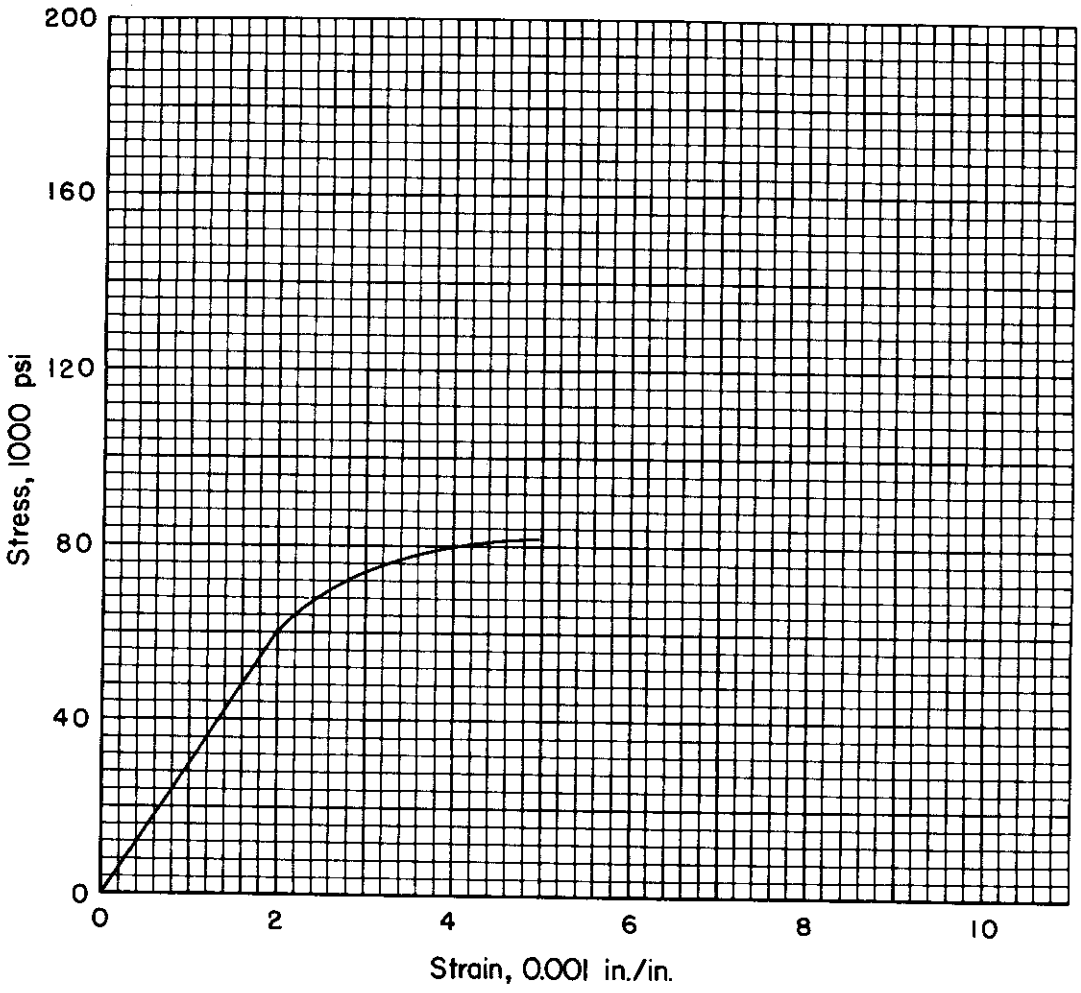

FIGURE 2. STRESS-STRAIN CURVE FOR NORMALIZED AND AGED 2800 STEEL AT ROOM TEMPERATURE

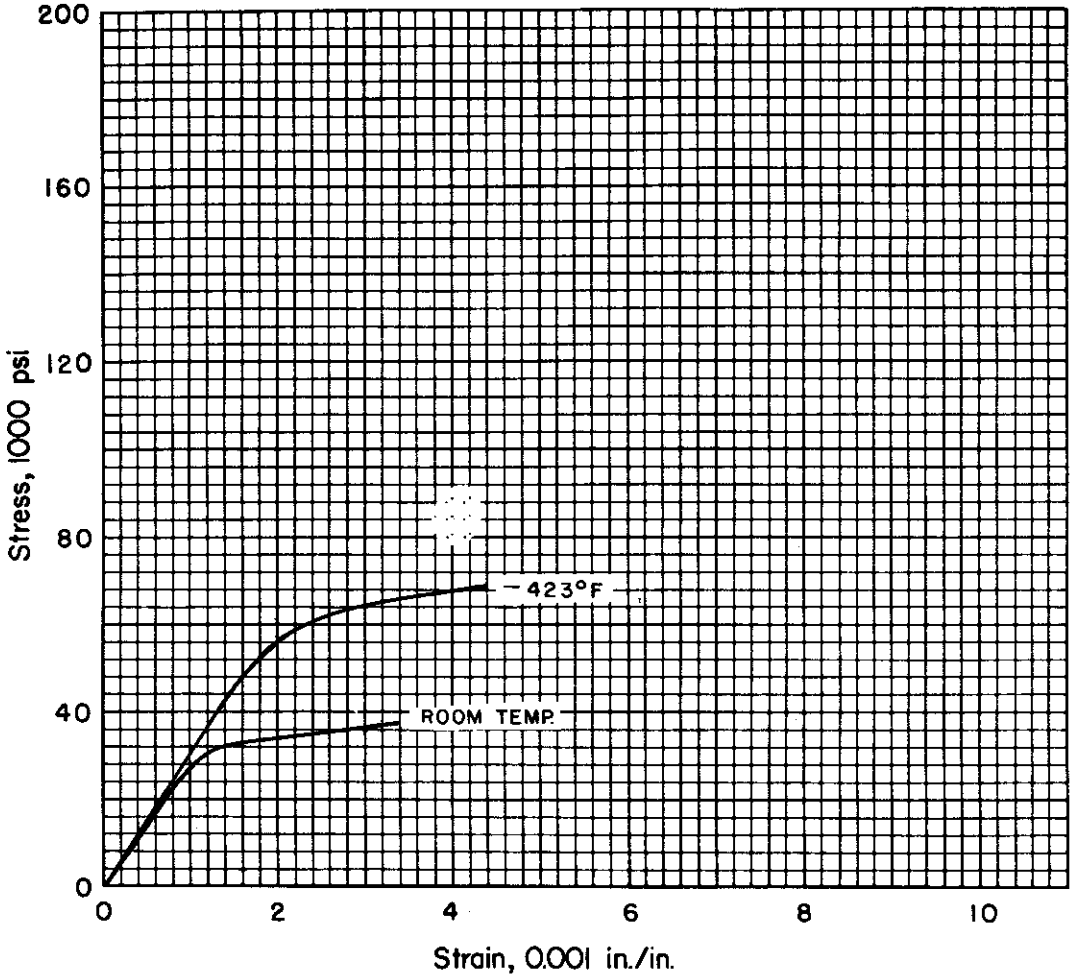

FIGURE 3. STRESS-STRAIN CURVES FOR ANNEALED 347 STAINLESS STEEL AT ROOM TEMPERATURE AND -423 F

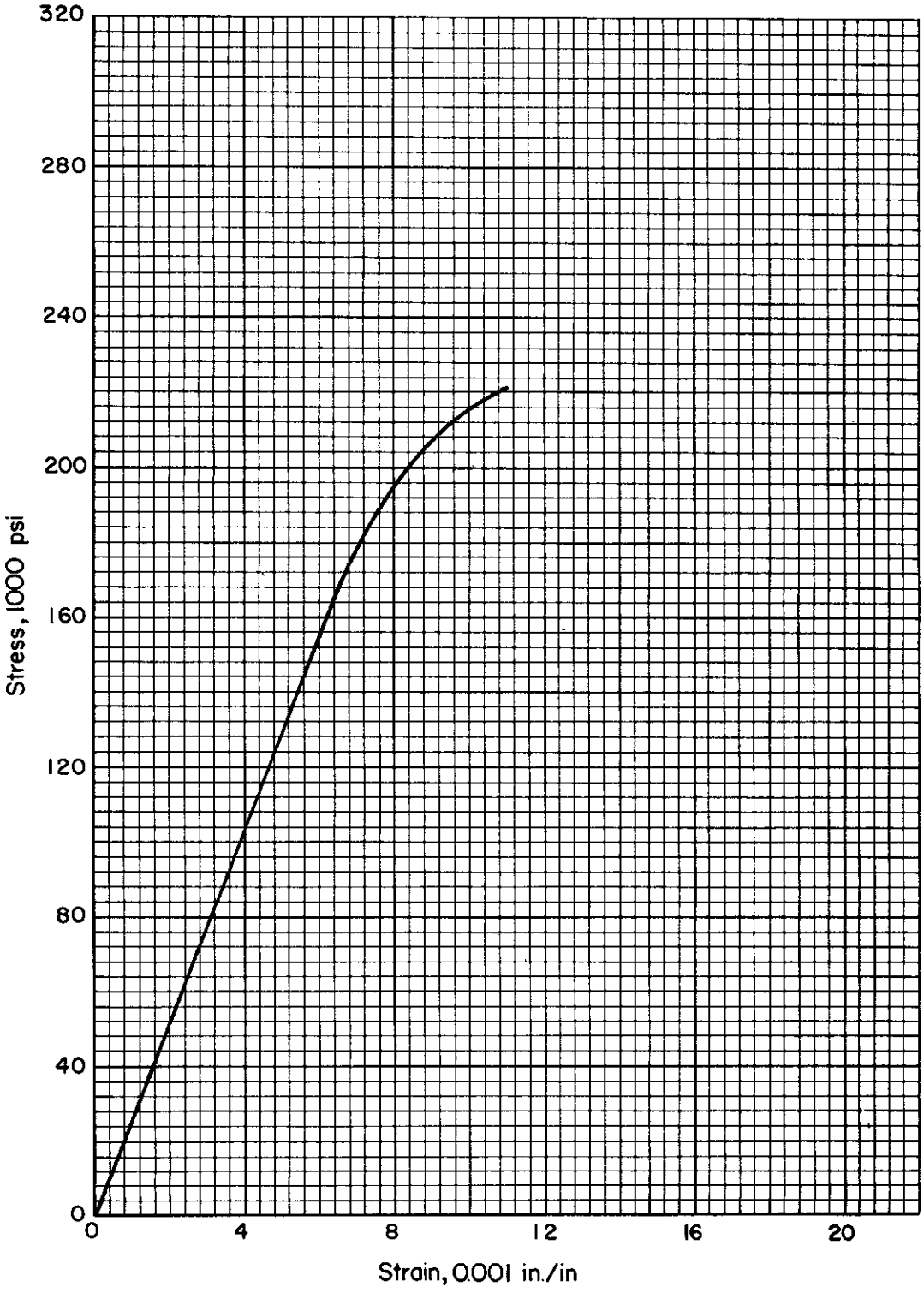

FIGURE 4. STRESS-STRAIN CURVE FOR COLD-ROLLED 301 STAINLESS STEEL AT ROOM TEMPERATURE

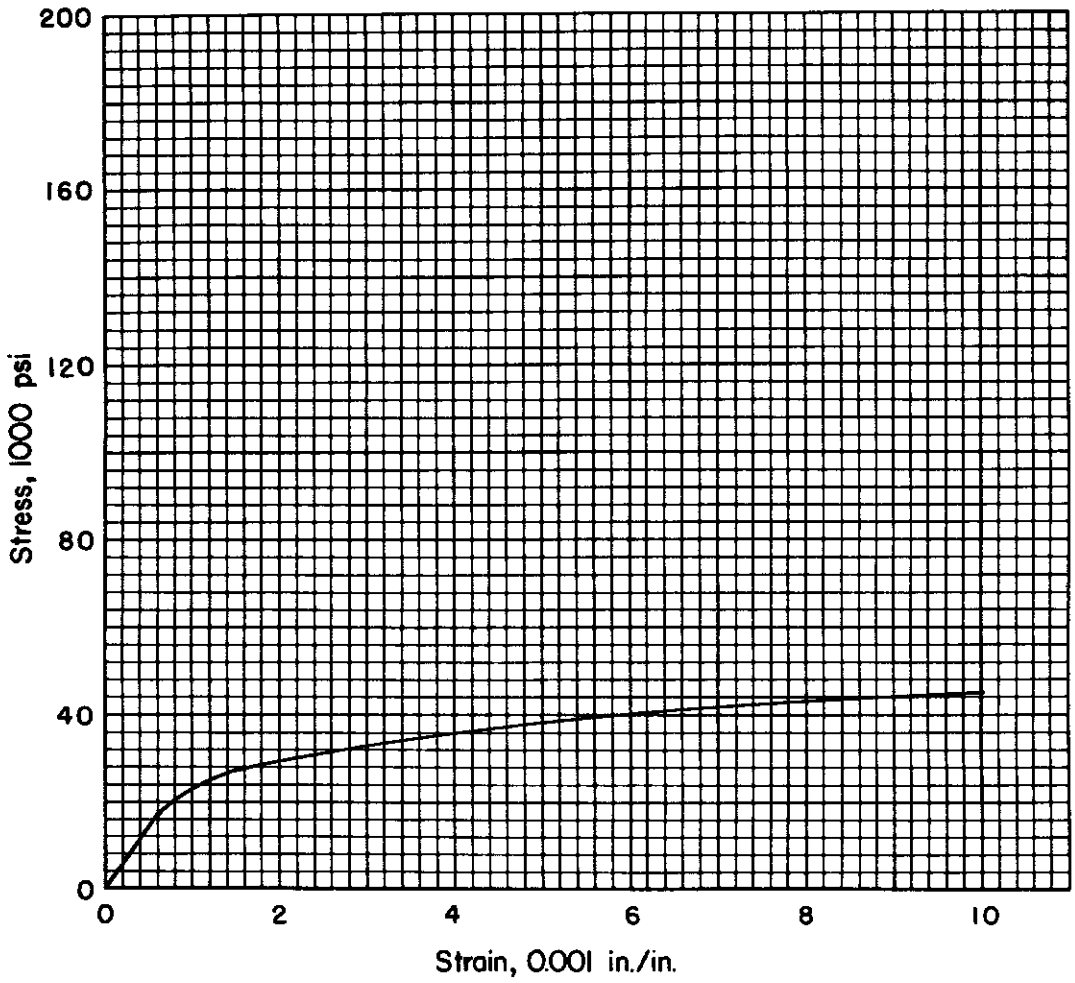

FIGURE 5. STRESS-STRAIN CURVE FOR ANNEALED "A" NICKEL AT ROOM TEMPERATURE

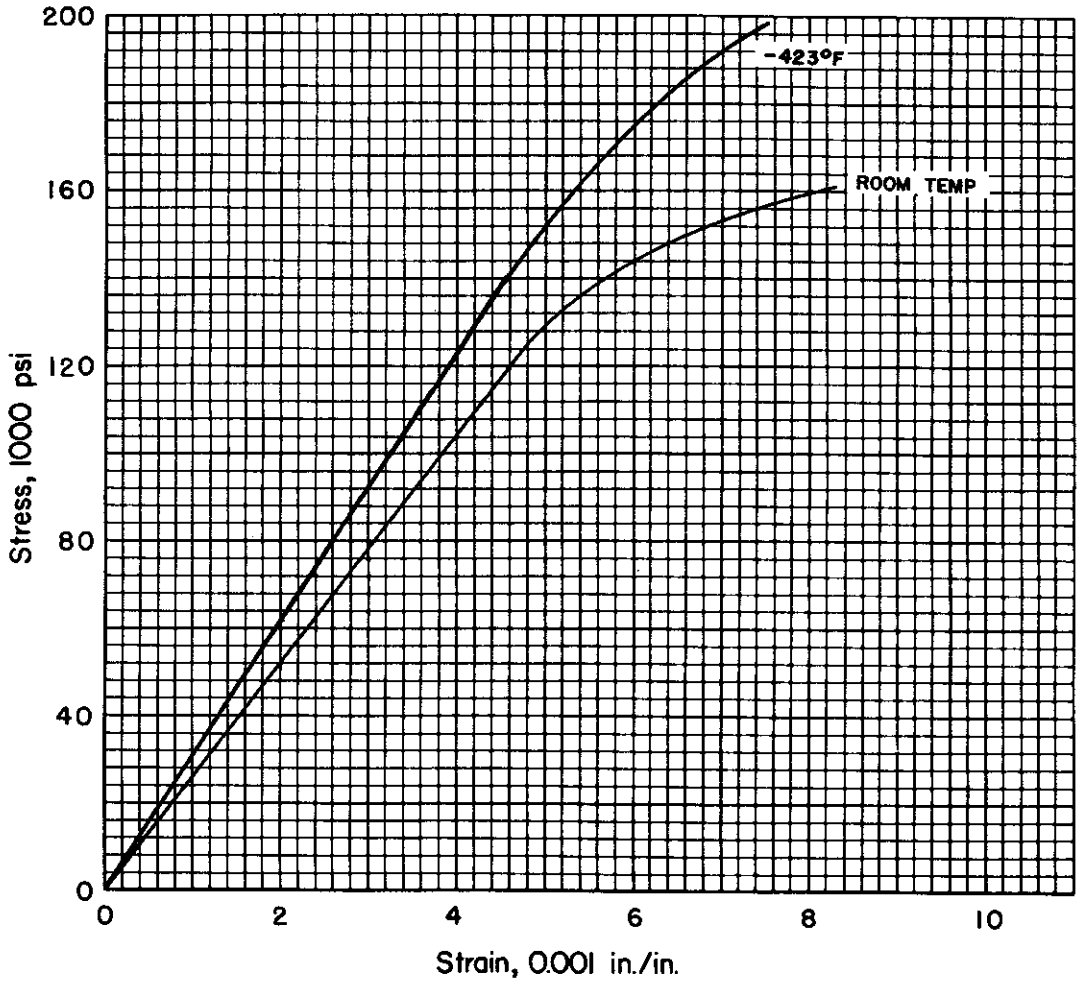

FIGURE 6. STRESS-STRAIN CURVES FOR COLD-ROLLED AND AGE-HARDENED "K" MONEL NICKEL AT ROOM TEMPERATURE AND -423 F

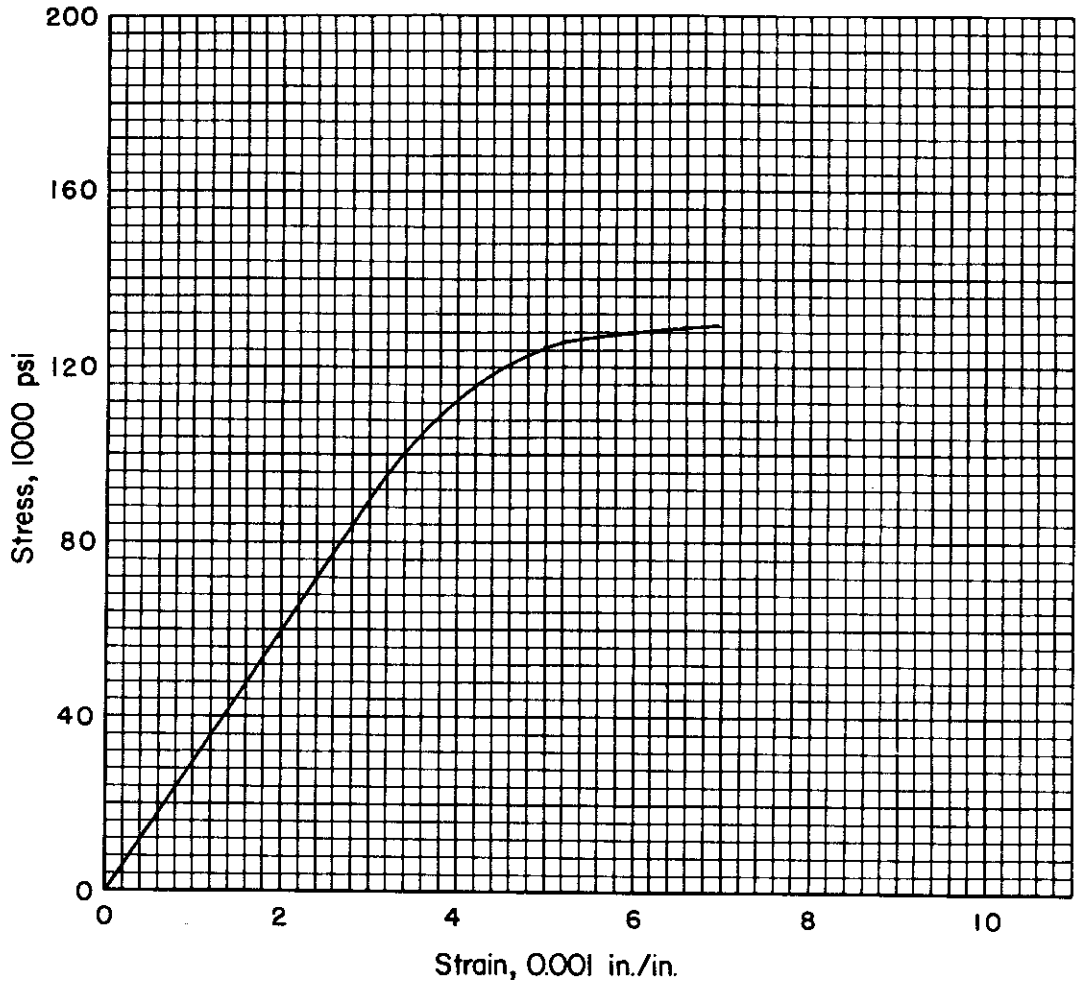

FIGURE 7. STRESS-STRAIN CURVE FOR COLD-ROLLED INCONEL NICKEL ALLOY AT ROOM TEMPERATURE

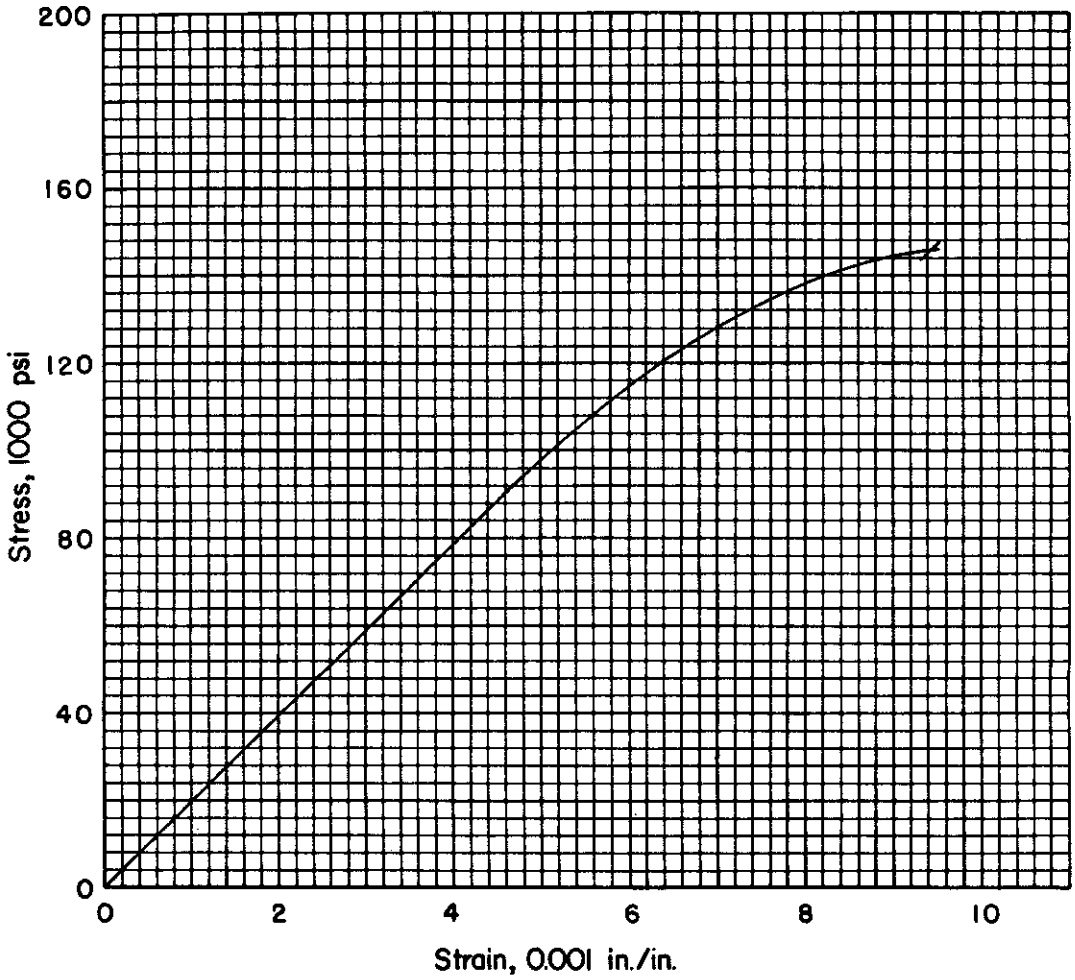

FIGURE 8. STRESS-STRAIN CURVE FOR ANNEALED AND AGE-HARDENED BERYLCO 25 BERYLLIUM-COPPER AT ROOM TEMPERATURE

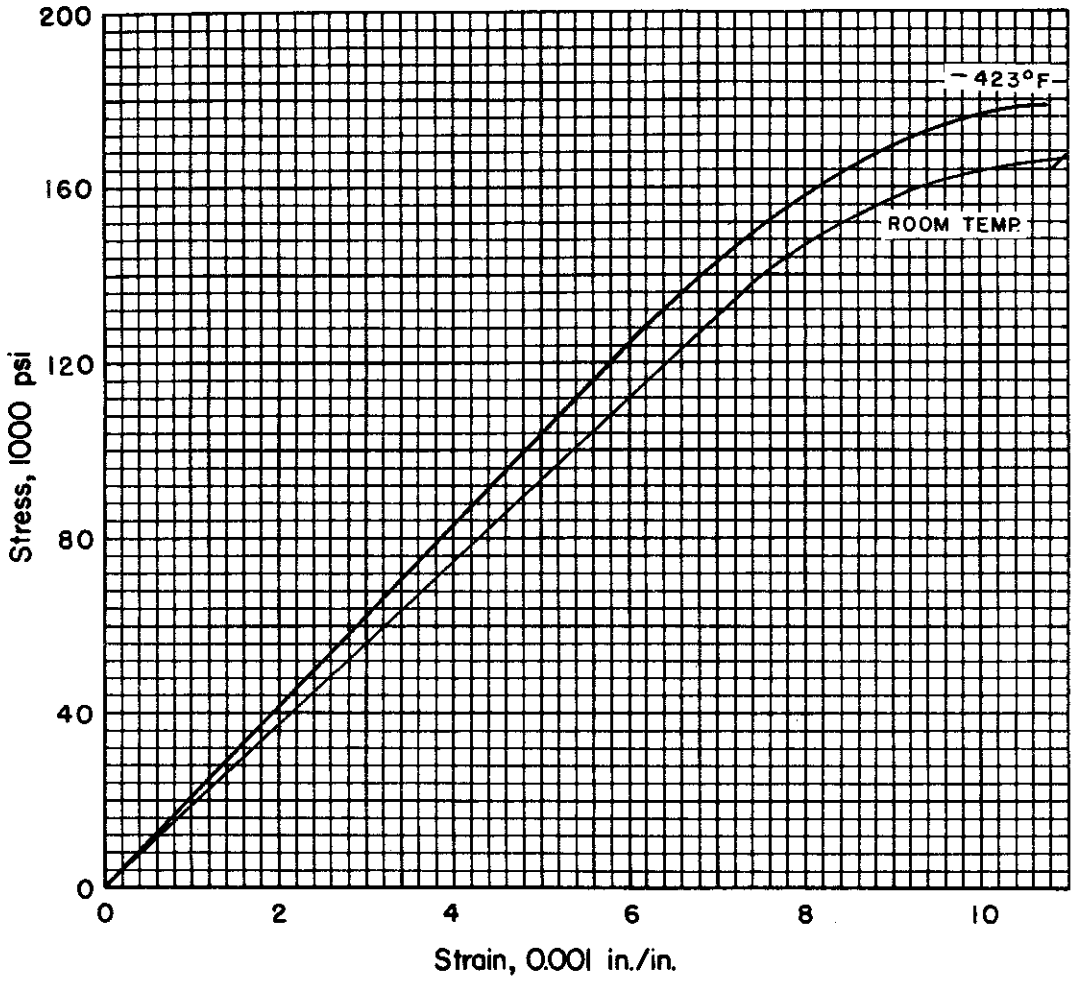

FIGURE 9. STRESS-STRAIN CURVES FOR COLD-ROLLED AND AGE-HARDENED BERYLCO 25 BERYLLIUM COPPER AT ROOM TEMPERATURE AND -423 F

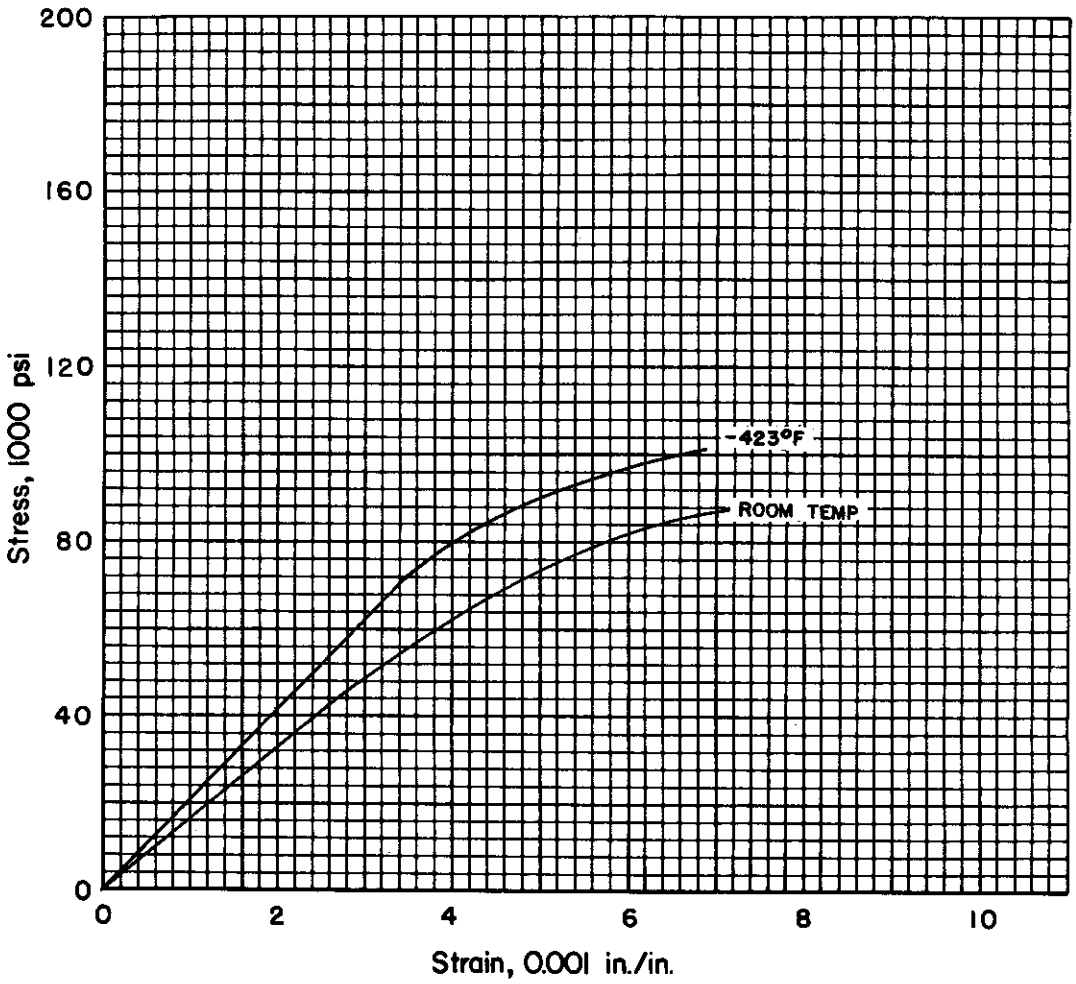

FIGURE 10. STRESS-STRAIN CURVES FOR COLD-ROLLED AND STRESS-RELIEVED 70/30 BRASS AT ROOM TEMPERATURE AND -423 F

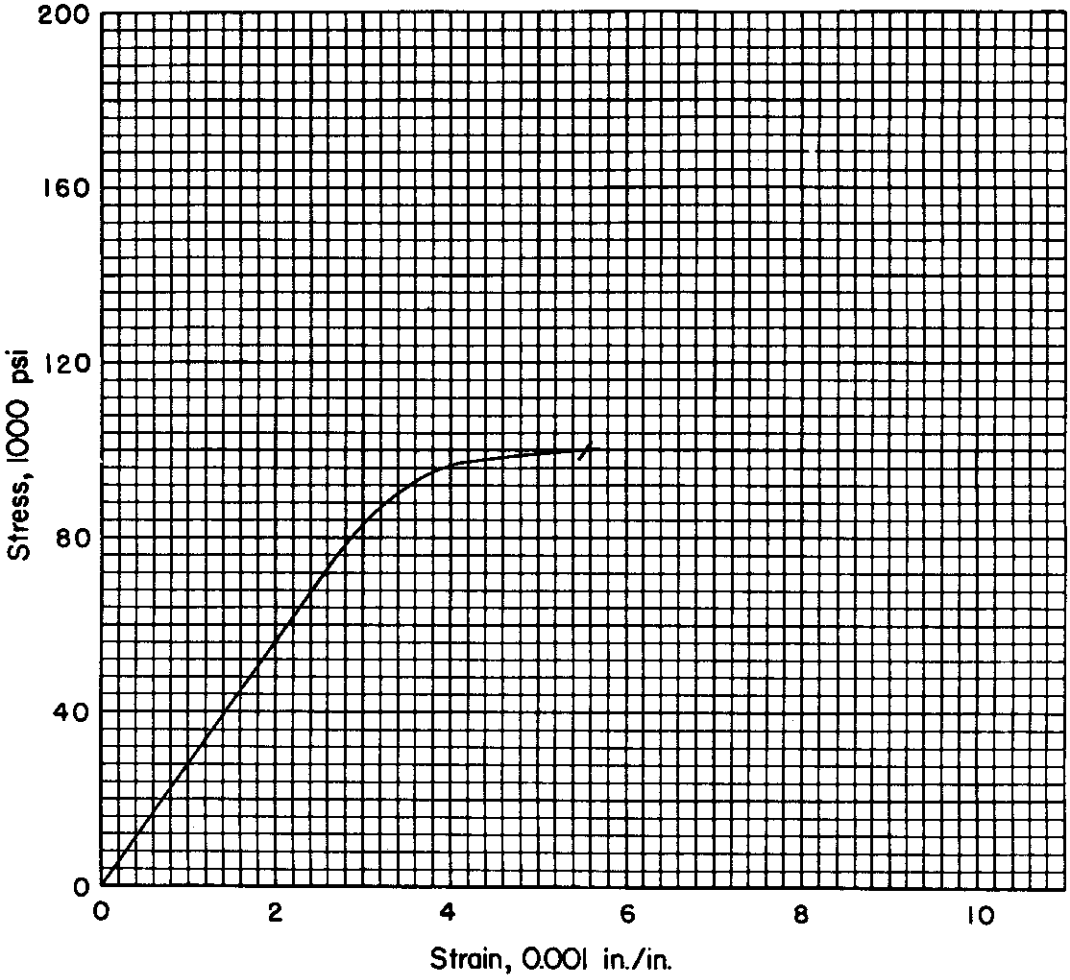

FIGURE 11. STRESS-STRAIN CURVE FOR ANNEALED AND AGE-HARDENED NI-SPAN C IRON-NICKEL ALLOY AT ROOM TEMPERATURE

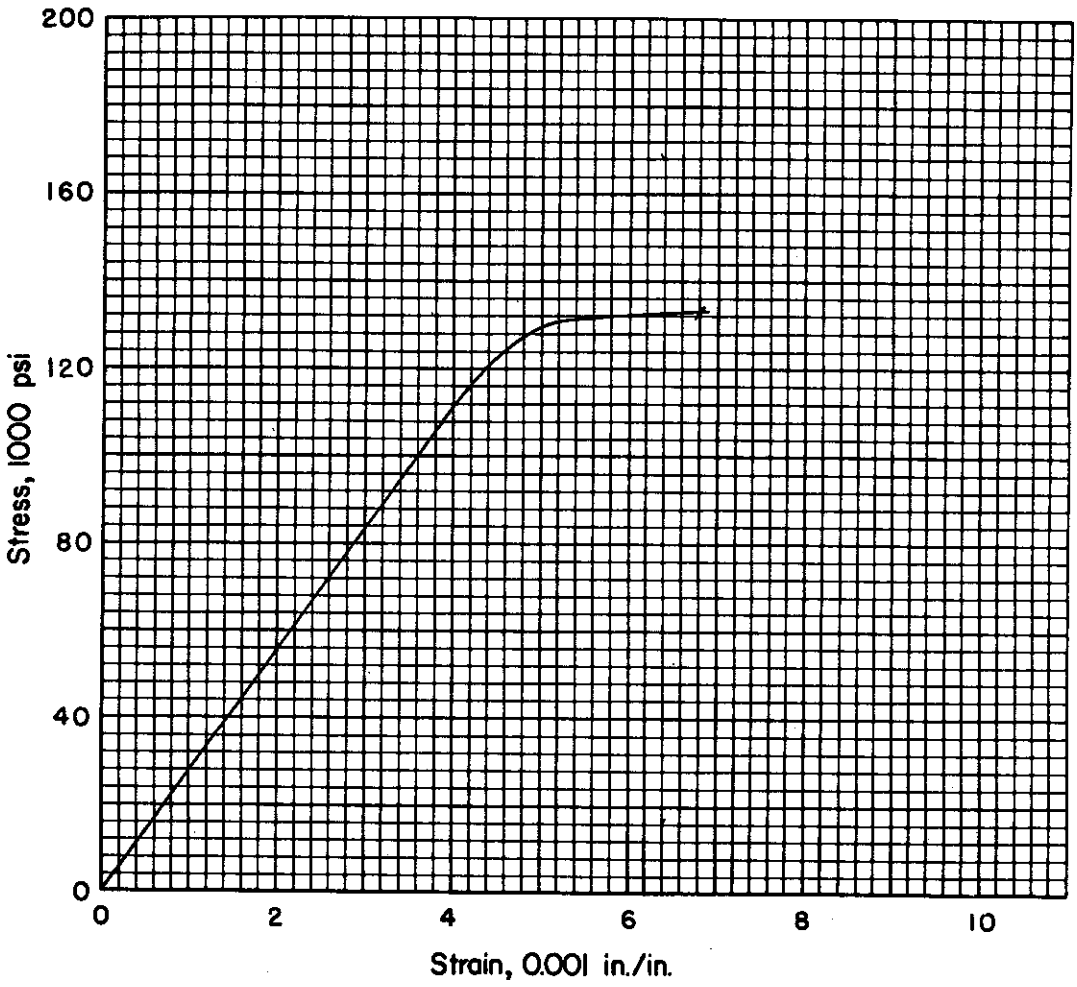

FIGURE 12. STRESS-STRAIN CURVE FOR QUENCHED AND TEMPERED 1075 CARBON STEEL AT ROOM TEMPERATURE

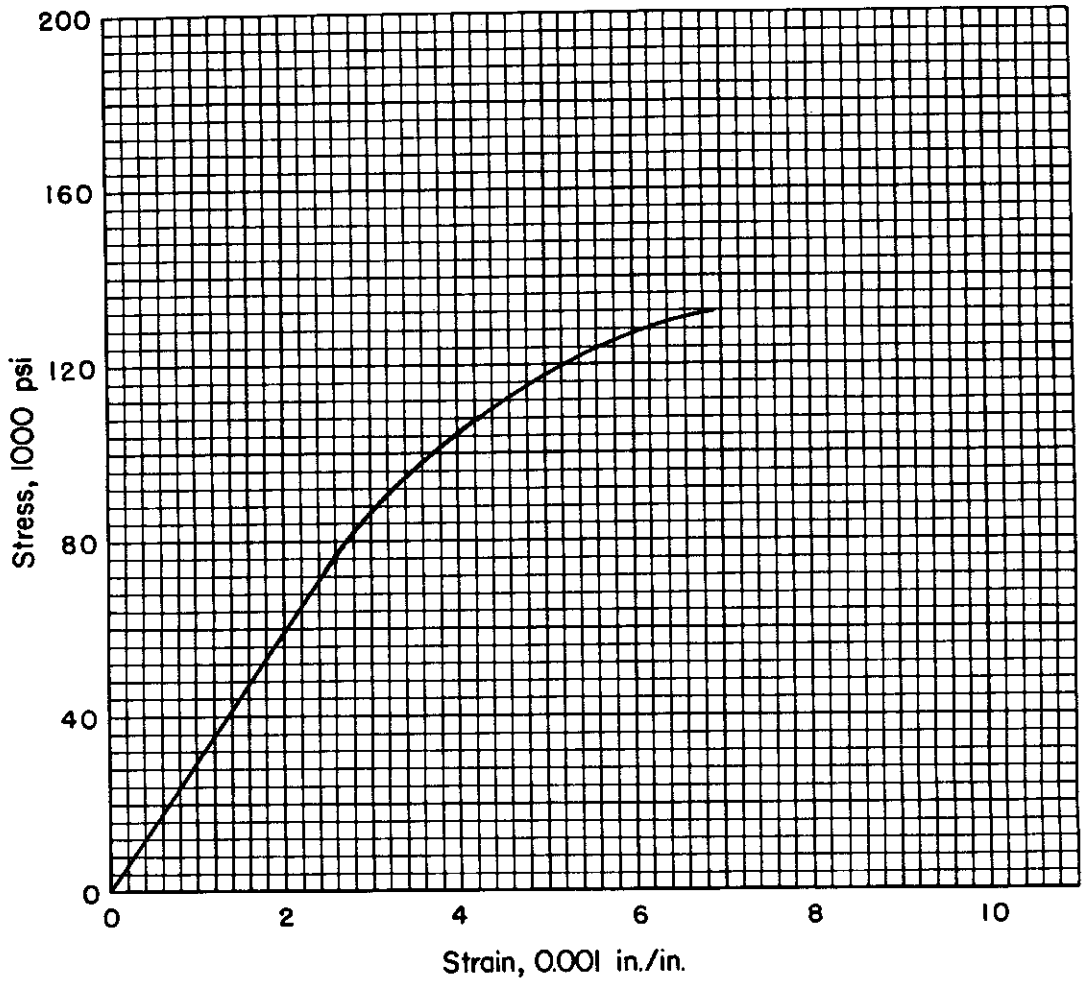

FIGURE 13. STRESS-STRAIN CURVE FOR 17-7PH (TH 1050) STAINLESS STEEL AT ROOM TEMPERATURE

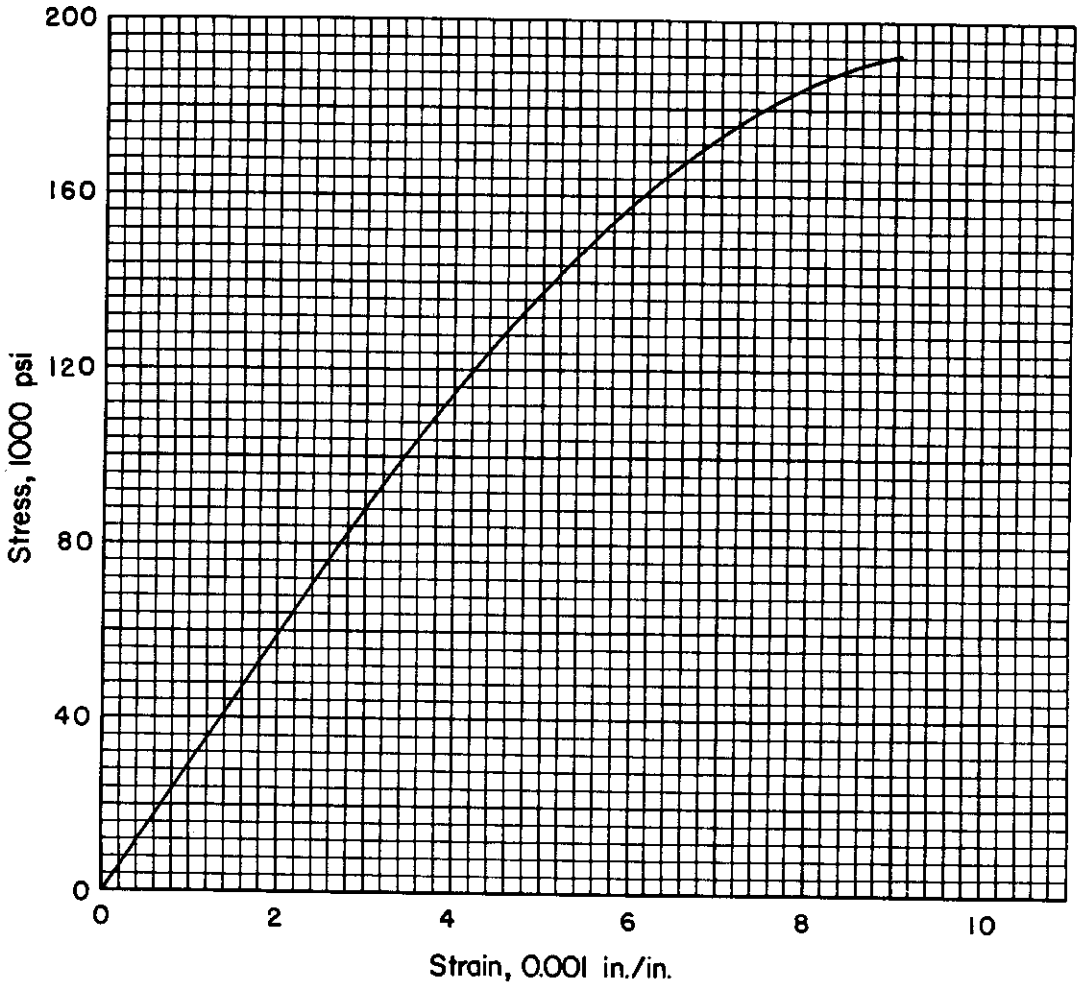

FIGURE 14. STRESS-STRAIN CURVE FOR 17-7PH (RH 950) STAINLESS STEEL AT ROOM TEMPERATURE

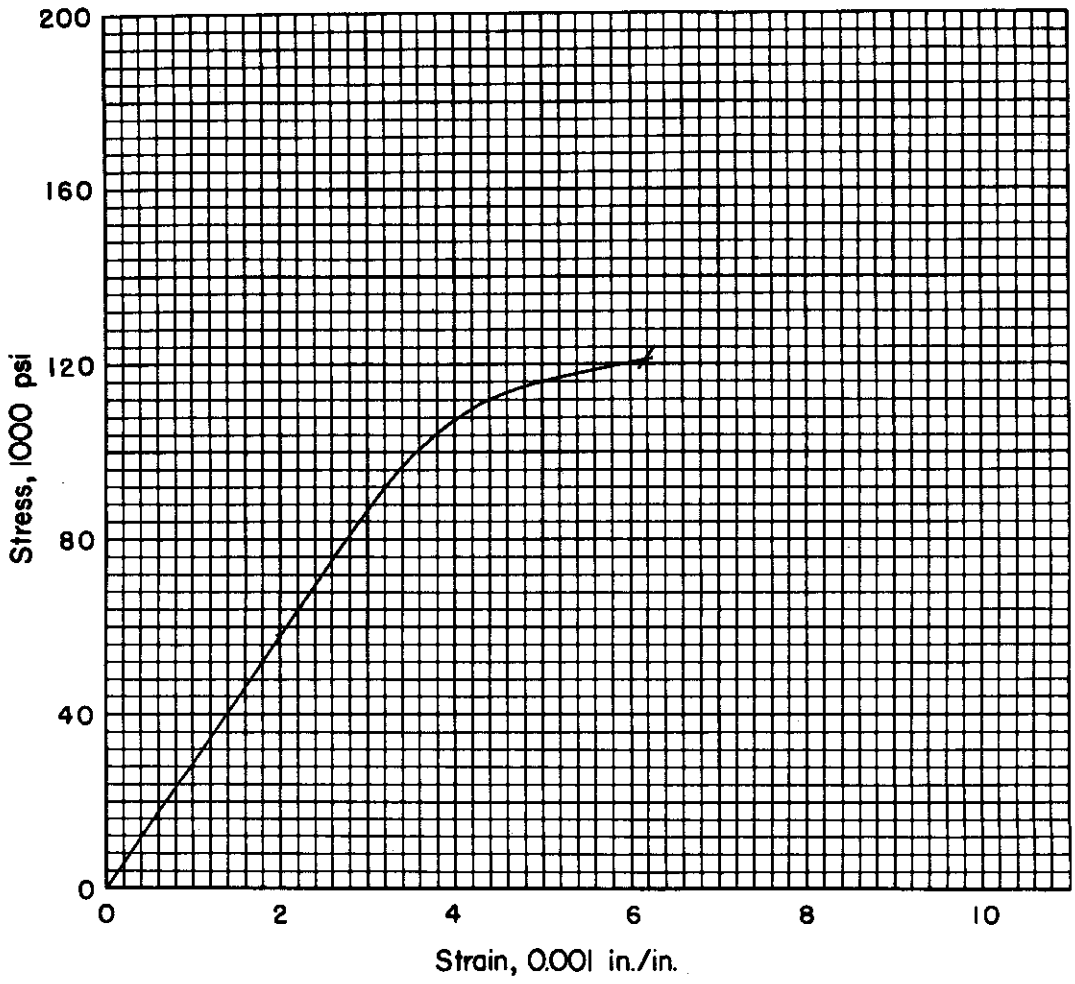

FIGURE 15. STRESS-STRAIN CURVE FOR ANNEALED AND AGE-HARDENED INCONEL "X" NICKEL AT ROOM TEMPERATURE

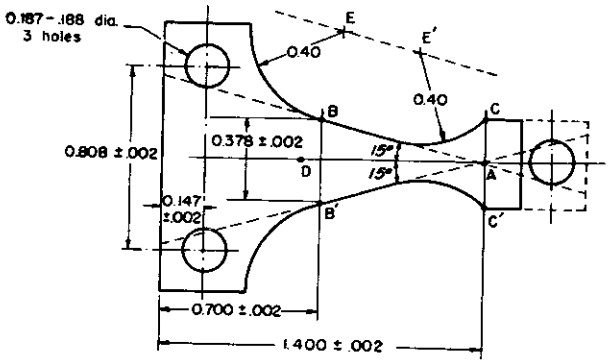

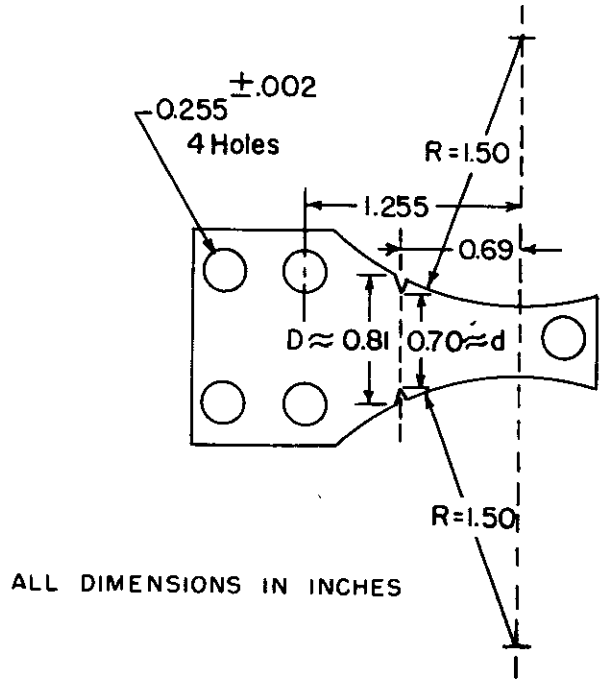

FIGURE 16. GEOMETRICAL DESIGNS OF NOTCHED AND UNNOTCHED FATIGUE SPECIMENS

A qualitative idea of the effect of finite plate width is suggested by a series solution of a plate with finite-depth notches recently accomplished by Tamate and Shroya[6]. Their results, modified for easier comparison with Lee's results, are shown in Figure 17. Inspection of the curve for semicircular notches shows that as the n/d ratio is increased (with n/r = 1), the K_T factor increases nearly linearly. This would indicate that for the n/d ratio of interest $\left(\frac{0.11}{0.7} = 0.16\right)$, the K_T value would be about 2.6, considerably less than the Peterson-Lee value for the same r/d ratio. However, the range of n/r of interest is from approximately 18 to 36. An estimate of the effect of increasing n/r from 1 to 18 or 36 is given by Figure 120 in Petersen's book. (This is strictly applicable only to tension or in-plane bending, but the K_T for the tension case is the upper limit for the transverse-bending K, since it represents the K_T for transverse bending for an infinitely thick plate). Figure 120[5] shows that for n/r values of 18 and 36, K_T has values greater than for n/r = 1. It is not known whether or not the effects of a small n/d and a large n/r cancel each other in the range of interest, but qualitatively they are opposite in effect.

The effect of plate thickness on K_T values is equally difficult to assess. The most widely used theory for moderately thick plates is Reissner's[7] which takes into account the effects of transverse shear deformation and the transverse normal stress. Another approach would be to consider the problem as one in three-dimensional elasticity. However, there is no known theoretical solution for transverse bending of an appreciably thick notched plate. Also, there are no experimental data for this case. In view of the paucity of information on this problem, the relation between plate thickness and K_T can only be inferred by consideration of analogous problems. Apparently the only available literature on this problem is that of Reissner[7] and of Naghdi[8], who applied Reissner's theory to an infinite plate with an elliptic hole. On this basis, it is estimated, for the range of thicknesses of interest (0.02 to 0.08 inch), the true values of K_T are only 0.05 and 0.10 (or about 1 to 3 per cent), respectively, higher than the thin-plate values.

The appropriate plots in Petersen's book for determination of K_T values for transverse bending are Figures 37 and 123 for K_T values equal to or less than 3 and greater than 3, respectively. The discussion above suggests that K_T values determined from Figures 37 and 123 may deviate somewhat from the true values. However, means of determining more exact values are not available, and use of these figures has the advantage that they are well known and generally accepted.

Fabrication of Specimens

The machining of the sheet specimens was done by clamping some 10 to 20 blanks between 1/4-inch-thick steel plates. Then, the holes for the grip section and the hole in the small end (which was cut off after machining, see Figure 16) were located and drilled. Allen head machine screws were installed in these holes to clamp the stacks of specimen blanks together for the entire machining process. The stacks were then squared to final over-all size by milling. In the case of the unnotched specimens, milling cutters with the appropriate radius and special jigs were used to produce the final shape.

In the case of the notched specimens, the notches were next roughed in within about 0.020 inch of the final value of d ($d \cong 0.70$ inch) using a milling cutter before milling the 1.5-inch radius. The final cuts in the notches were made with carbide tools

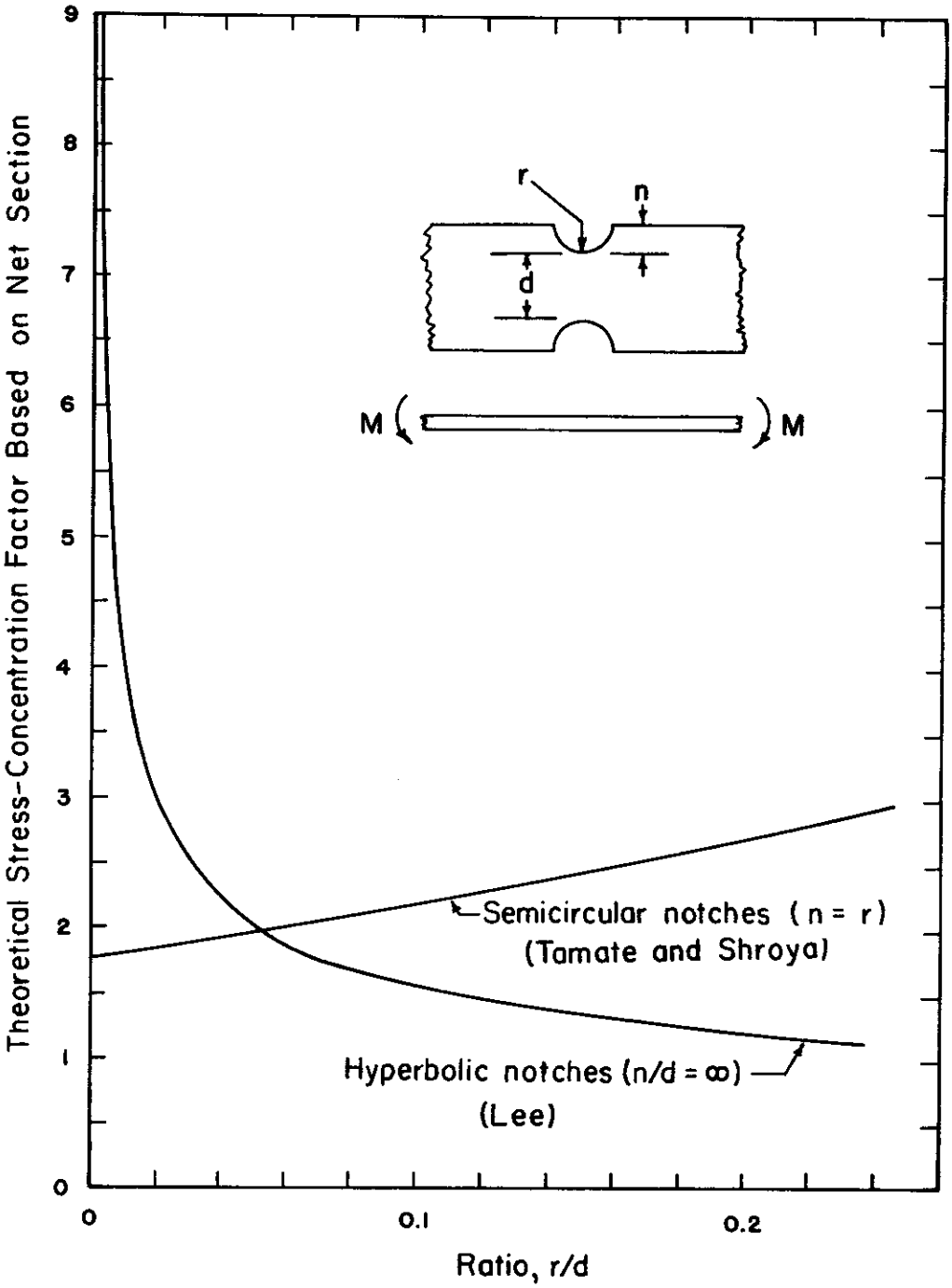

FIGURE 17. EFFECT OF r/d AND n/d RATIOS ON THEORETICAL STRESS-CONCENTRATION FACTOR BASED ON NET SECTION

used as fly cutters. These tools had been precision ground to a sharp 60-degree V and the tips hand-honed to appropriate radii measured on a 50X shadowgraph. In order to achieve nearly the same values of K_T (either 3 or 6.3) for all the materials, minor variations in tool dimensions were taken into account during machining in arriving at the final exact values of net widths d.

Finally, after the notches were finished, the radii of 1.50 inches were formed by milling, using cutters with 3.00 inches diameter. The center of a cutter was moved during cutting toward the stack of specimens along the dashed line shown in Figure 16, so as to achieve the desired gross width D = 0.81 inch on the notch line.

Procedure for Determining the Values of K_T

After machining (and heat treatment, when appropriate) the stacks of specimens were opened and all specimens numbered consecutively according to their positions in the stacks. The value of the theoretical stress concentration factor for each material was then determined by measuring accurately the actual final dimensions. A number of specimens were selected from each stack, generally one from each end and one from the center. The notches of these specimens were then photographed on a Bausch and Lomb Research Metallograph at magnifications of 50X and 100X for the medium and the sharp notches, respectively. Figure 18 shows such photographs of notches in three different stacks. An average root radius and an average notch depth were then obtained from measurements made on all the photographs obtained for the material. The net width d of the specimens was measured on a shadowgraph at 50X by micrometric translation of a specimen from each stack. The gross width D of the specimens at the notch line was then obtained as the sum of the net width d and twice the notch depth. The ratio $\frac{r}{d}$, root radius to net width, and the ratio $\frac{D}{d}$, the gross width to the net width, were then used to find the value of K_T from Figure 37 or Figure 123 in Petersen's[5] book, for K_T values near 3 or 6, respectively. The medium notch factors, which were mostly in the range slightly above 3, were determined by extrapolating the curves in Petersen's Figure 37.

Description of Experimental Equipment

The specimens were tested at a stress ratio R = -1 (fully reversed bending) in three modified Krouse-type plate and sheet fatigue machines. Figure 19 is a view of the specimen support and drive mechanism of one of the two identical machines used at -320 F, -110 F, and at room temperature. Although the same specimens were used at -423 F as at the other temperatures and were mounted and driven in the same way, the design of the -423 F fatigue machine, shown schematically in Figure 20, resulted from an effort to minimize the heat capacity of the supporting structure and the heat transfer into the working space.

The specimens were clamped to the base in each machine with four machine screws (two screws for the unnotched specimens) through a 1/4-inch-thick steel plate. Double V-block or knife edge arrangements, which are attached to the drive rods of the machines, deflected the specimens. The separation of the knife edges was adjusted for

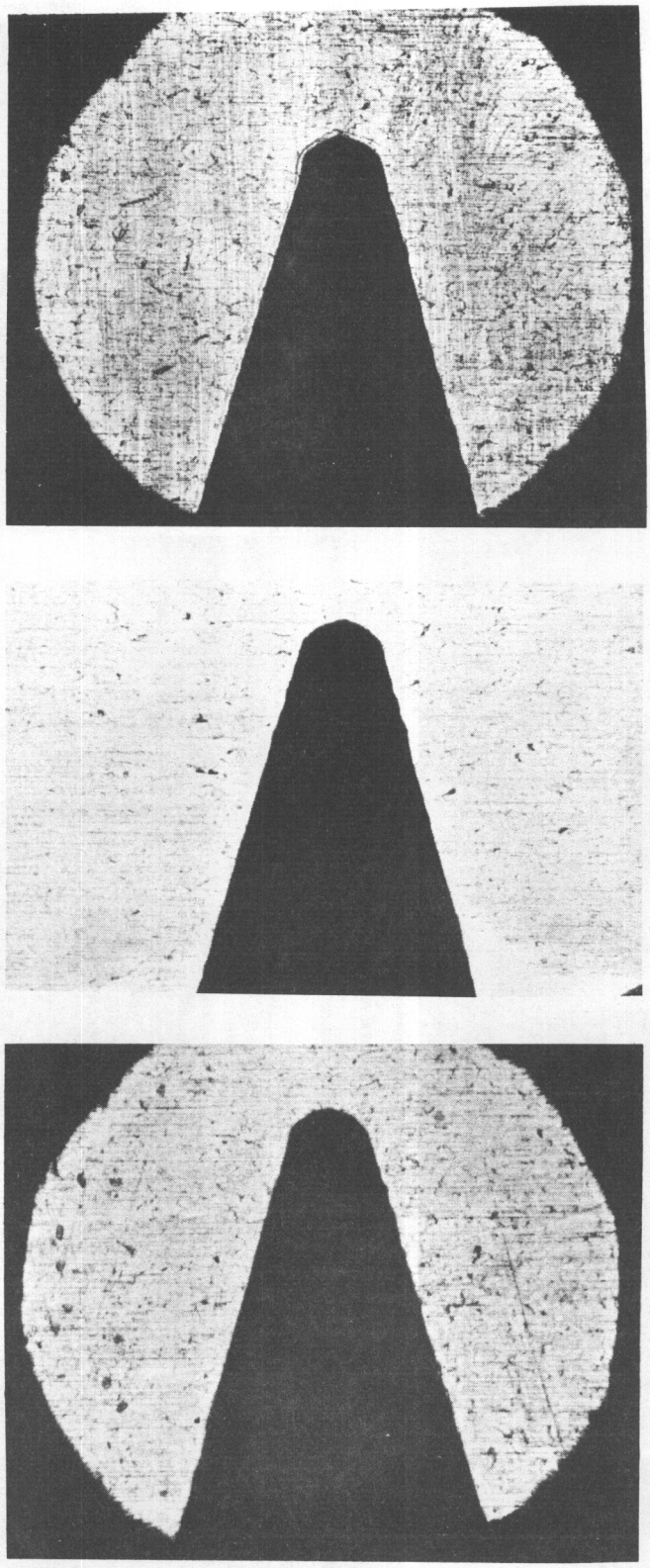

50X

FIGURE 18. NOTCH ROOTS OF THREE TYPICAL 301 STAINLESS STEEL FATIGUE SPECIMENS

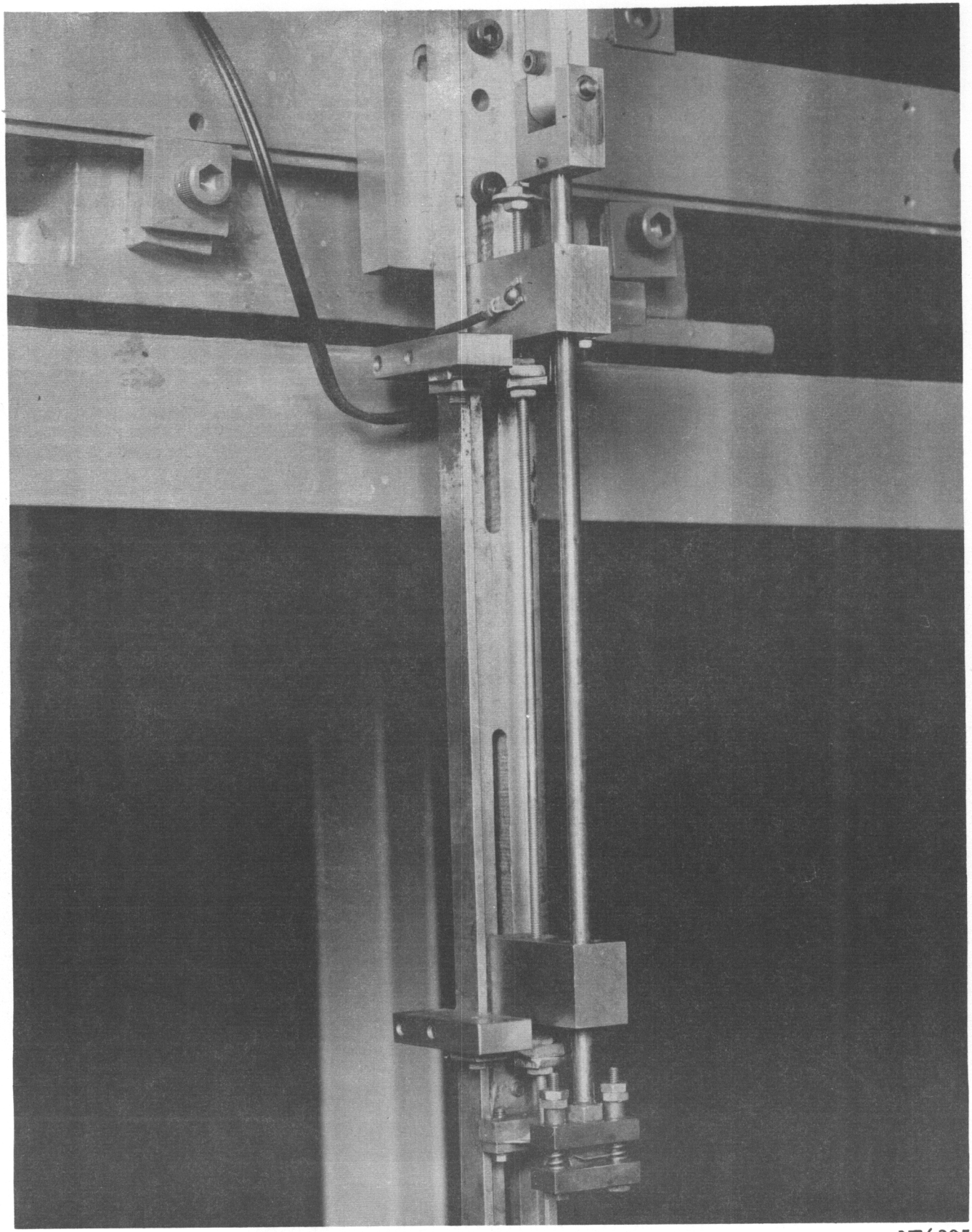

N76285

FIGURE 19. CLOSE-UP VIEW OF MACHINE FOR USE TO -320 F

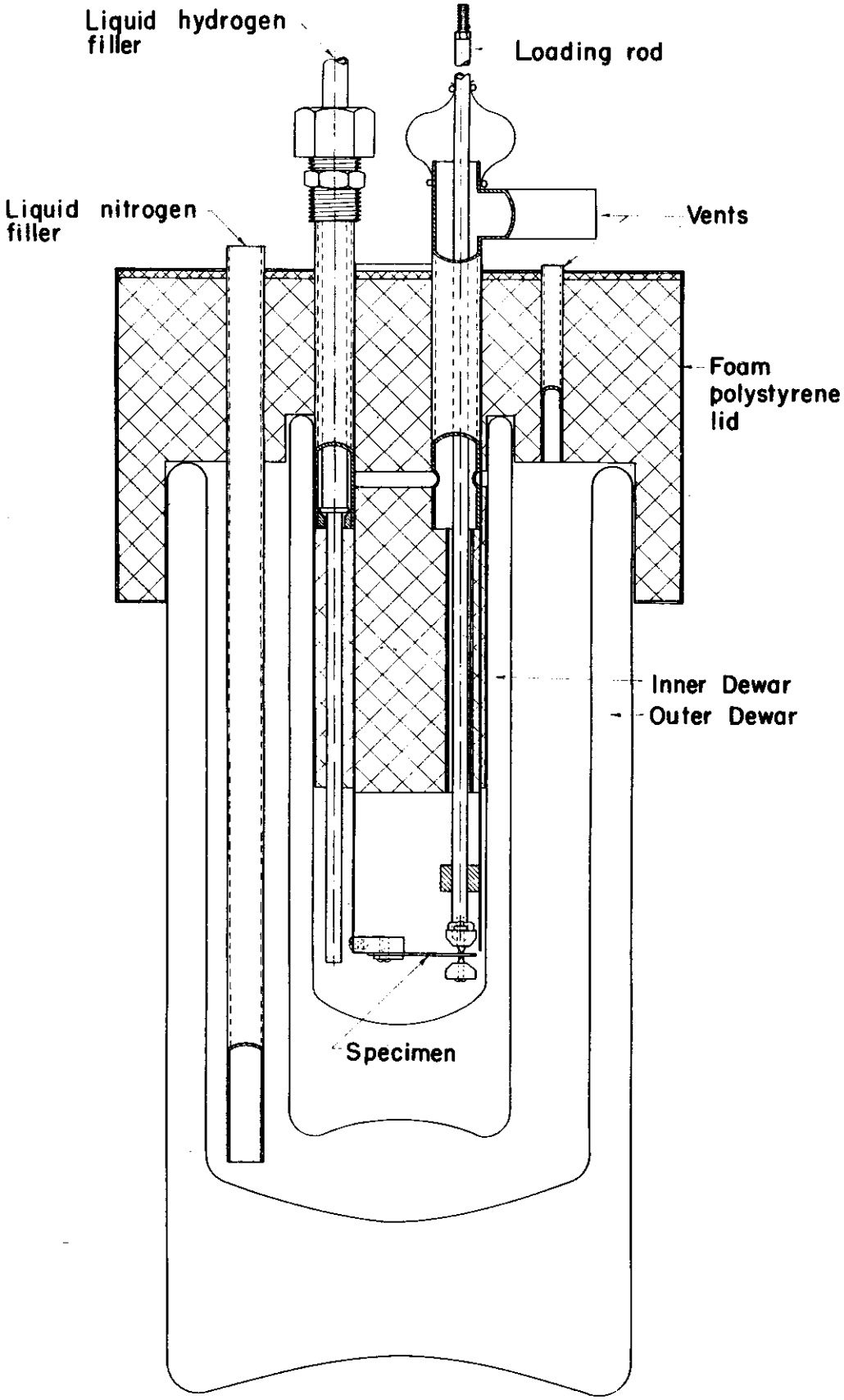

FIGURE 20. CROSS SECTION OF LIQUID-HYDROGEN DEWAR AND CONTENTS

each material so that their total separation was about 0.005 inch greater than the fatigue specimen thickness. Thus, only one knife edge was in contact with the specimens at a time, allowing free sliding between knife edges and the specimens during the deflections. Each of the drive shafts, restricted to movement on its own axis by ball bushings, is attached through a yoke and pin to a crank and in turn to an adjustable cam.

The cycling rate in the two machines used at -320 F and above was 1725 cpm. The third machine was adjustable to one of three rates: 1725, 3450, and 5175 cpm. This latter machine was run mostly at the higher rate of 3450 cpm rather than at 1725 cpm in order to minimize liquid-hydrogen consumption. In the development of S-N curves over the range from 10^4 to 10^6 cycles, the initial cooling and heat input during cycling were such that about 15 experiments could be completed with 150 liters of liquid hydrogen.

After clamping a specimen into a machine, a Dewar containing the appropriate liquid for the desired temperature (methanol and Dry Ice for -110 F and liquid nitrogen for -320 F) was raised around the specimen. In the liquid-hydrogen tests, two Dewars (one within the other, each double walled and evacuated) with a close fitting foamed polystyrene lid enclosed the specimen. Both Dewars were first precooled with liquid nitrogen; the outer Dewar was kept full and the smaller inner Dewar after being precooled was emptied by purging with warm hydrogen gas. This inner Dewar was then filled with liquid hydrogen.

In order to monitor the level of liquid hydrogen (or sometimes nitrogen) around the specimen, a liquid-level device was constructed, based on the change of resistance with temperature of carbon resistors. A Wheatstone bridge circuit was built similar to one described by Scott[9]. Three 1000-ohm Allen Bradley carbon resistors were mounted with their axes horizontal on the outside surface of the 2-inch tube, the lowest one level with the specimen and the others about 3/4 inch and 1-1/2 inches above the first. The three resistors could, in turn, be connected to the circuit by means of a switch. When one of the three resistors was immersed in liquid hydrogen and was switched into the circuit, the circuit meter read near zero; if the resistor was above the liquid surface, the meter read above half-scale. When liquid nitrogen was used around the specimen, the corresponding meter indications were about 0.6 full scale and greater than full scale, respectively.

The shutoff mechanism of each of the machines used at -320 F and above, part of which is visible in Figure 19, consists of a rod in light, spring-loaded contact with the specimen on its axis and about 1/8 inch outside of the failure zone. The rod is driven up and down by the specimen until the specimen breaks, at which time the broken specimen stub comes to rest in its neutral position. The upper end of the driven rod operates an electrical switch. When a specimen breaks, the switch stands open and an electronic circuit shuts off the motor by means of a relay. This shutoff mechanism was designed after various attempts to set up a switch with the specimen itself an element in a circuit. Such switches were unsuccessful mainly because of too great an electrical conductivity of liquids usable with Dry Ice. No shutoff mechanism was incorporated in the liquid-hydrogen machine.

Procedure in Fatigue Experiments

After mounting a notched specimen in its grip and adjusting the separation of the knife edges as described above, the load-deflection characteristic of the specimen was measured.

Figure 21 shows a schematic diagram of the arrangements used to obtain deflection measurements by handing weights on each specimen. After a specimen had reached the desired test temperature the pin was removed from the clevis and a beam set on the clevis. Positions of the specimen were read on a micrometer before and after increments of load. For convenience, the first specimen of a material to be tested at each temperature was usually loaded in some 8 to 10 increments up to the estimated maximum load required. Succeeding specimens were then loaded with only that load giving the desired maximum stress level for that experiment. The cam was then adjusted in each experiment so that the specimen deflection, measured by the micrometer, agreed with the value just obtained in static loading. The motor was then run until failure of the specimen.

After completion of an S-N curve, the static load-deflection data were combined to obtain an average load/deflection ratio for use in calculating the stresses. The maximum stress in each experiment was calculated in terms of the actual maximum deflection, the load/deflection ratio, and the geometry of the specimen by means of the formula $S = \frac{Mc}{I}$, where S is the stress, M is the moment at the notch line, and I/c is the section modulus of the specimen at the notch line. This method of calculation of stresses for constant-deflection experiments does not, of course, account for possible changes in the stress-strain characteristic of a material during fatigue experiments. However, for materials which are strengthened by strain cycling the calculated stresses should be conservative from a fatigue-design viewpoint.

Figure 22 shows typical notched specimens before and after fatigue failure.

In the first year's work with unnotched specimens, it had been planned to calculate stresses from measured strains and modulus values obtained at the Cryogenic Engineering Laboratory at Boulder. Accordingly, calibration experiments were carried out with two specimens of each of the materials, one specimen being used in the liquid-hydrogen fatigue machine and the other specimen in one of the two other identical fatigue machines.

Two Type A-7 SR-4 bonded wire strain gages were applied to each of the calibration specimens. The gages were cemented on opposite faces of the specimen at points centrally located on the axis in the constant-stress section. In use, the two gages were connected in adjacent arms of a bridge to a Type N strain-gage indicator. The specimens were mounted in the usual way, but for calibration, the drive shaft was disconnected from the crank and cam. The dial indicator was mounted under the knife-edge grip to measure deflections as it was for fatigue experiments. The drive shaft was pushed downward against the specimen and dial indicator by a micrometer screw, which permitted accurate increments of deflection and a check on dial-gage readings. Strain readings were taken at small deflection increments up to the maximum deflection used for each material in fatigue experiments. The resulting calibration curves were used to convert deflections in fatigue experiments into strains.

The calibration procedure described above had the advantages that each material was calibrated with a specimen identical in geometry and in metallurgical condition to the fatigue specimens, and that deviations from ideal rigidity of the mounts for the specimens of different stiffness were automatically accounted for in the calibration.

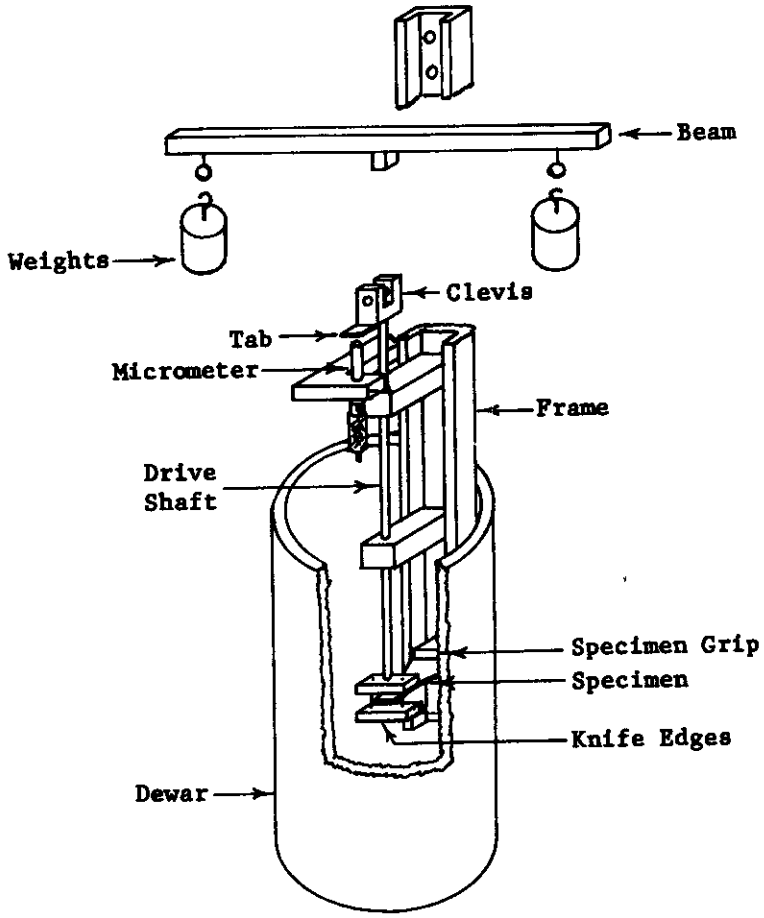

FIGURE 21. ARRANGEMENT FOR MEASURING DEFLECTION OF SPECIMENS UNDER DEAD-WEIGHT LOADING

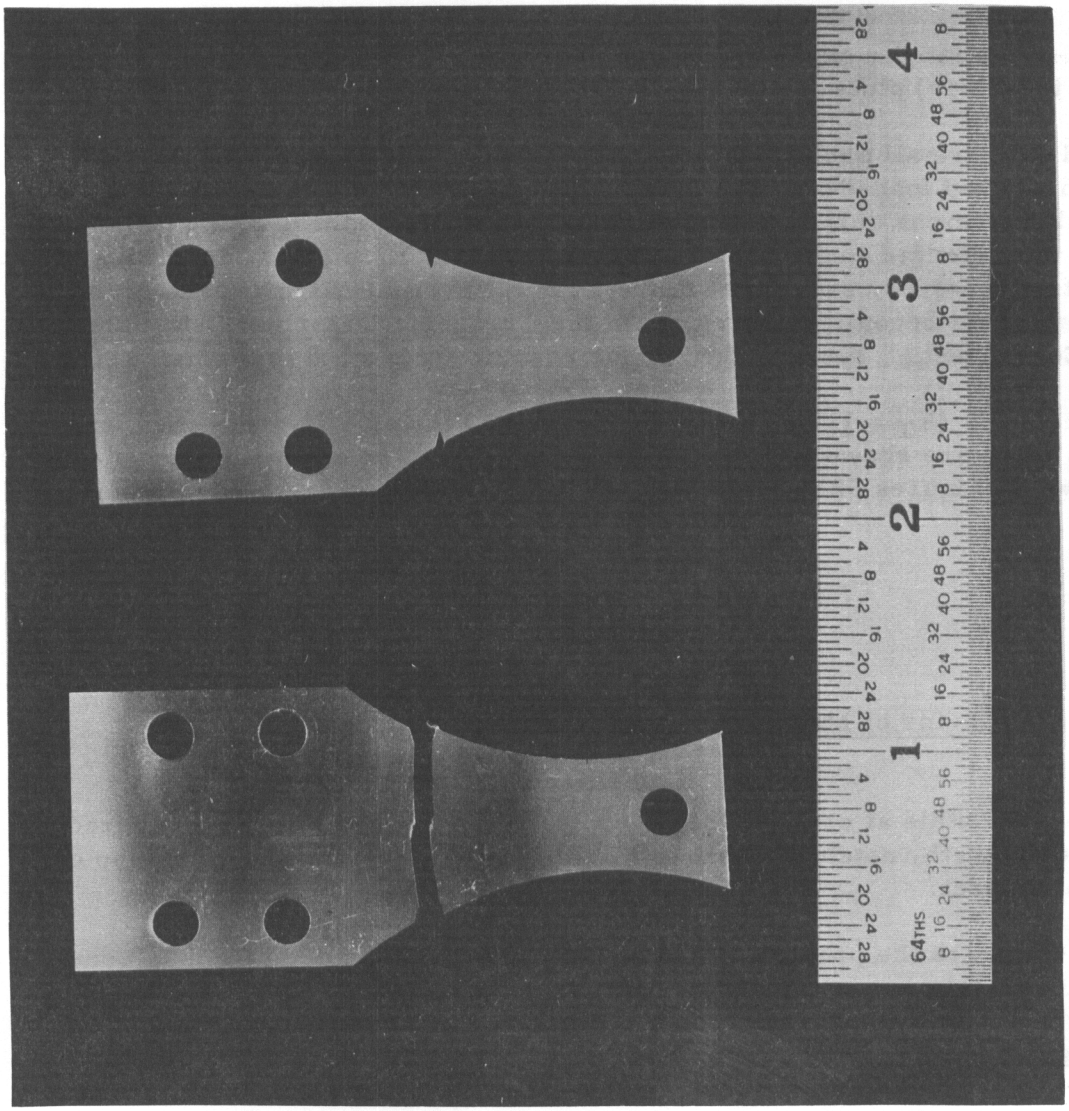

FIGURE 22. TYPICAL NOTCHED FATIGUE SPECIMEN BEFORE AND AFTER FATIGUE EXPERIMENT

In addition to the static calibration carried out as described above, experiments were conducted to verify that the deflections with the machine running were close to the statically measured values. Several experiments of this kind were performed which included the most extreme conditions of specimen thickness and cycling rate (in the case of the liquid-hydrogen apparatus). Deflections of the knife-edge grips were measured by means of a micrometer screw. With the machine running, the micrometer screw was slowly advanced until it was touched by a point of the knife-edge grip upon each downward excursion. The touching of the grip and the micrometer was detected by means of a very sensitive electronic ohmmeter device which gave indications on an electric "eye". This device permits easy detection of deflections of less than 0.001 inch. It was found from these experiments that dynamic and static deflections did not differ by more than about 0.001 inch.

RESULTS

The results of the fatigue experiments are shown in S-N (stress or strain versus number of cycles to failure) plots.

The notched data are all presented in terms of stress. The stress values were calculated from measured load-deflection data as described above. In the first year's work on unnotched specimens only strain-deflection data were obtained (using SR-4 strain gages). It was intended to convert these data from strain to stress by means of stress-strain plots. However, stress-strain data for all the materials at each of the four temperatures did not become available from the Cryogenic Materials Data Handbook program. Consequently, some of the fatigue results are plotted in terms of strain.

The unnotched data (K_T = 1) are shown in Figures 23 through 37. The medium notched (K_T = 3.1) data are shown in Figures 38 through 51. The sharp notched (K_T = 6.3) data are shown in Figures 52 through 56.

DISCUSSION

Beahvior of Metals at Cryogenic Temperatures

The behavior of metals at cryogenic temperatures has generally been measured in terms of tensile strength, notched tensile strength, yield strength, and reduction of area at fracture or impact.

In more recent years the problem of brittle fracture has been identified as comprising two questions: (1) what is involved in initiating a crack, and (2) what is involved in propagating a crack? The separate aspects of initiation and propagation have been recognized in fatigue and work is now being carried out in a number of laboratories on these aspects. Current fracture mechanics analyses that have been undertaken to generate design data have usually made the basic assumption that cyclic loading is not involved[10]. Research efforts are being carried out on fatigue damage and fracture, with the aim of providing design data[11].

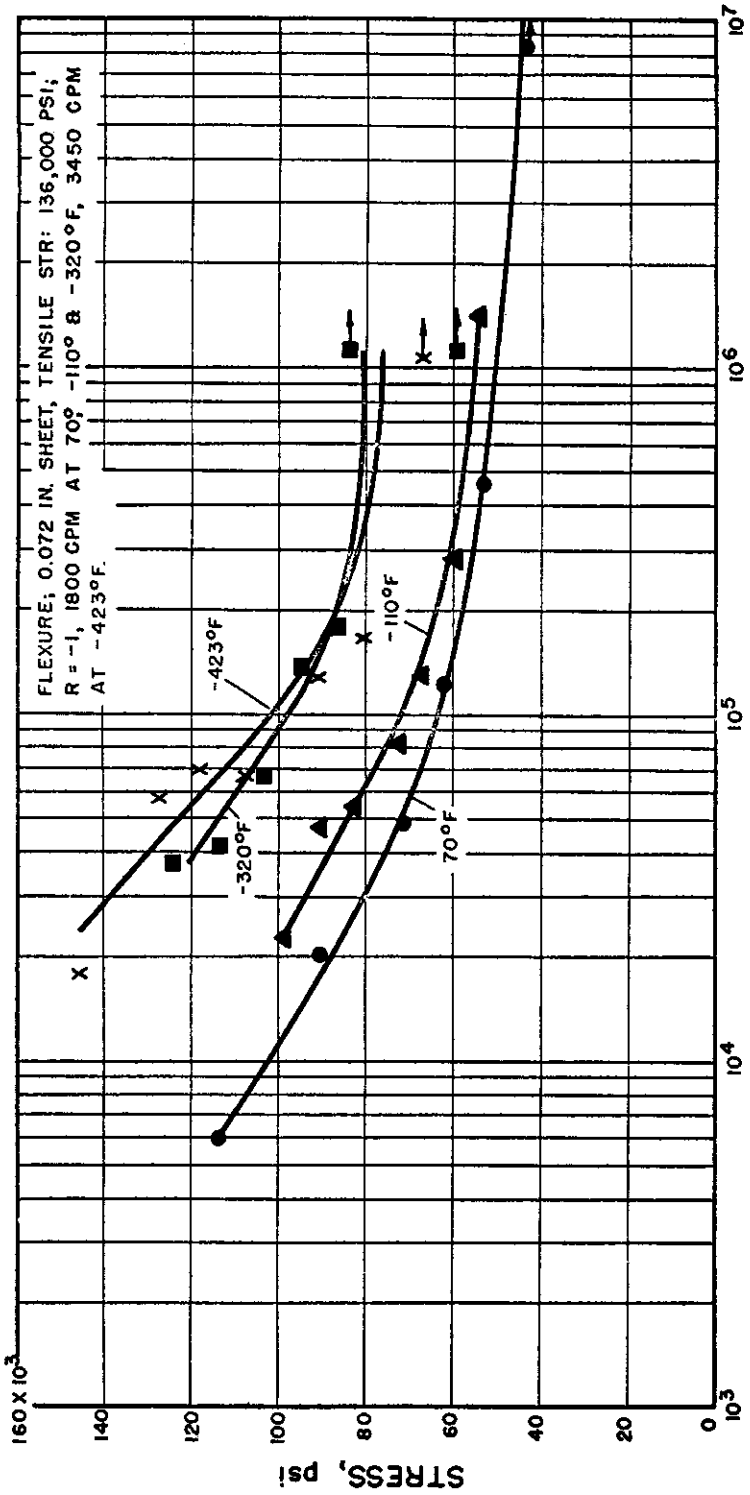

FIGURE 23. UNNOTCHED (K_T = 1) FATIGUE BEHAVIOR OF ANNEALED 6Al-4V TITANIUM

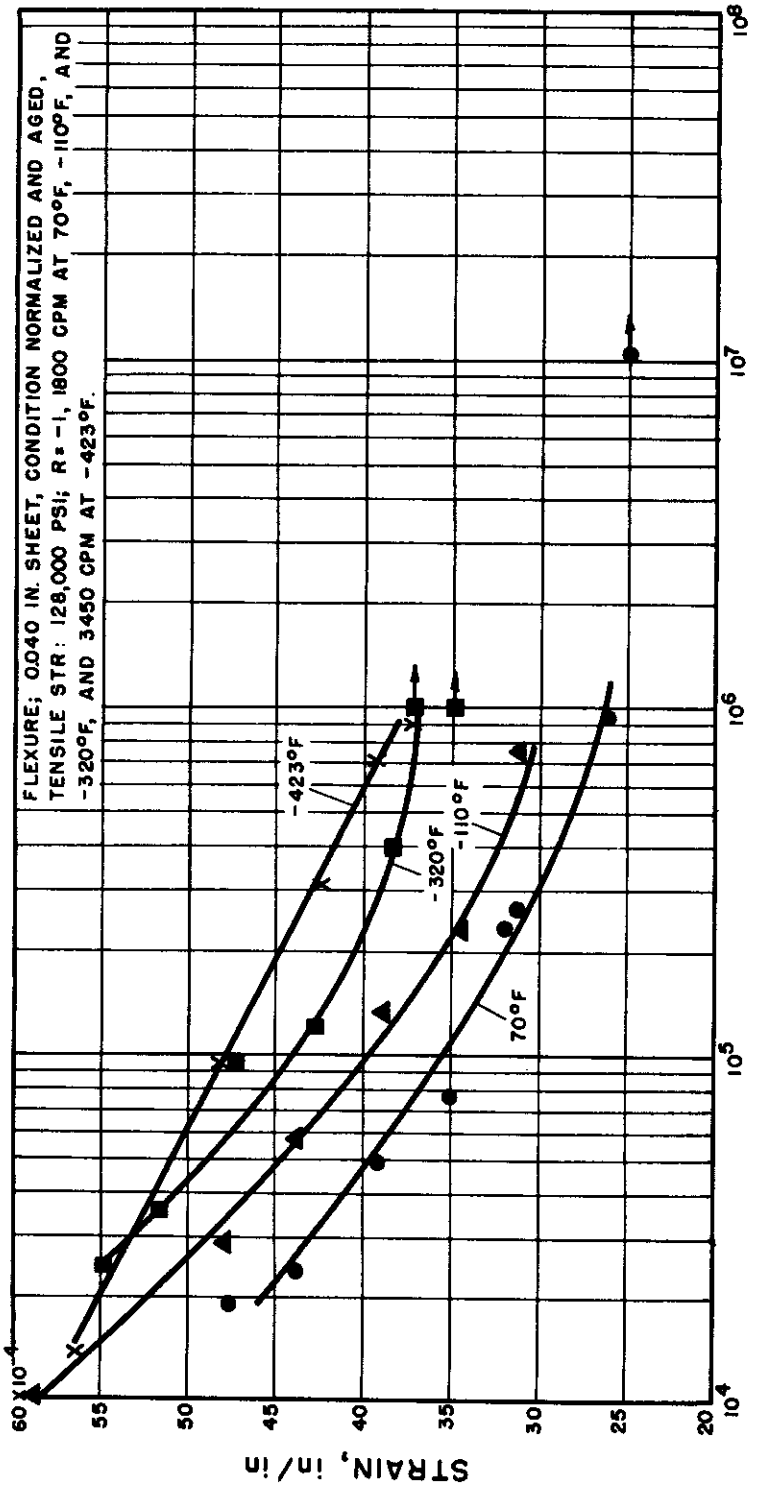

FIGURE 24. UNNOTCHED (K_T = 1) FATIGUE BEHAVIOR OF NORMALIZED AND AGED 2800 STEEL

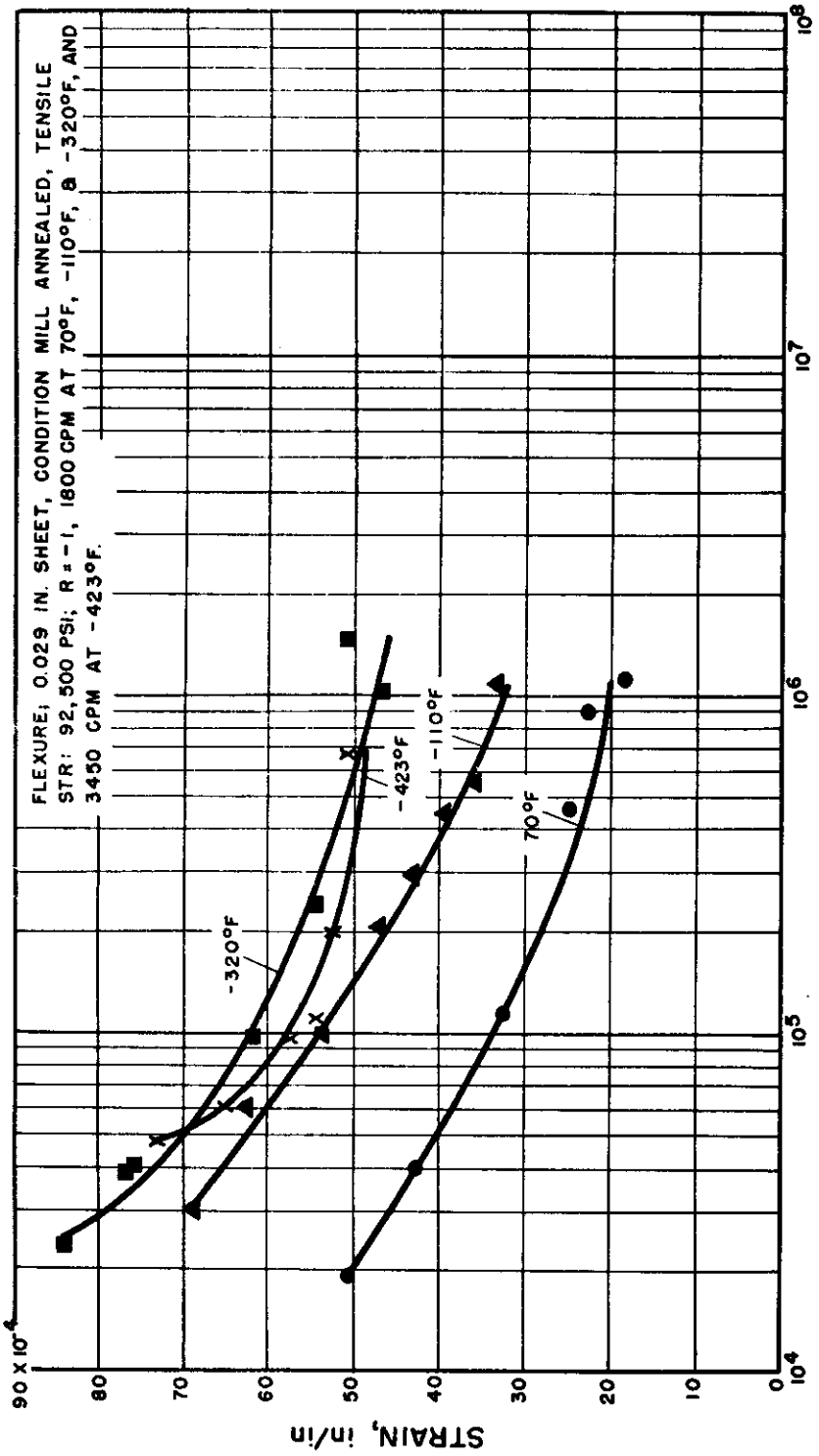

FIGURE 25. UNNOTCHED (K_T = 1) FATIGUE BEHAVIOR OF ANNEALED 347 STAINLESS STEEL

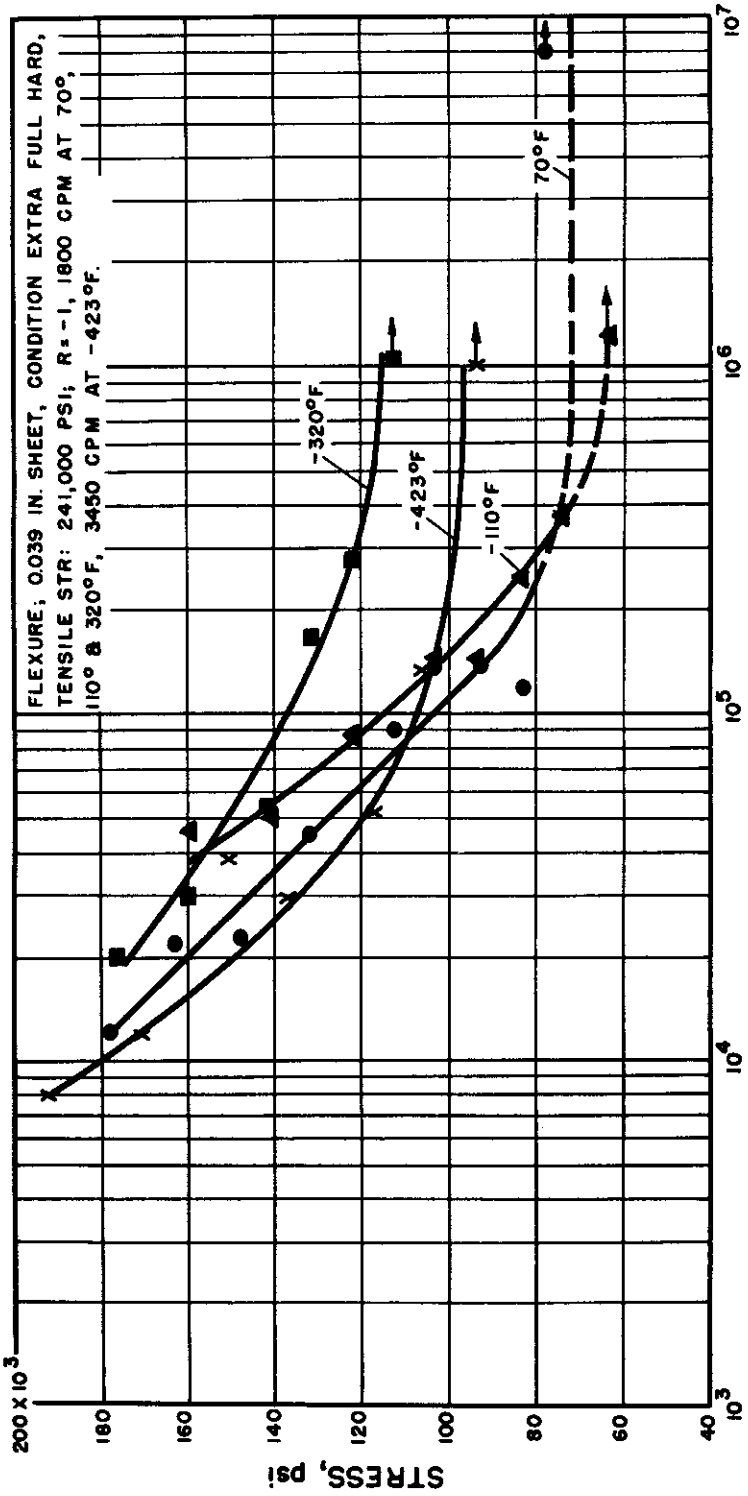

FIGURE 26. UNNOTCHED (K_T = 1) FATIGUE BEHAVIOR OF COLD-ROLLED 301 STAINLESS STEEL

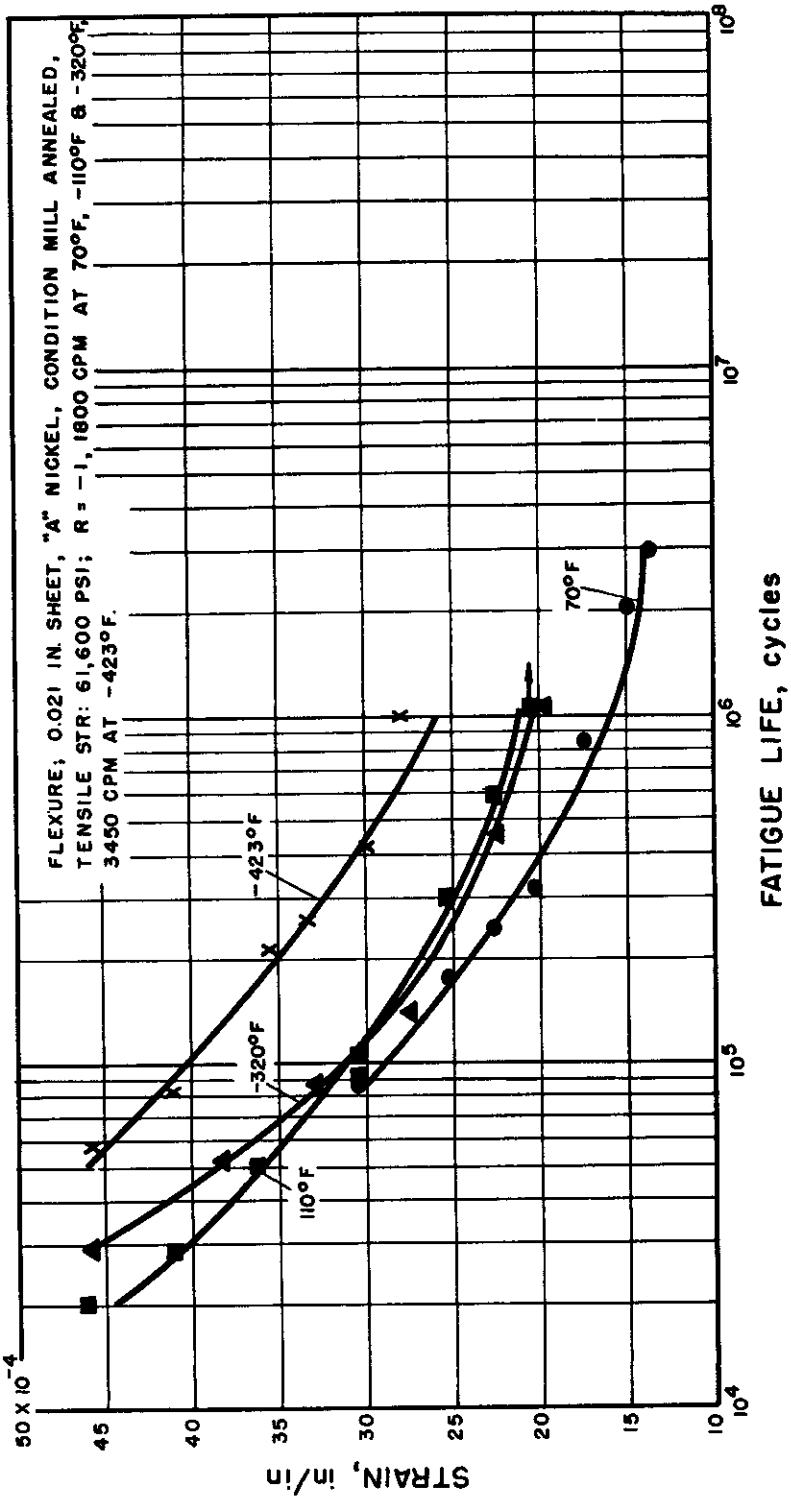

FIGURE 27. UNNOTCHED (K_T = 1) FATIGUE BEHAVIOR OF ANNEALED "A" NICKEL

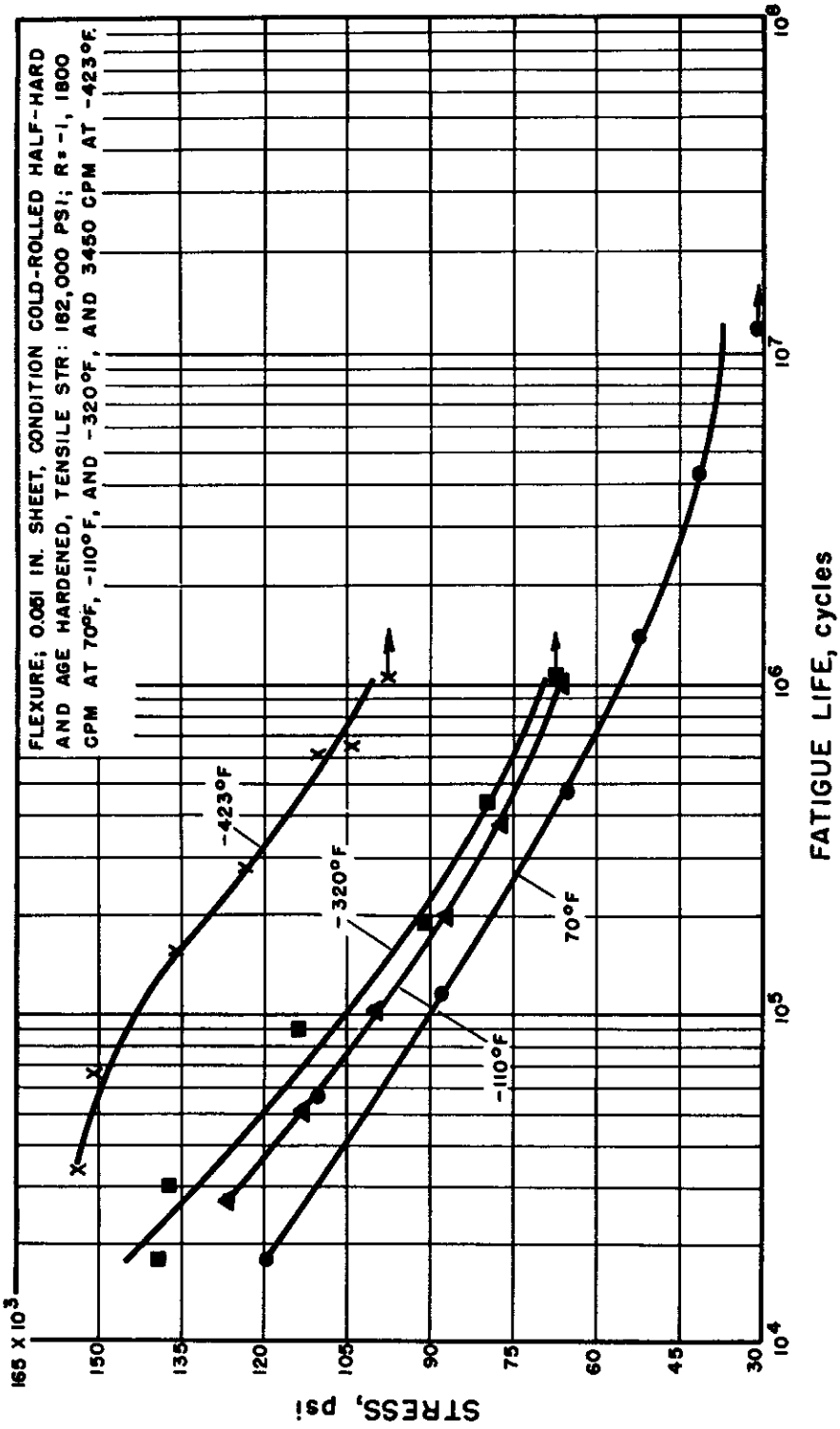

FIGURE 28. UNNOTCHED (K_T = 1) FATIGUE BEHAVIOR OF COLD-ROLLED AND AGE-HARDENED "K" MONEL NICKEL

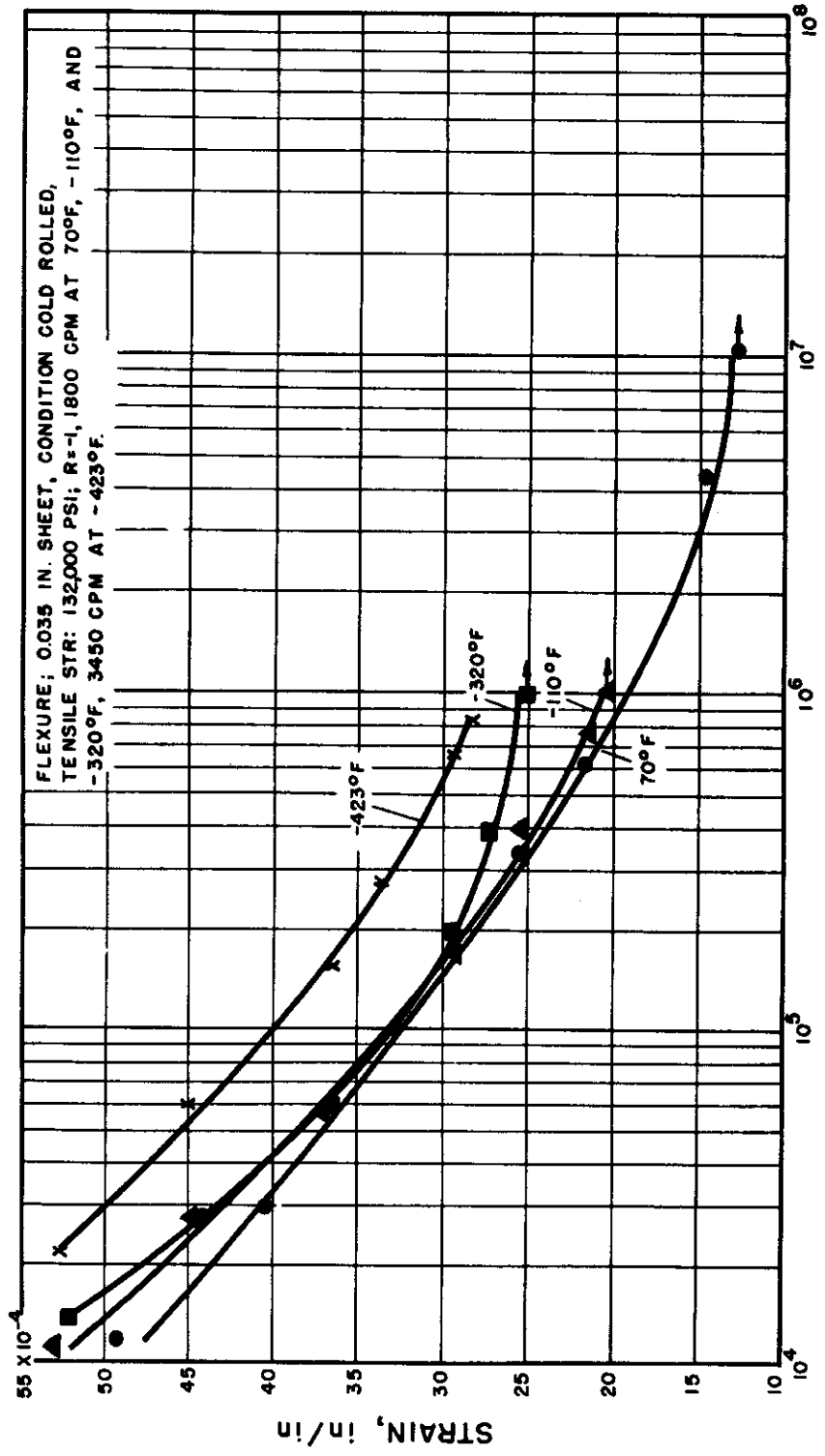

FIGURE 29. UNNOTCHED (K_T = 1) FATIGUE BEHAVIOR OF COLD-ROLLED INCONEL NICKEL

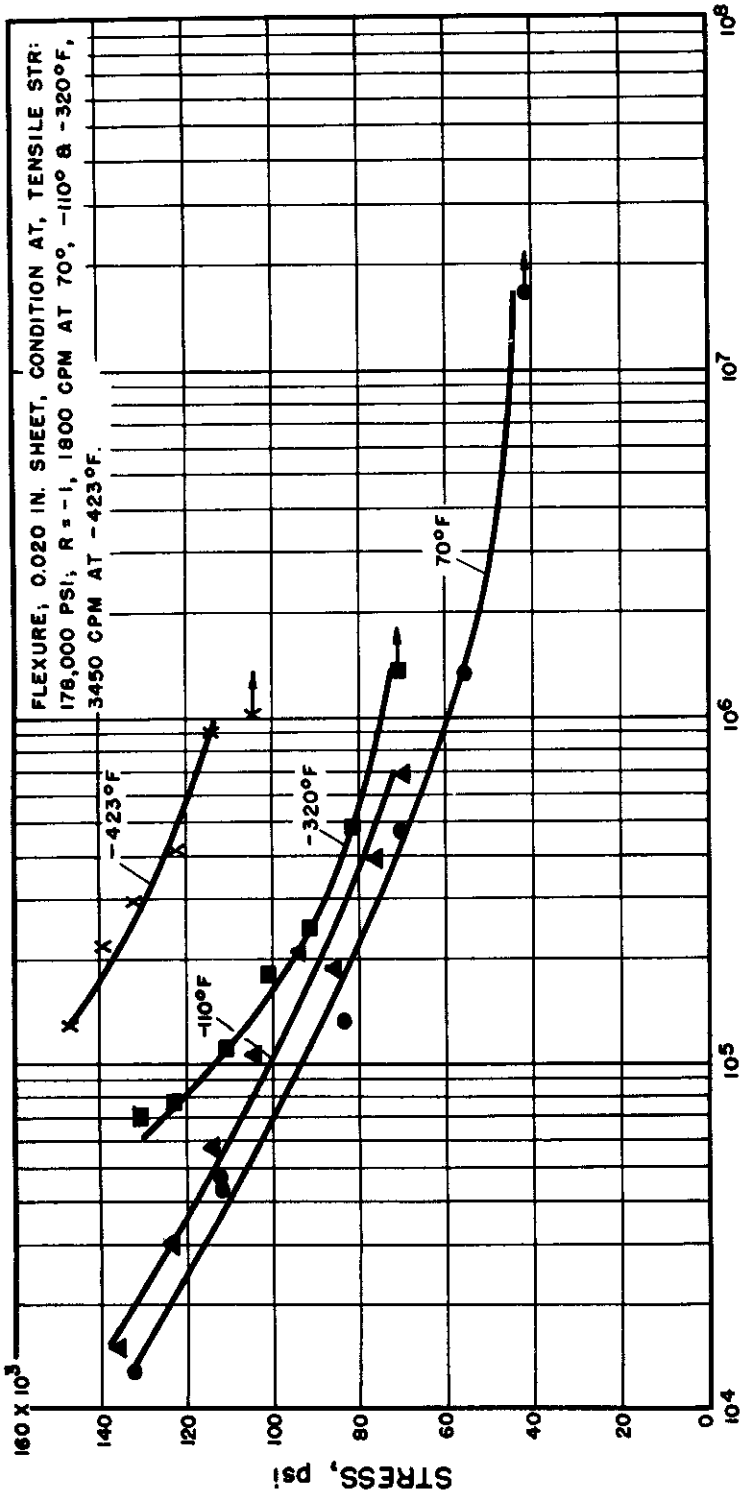

FIGURE 30. UNNOTCHED (K_T = 1) FATIGUE BEHAVIOR OF ANNEALED AND AGE-HARDENED BERYLCO 25 BERYLLIUM-COPPER

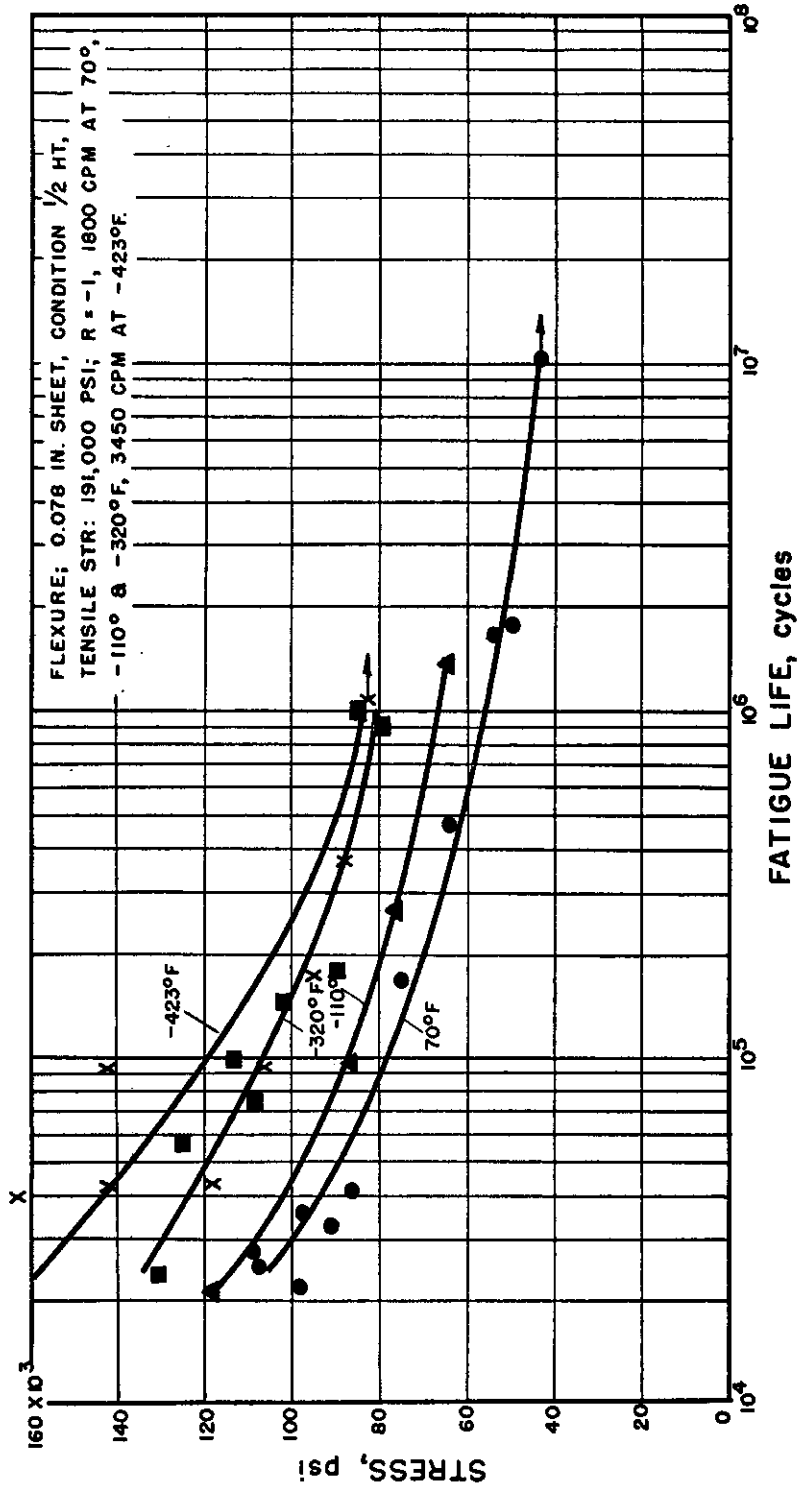

FIGURE 31. UNNOTCHED (K_T = 1) FATIGUE BEHAVIOR OF COLD-ROLLED AND AGE-HARDENED BERYLCO 25 BERYLLIUM-COPPER

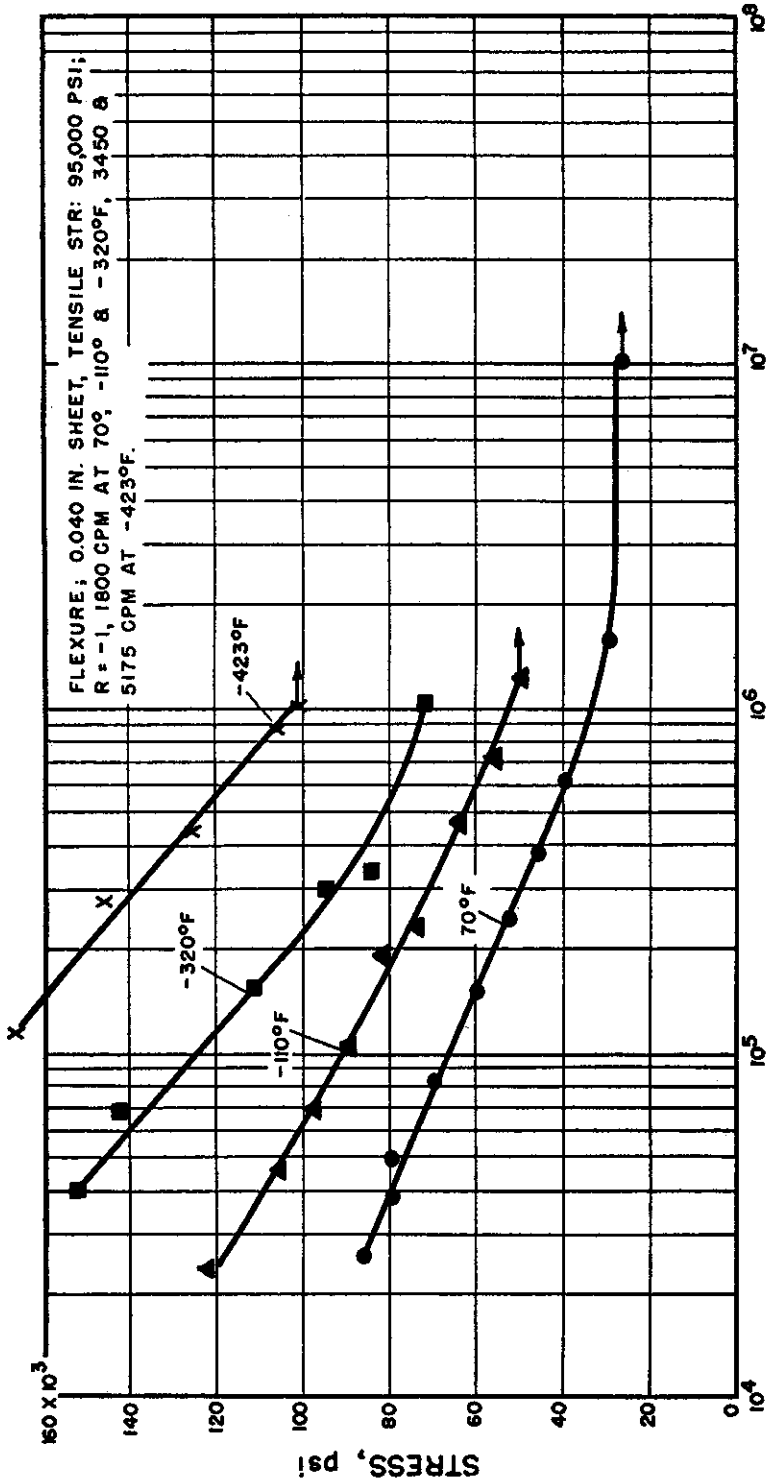

FIGURE 32. UNNOTCHED (K_T = 1) FATIGUE BEHAVIOR OF COLD-ROLLED AND STRESS-RELIEVED 70/30 BRASS

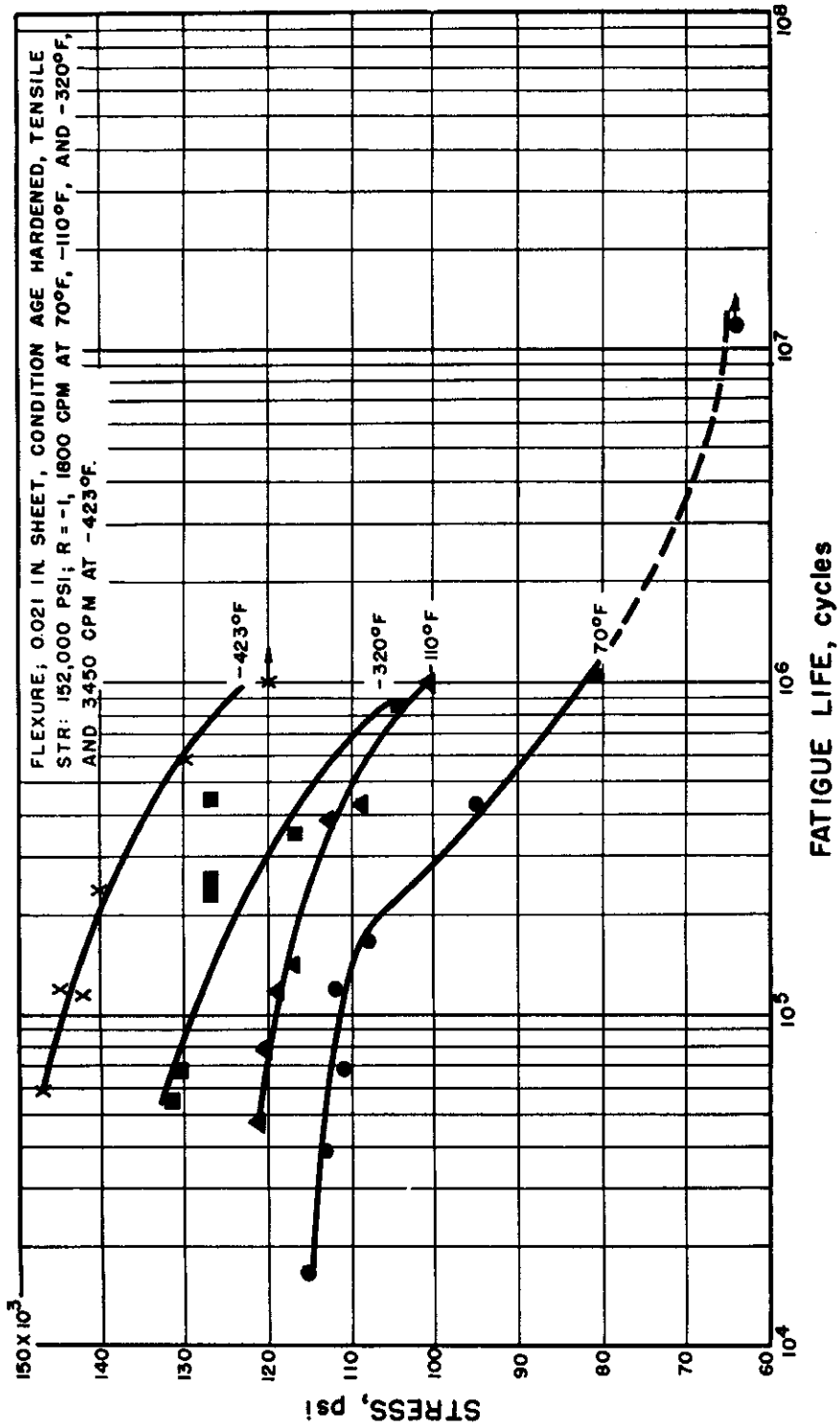

FIGURE 33. UNNOTCHED (K_T = 1) FATIGUE BEHAVIOR OF ANNEALED AND AGE-HARDENED NI-SPAN C IRON-NICKEL ALLOY

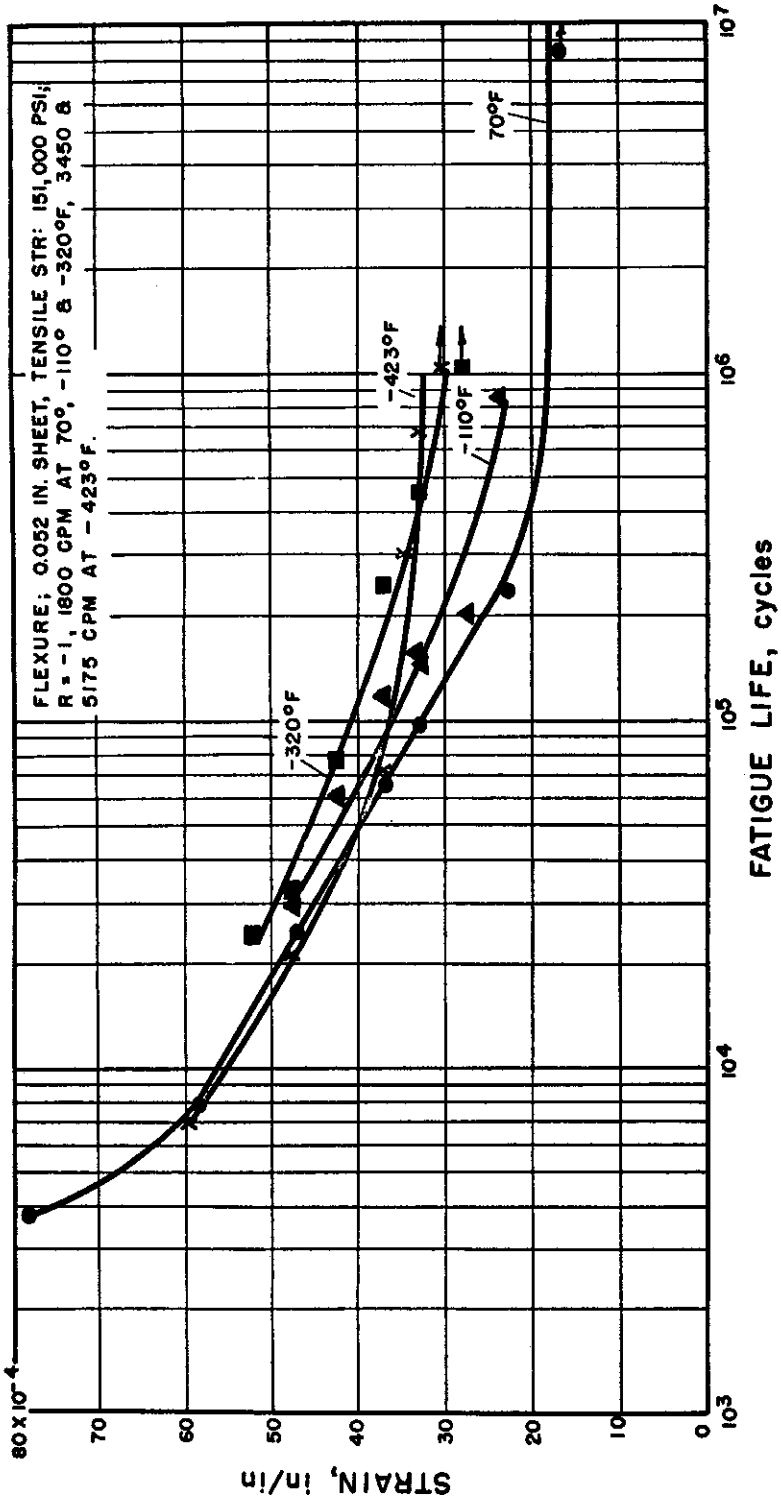

FIGURE 34. UNNOTCHED (K_T = 1) FATIGUE BEHAVIOR OF QUENCHED AND TEMPERED 1075 CARBON STEEL

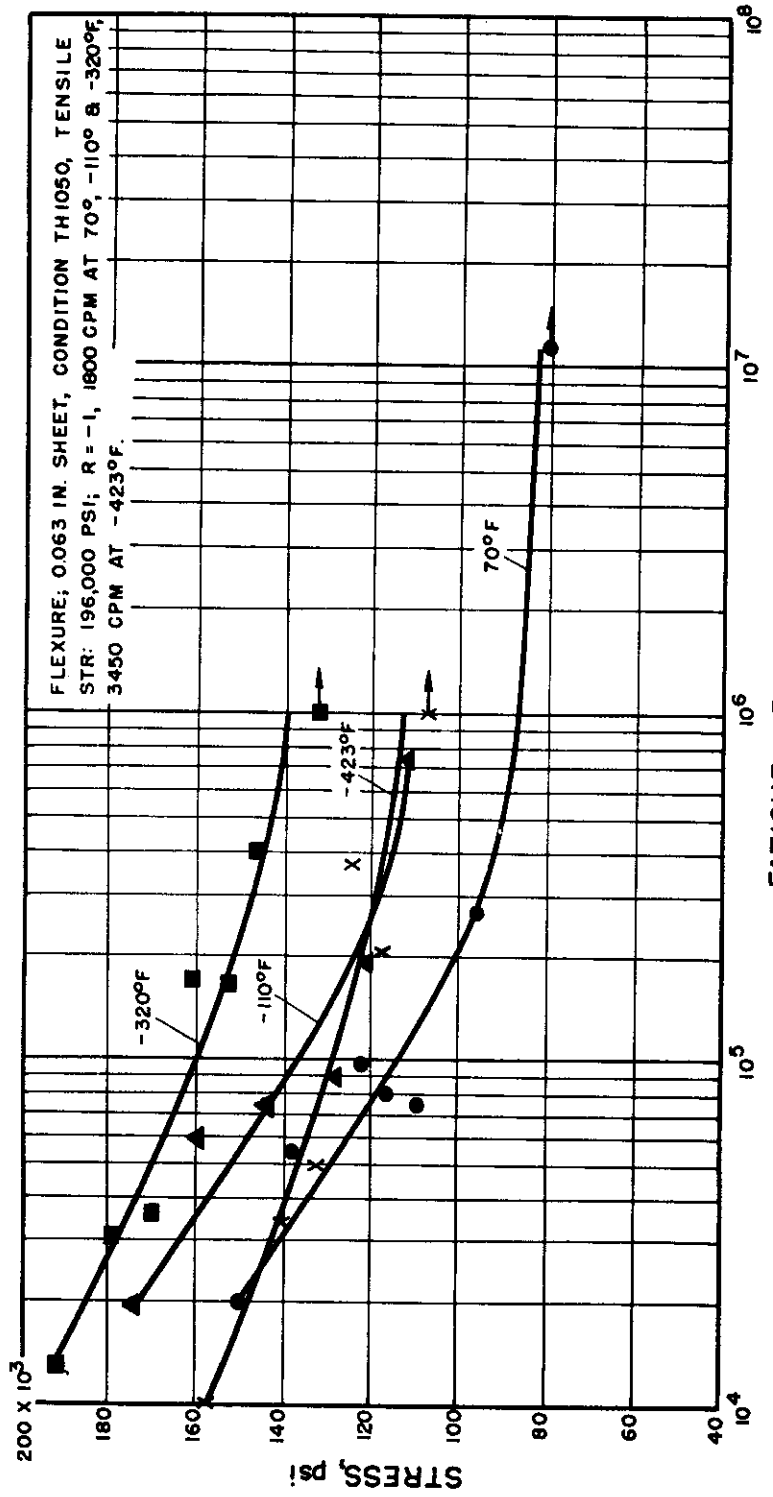

FIGURE 35. UNNOTCHED (K_T = 1) FATIGUE BEHAVIOR OF 17-7PH (TH 1050) STAINLESS STEEL

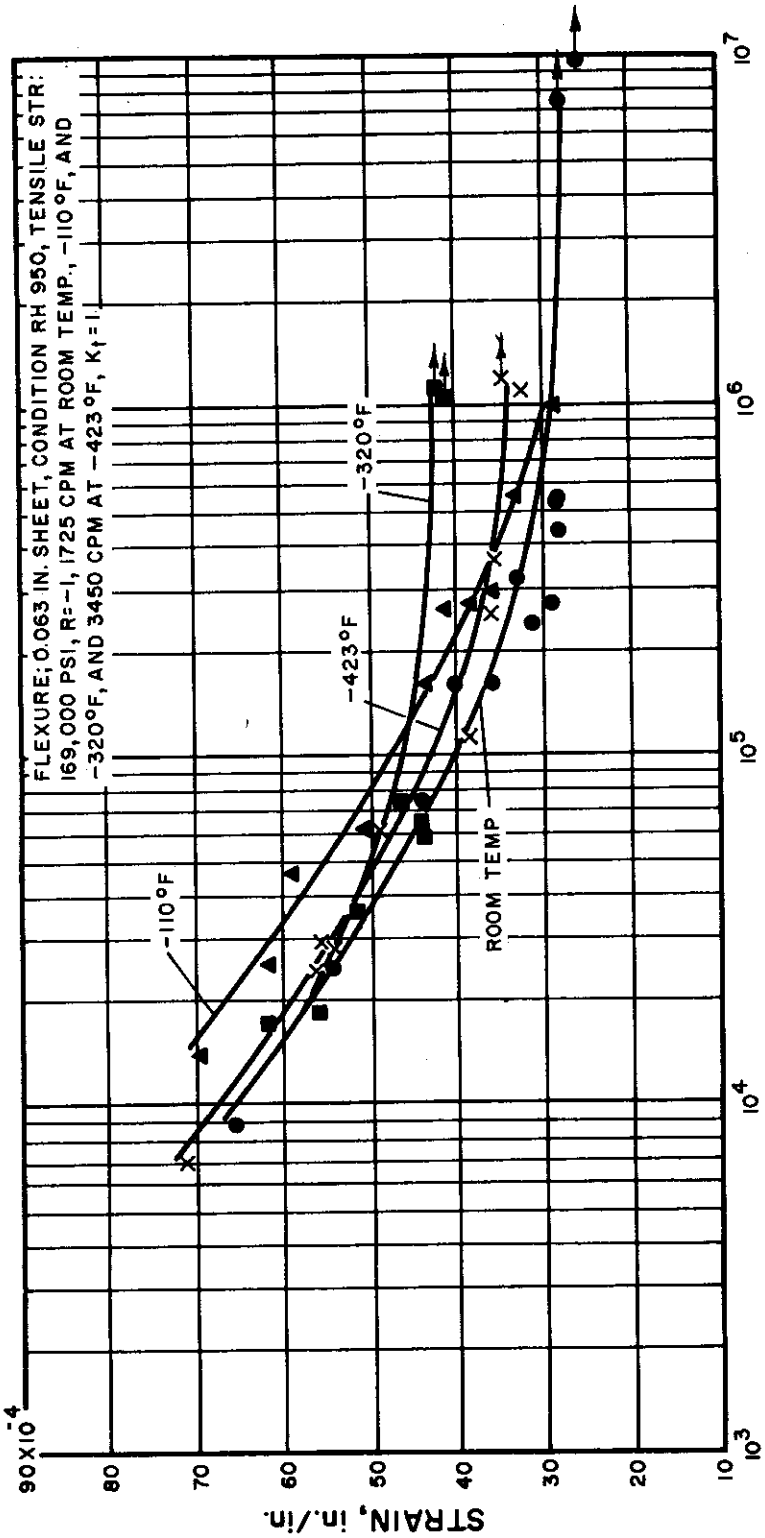

FIGURE 36. UNNOTCHED (K_T = 1) FATIGUE BEHAVIOR OF 17-7PH (RH 950) STAINLESS STEEL

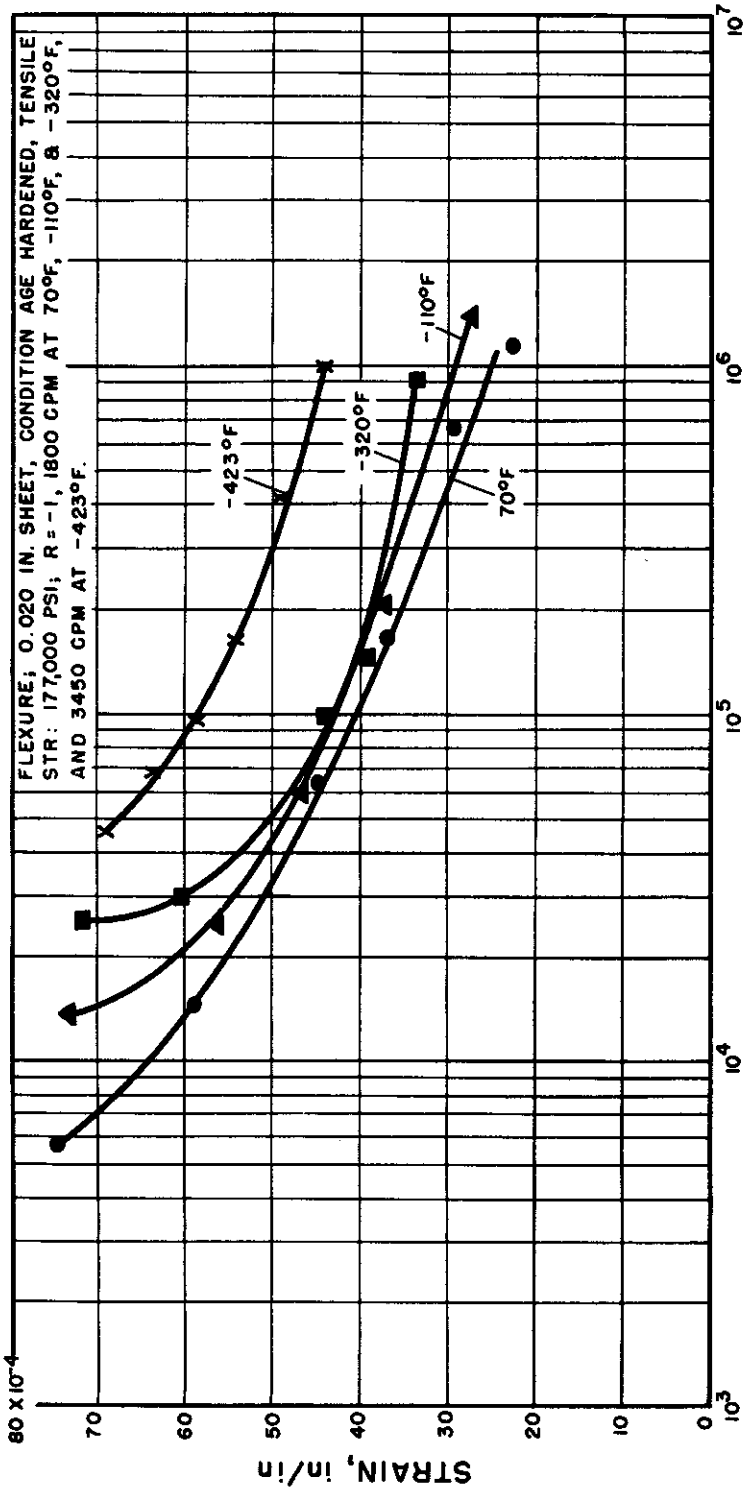

FIGURE 37. UNNOTCHED (K_T = 1) FATIGUE BEHAVIOR OF ANNEALED AND AGE-HARDENED INCONEL "X" NICKEL

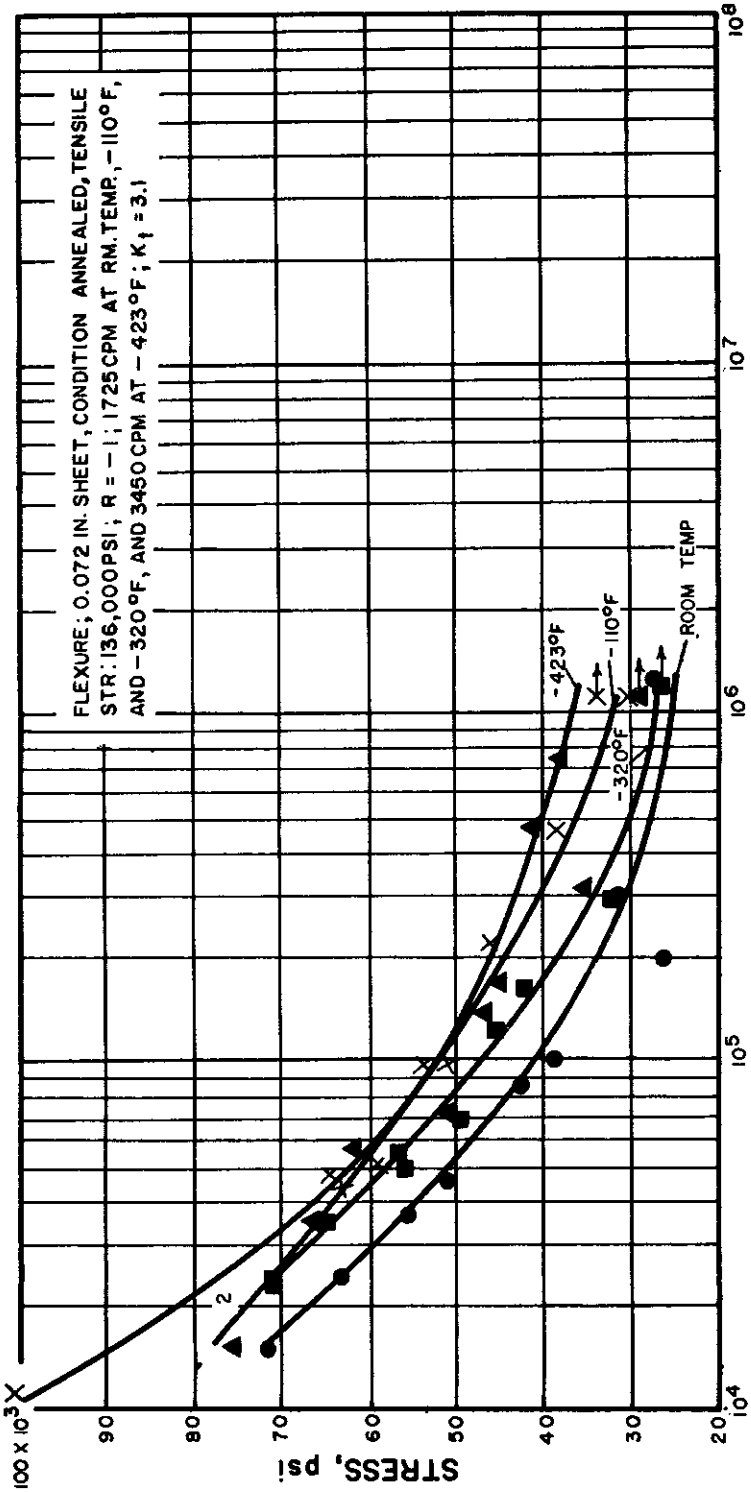

FIGURE 38. NOTCHED (K_T = 3.1) FATIGUE BEHAVIOR OF ANNEALED 6Al-4V TITANIUM

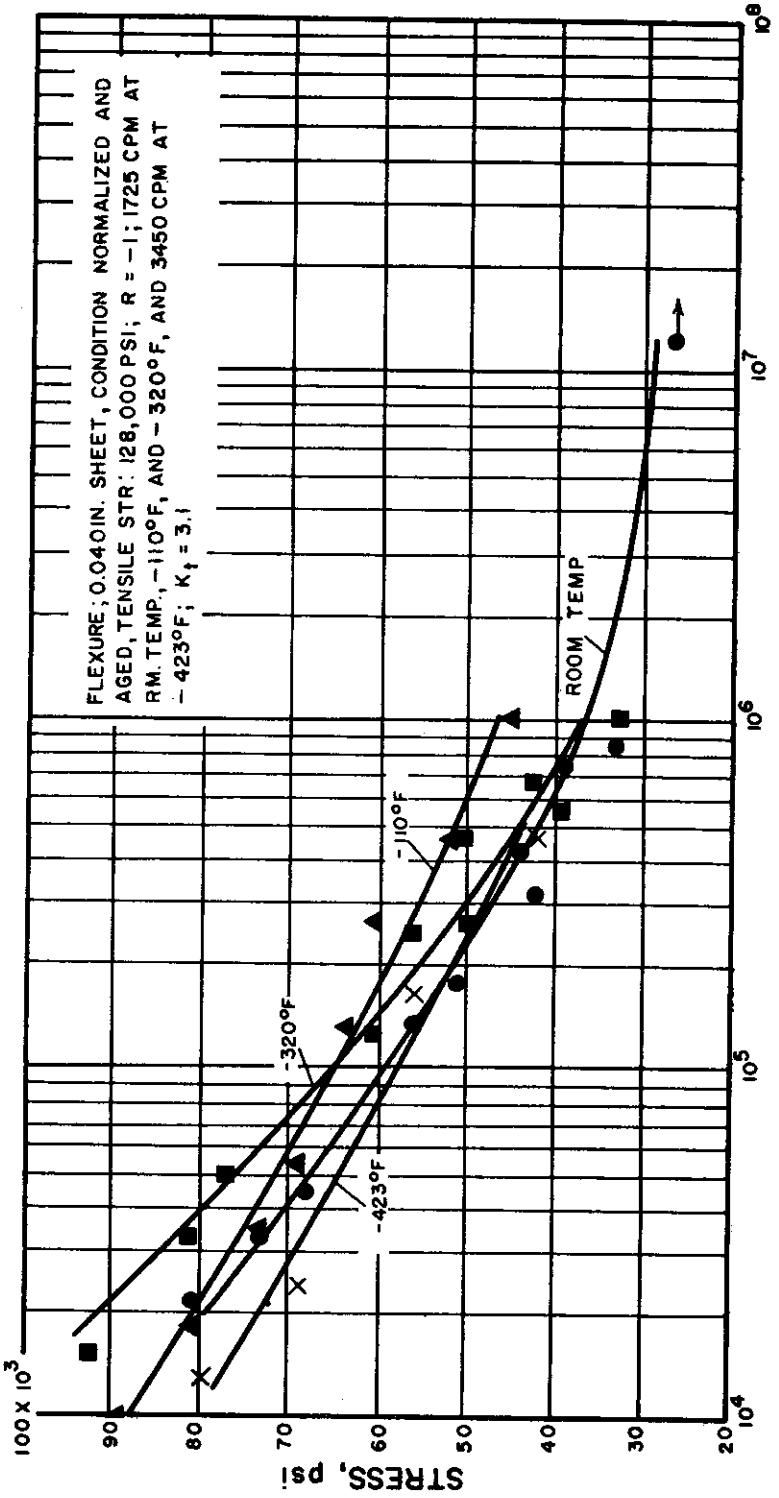

FIGURE 39. NOTCHED (K_T = 3.1) FATIGUE BEHAVIOR OF NORMALIZED AND AGED 2800 STEEL

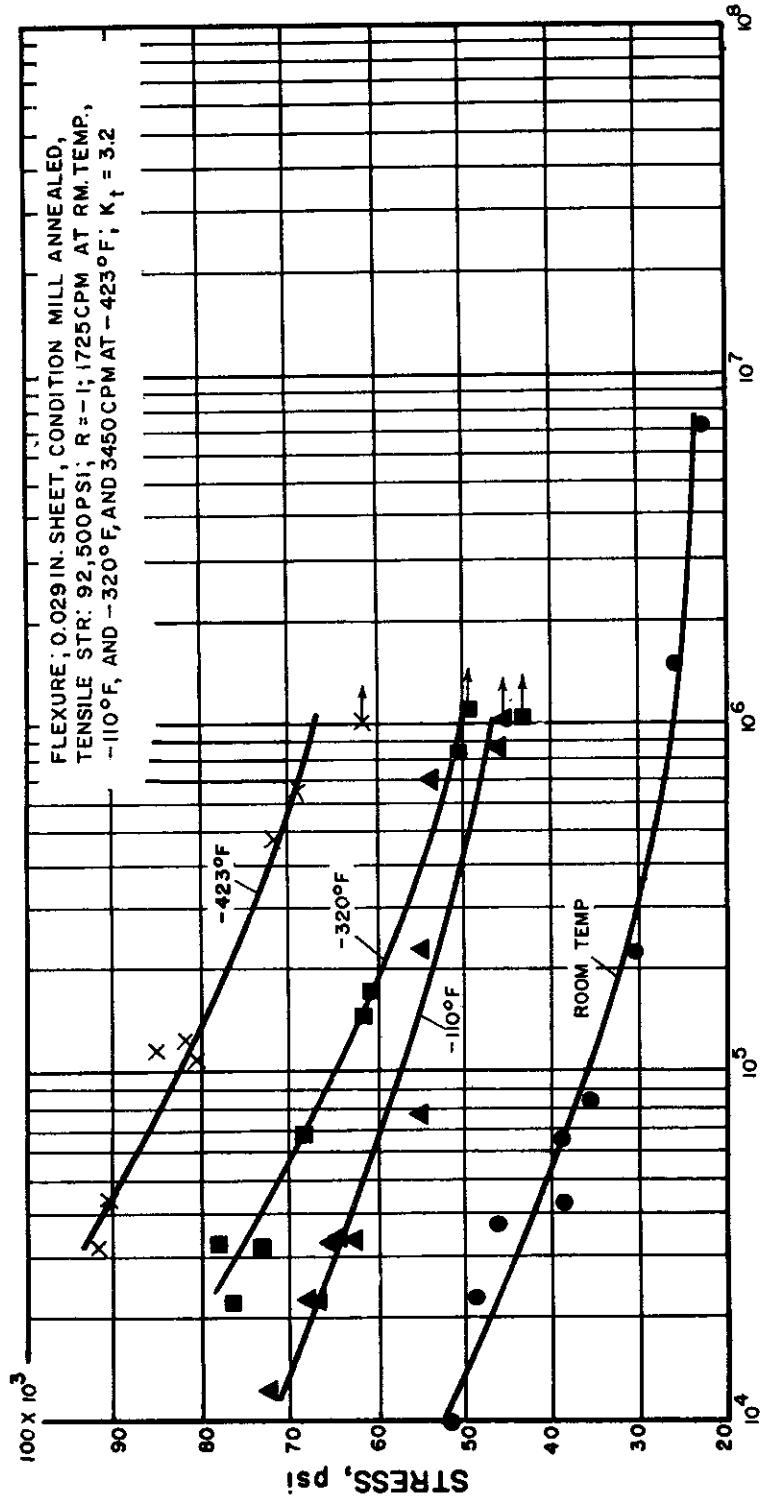

FIGURE 40. NOTCHED (K_T = 3.2) FATIGUE BEHAVIOR OF ANNEALED 347 STAINLESS STEEL

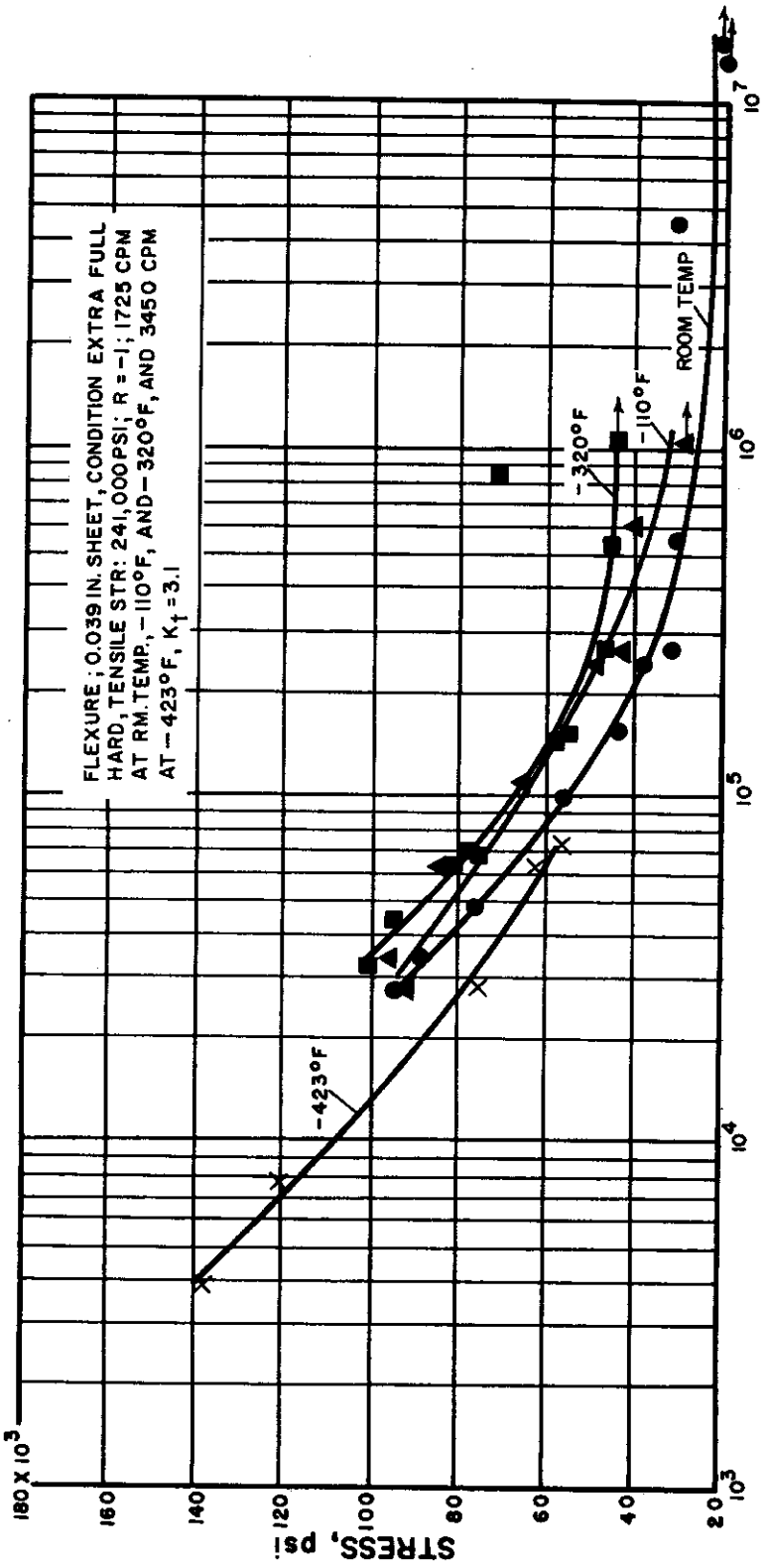

FIGURE 41. NOTCHED (K_T = 3.1) FATIGUE BEHAVIOR OF COLD-ROLLED 301 STAINLESS STEEL

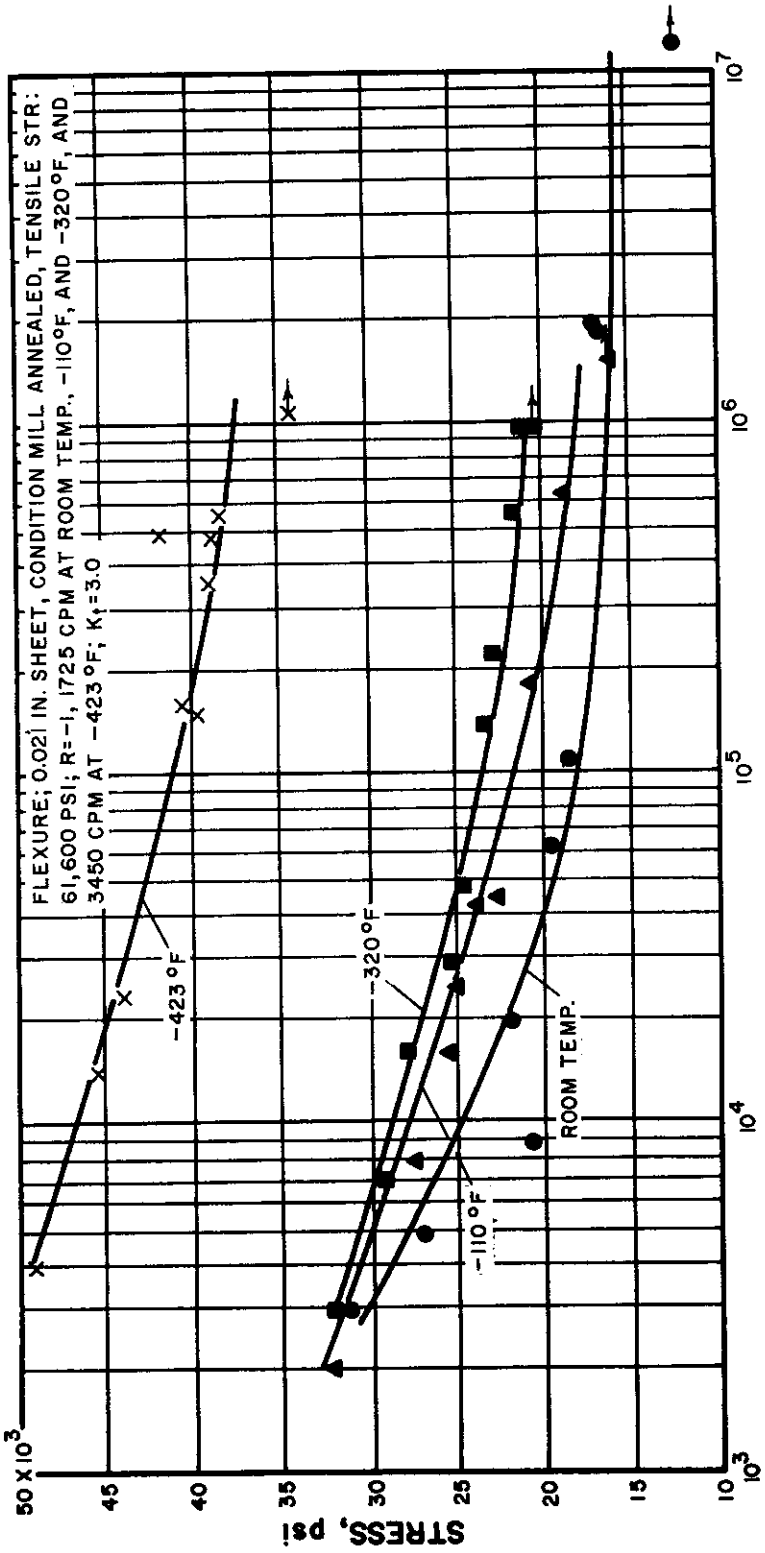

FIGURE 42. NOTCHED (K_T = 3.0) FATIGUE BEHAVIOR OF ANNEALED "A" NICKEL

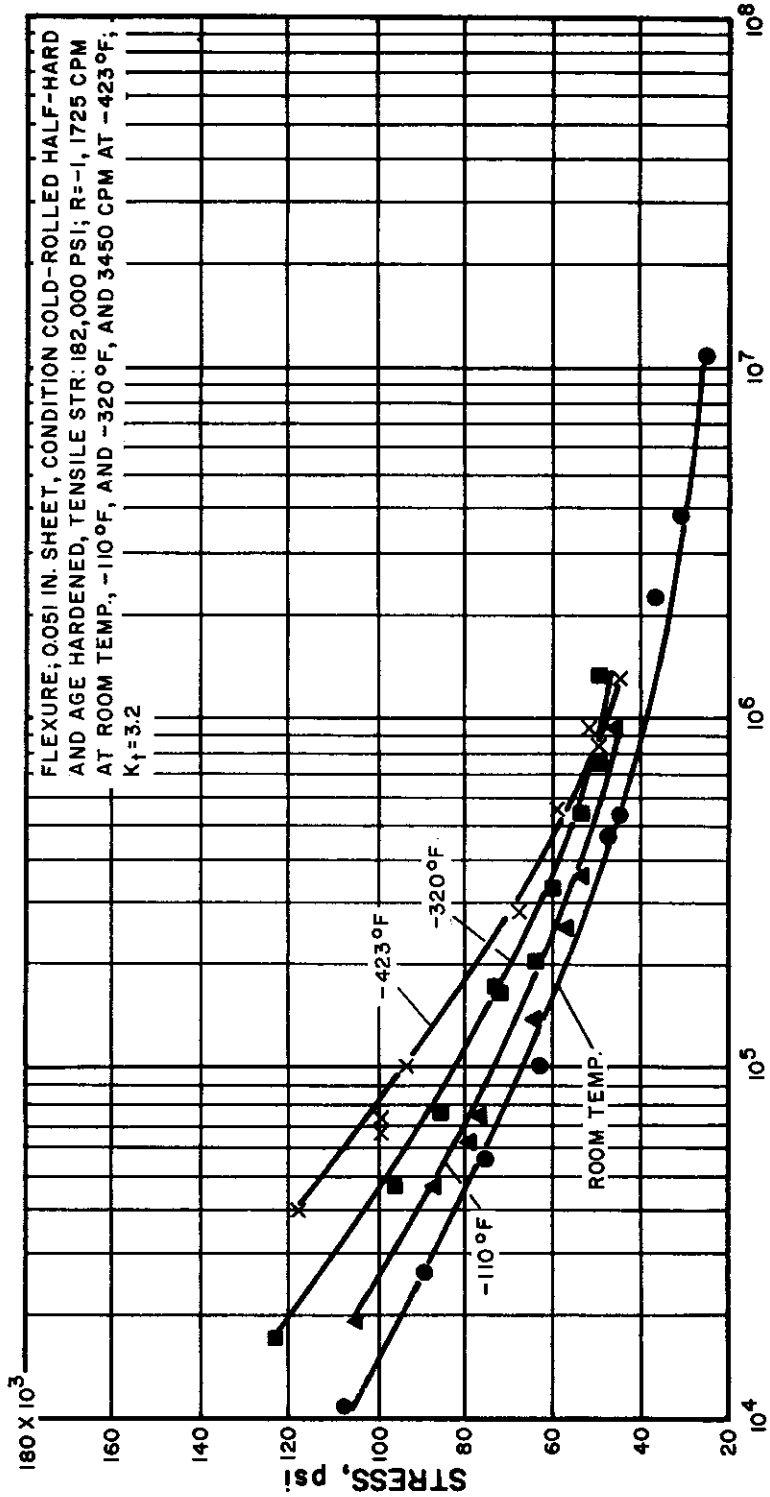

FIGURE 43. NOTCHED (K_T = 3.2) FATIGUE BEHAVIOR OF COLD-ROLLED AND AGE-HARDENED "K" MONEL NICKEL

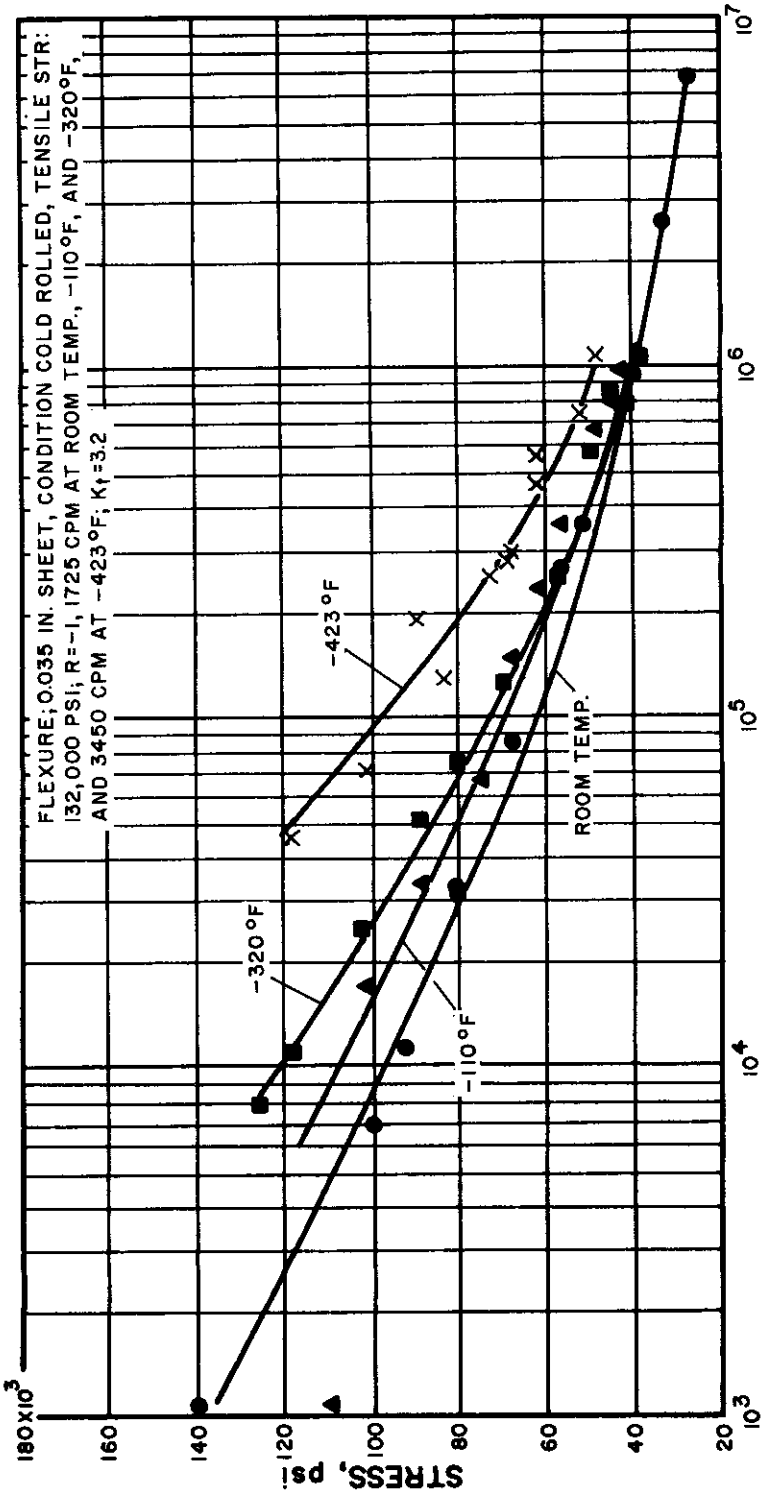

FIGURE 44. NOTCHED (K_T = 3.2) FATIGUE BEHAVIOR OF COLD-ROLLED INCONEL NICKEL

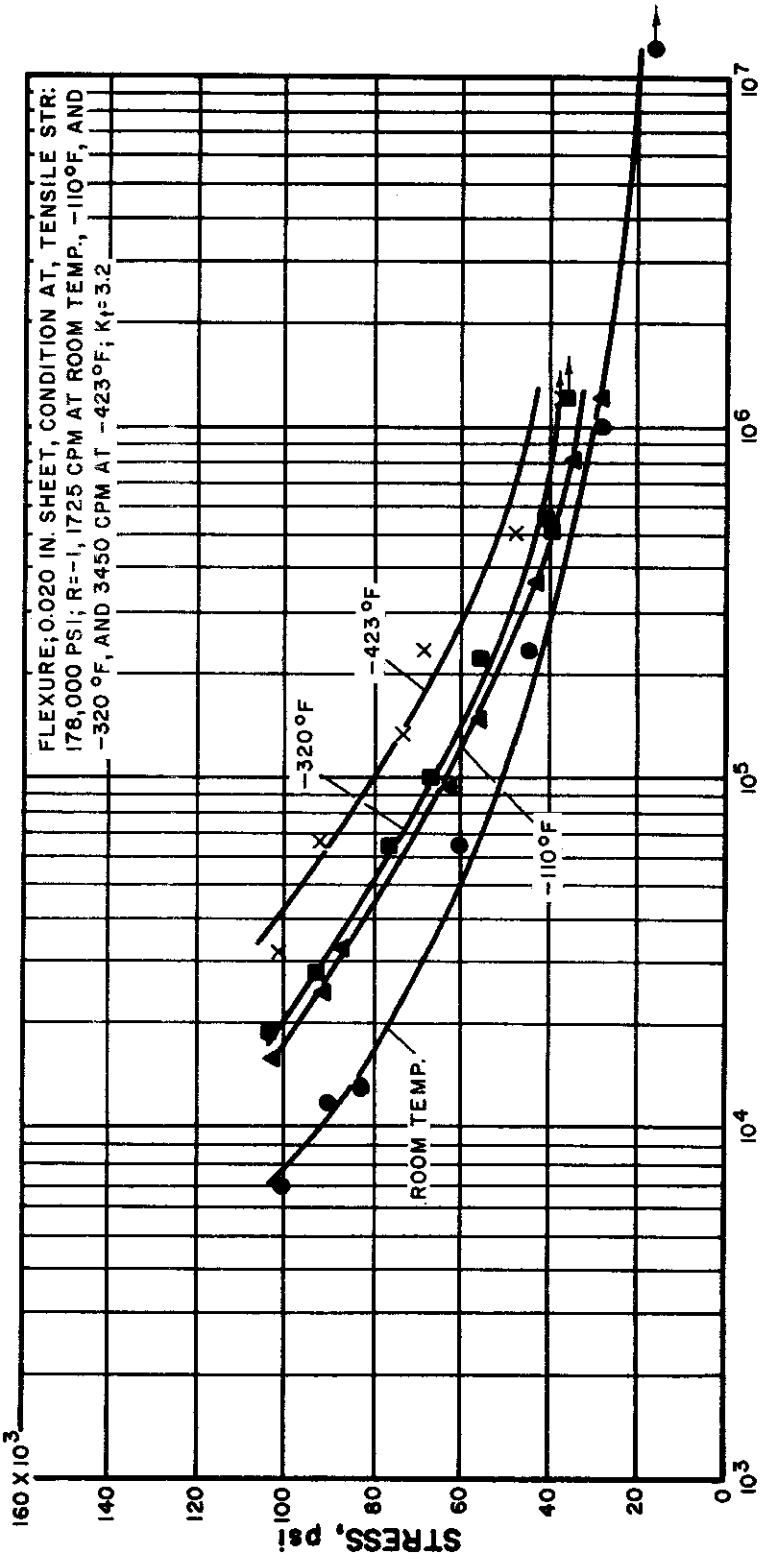

FIGURE 45. NOTCHED (K_T = 3.2 FATIGUE BEHAVIOR OF ANNEALED AND AGE-HARDENED BERYLCO 25 BERYLLIUM COPPER

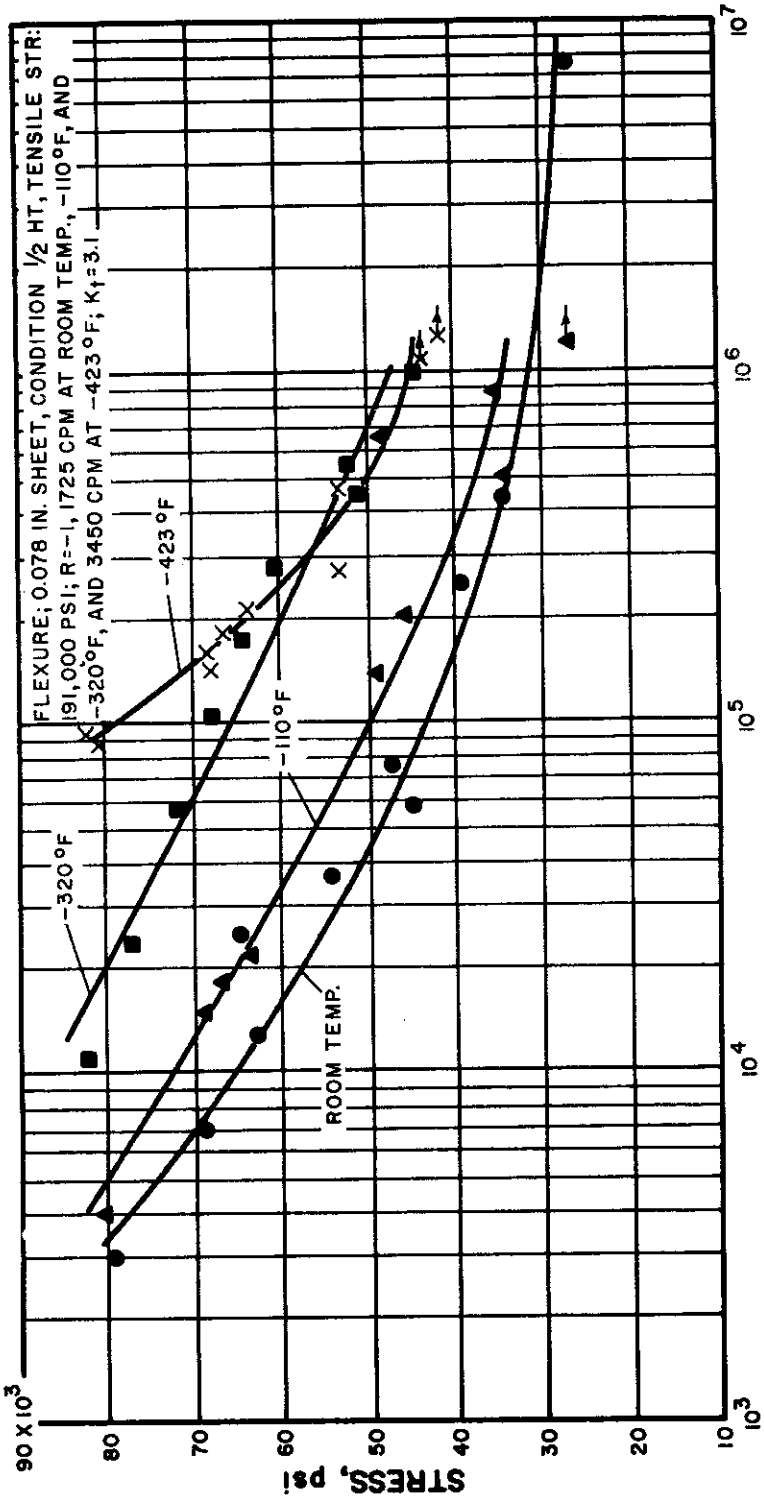

FIGURE 46. NOTCHED (K_T = 3.1) FATIGUE BEHAVIOR OF COLD-ROLLED AND AGE-HARDENED BERYLCO 25 BERYLLIUM-COPPER

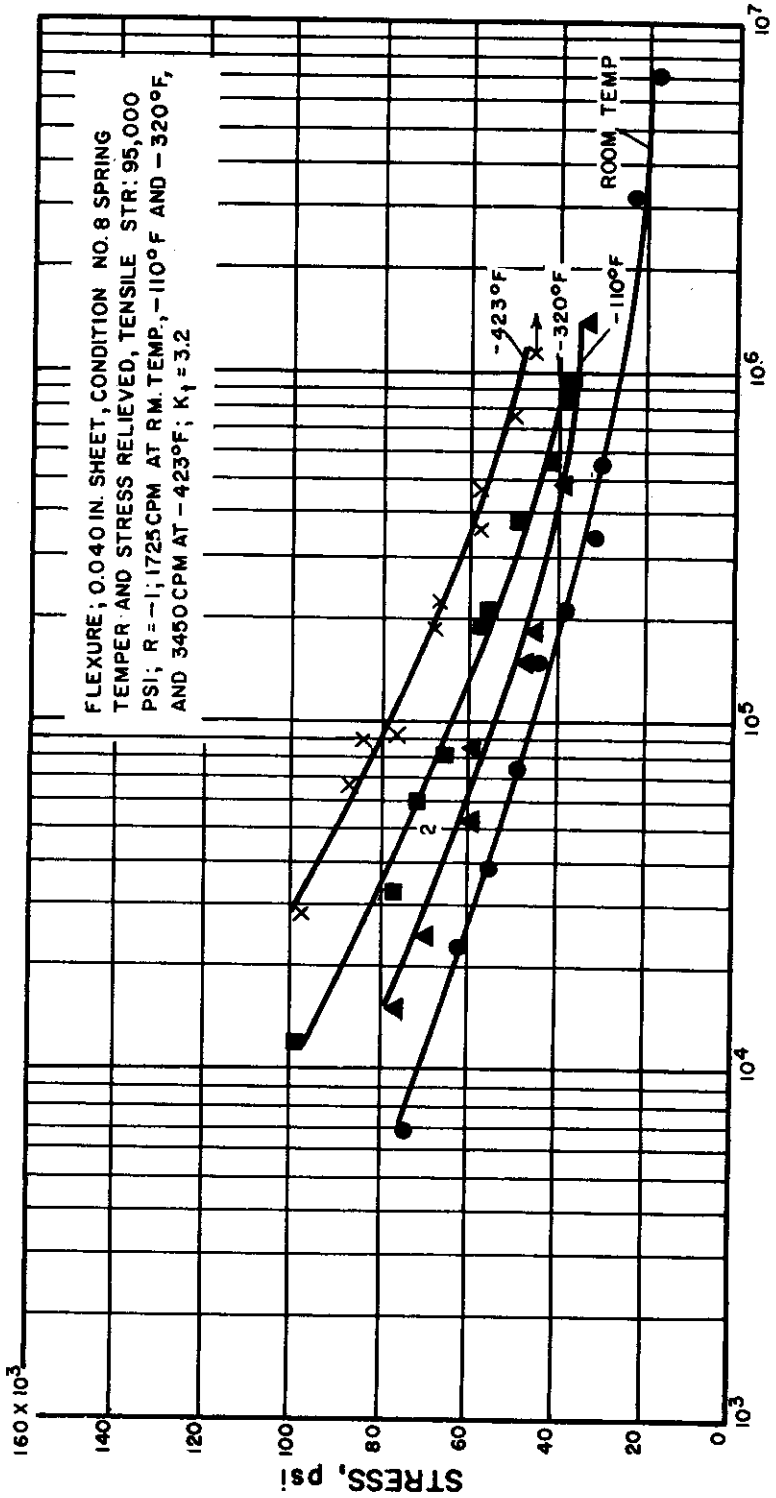

FIGURE 47. NOTCHED (K_T = 3.2) FATIGUE BEHAVIOR OF COLD-ROLLED AND STRESS-RELIEVED 70/30 BRASS

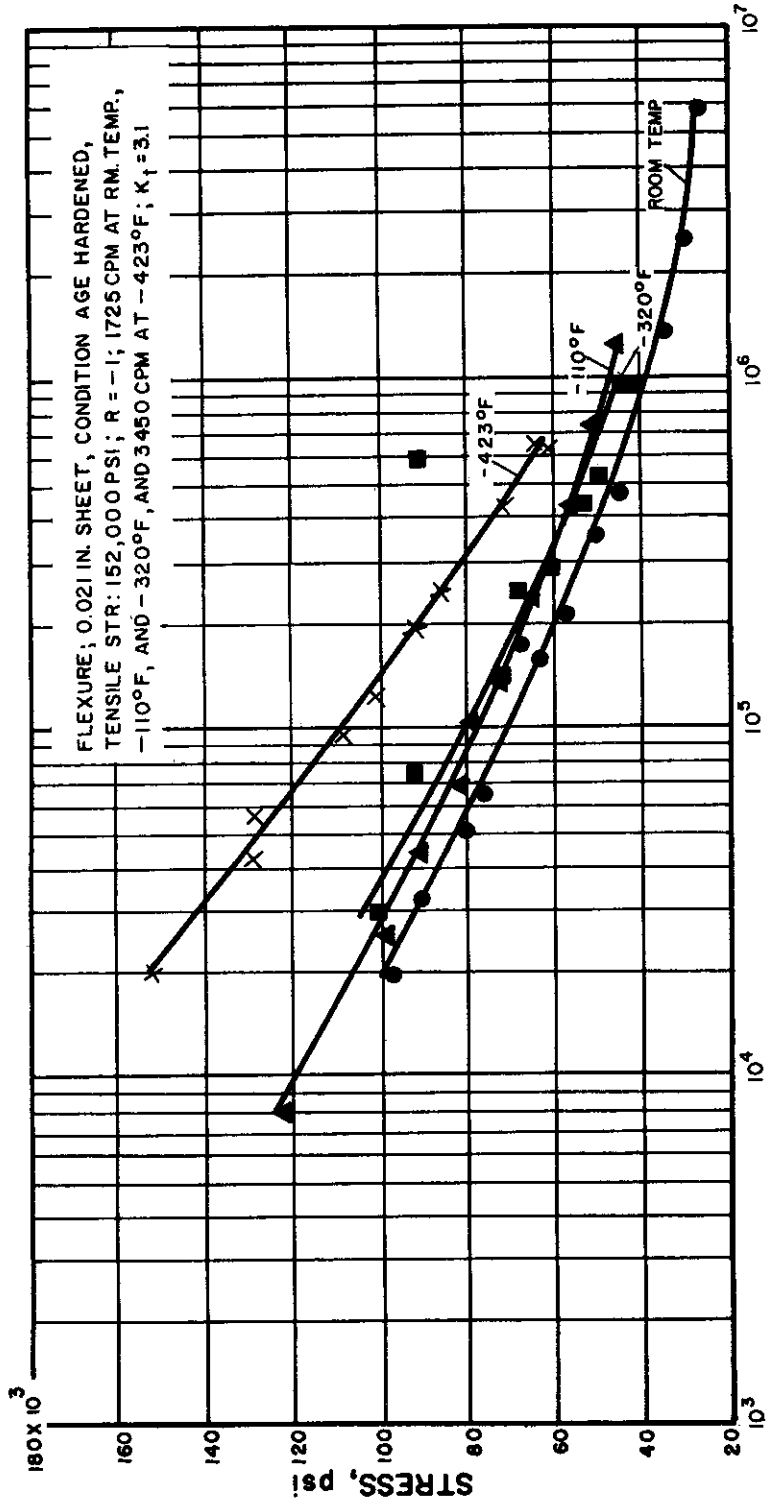

FIGURE 48. NOTCHED (K_T = 3.1) FATIGUE BEHAVIOR OF ANNEALED AND AGE-HARDENED NI-SPAN C IRON-NICKEL ALLOY

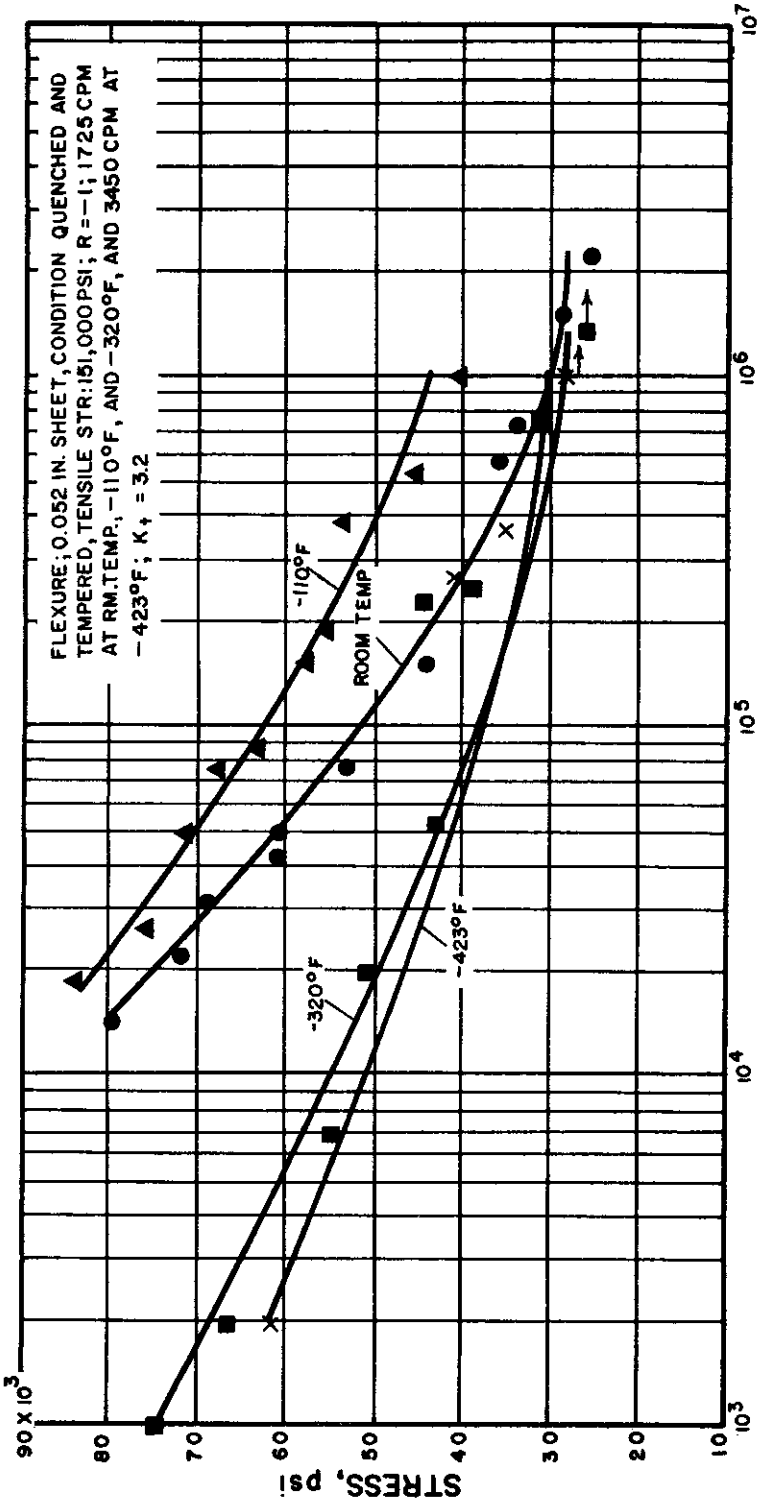

FIGURE 49. NOTCHED (K_T = 3.2) FATIGUE BEHAVIOR OF QUENCHED AND TEMPERED 1075 CARBON STEEL

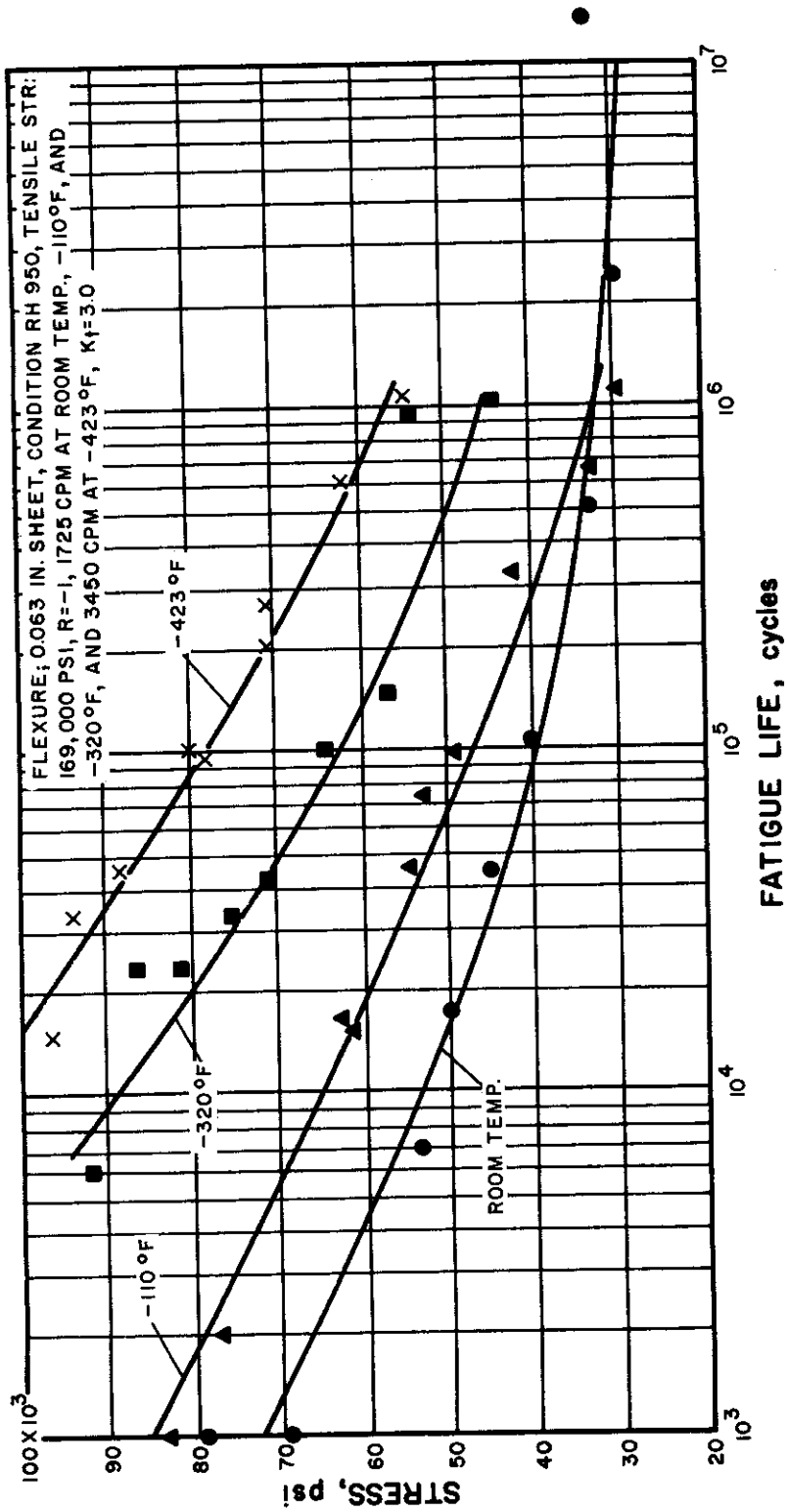

FIGURE 50. NOTCHED (K_T = 3.0) FATIGUE BEHAVIOR OF 17-7PH (RH 950) STAINLESS STEEL

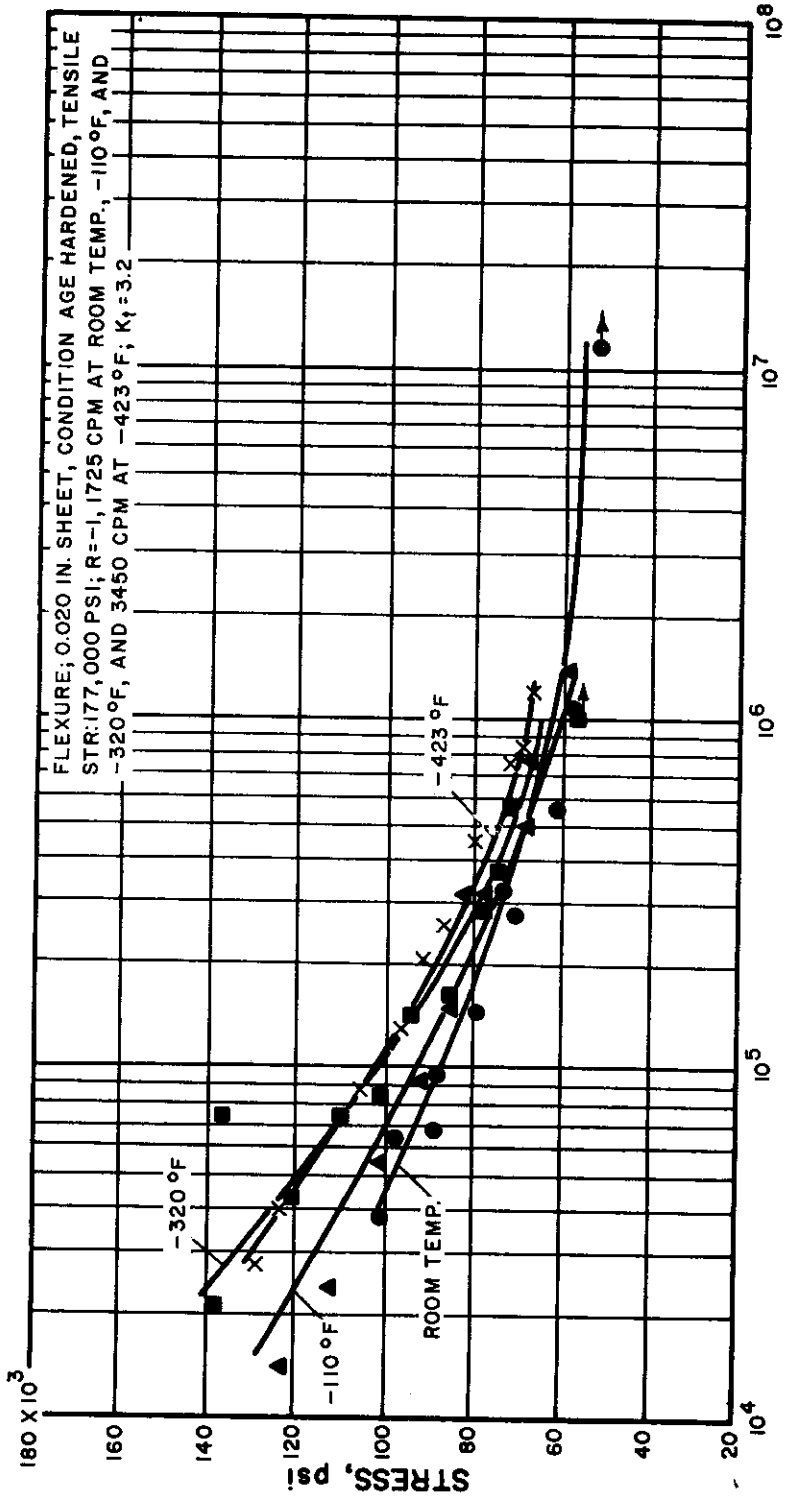

FIGURE 51. NOTCHED (K_T = 3.2) FATIGUE BEHAVIOR OF ANNEALED AND AGE-HARDENED INCONEL "X" NICKEL

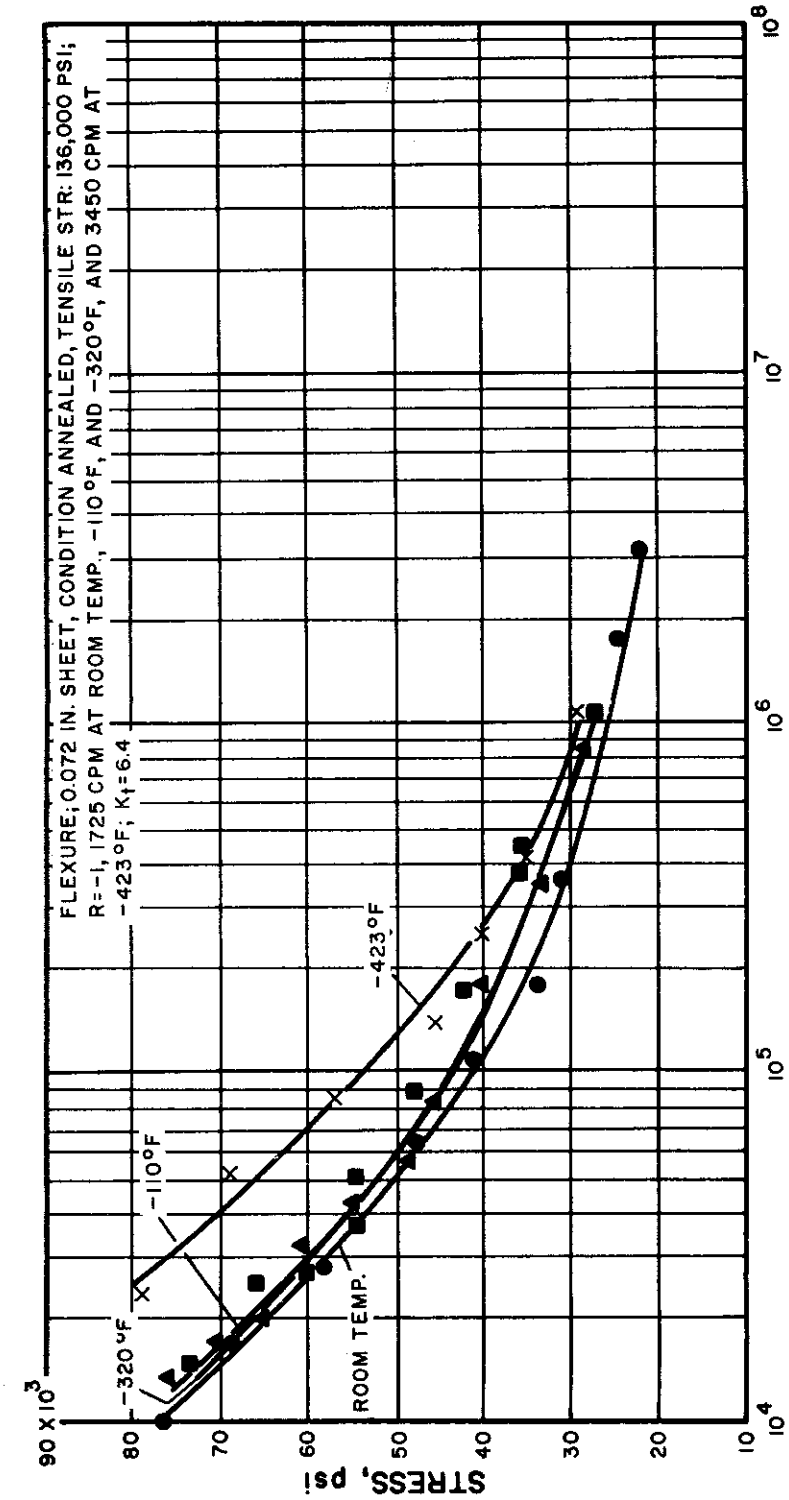

FIGURE 52. NOTCHED (K_T = 6.4) FATIGUE BEHAVIOR OF ANNEALED 6Al-4V TITANIUM

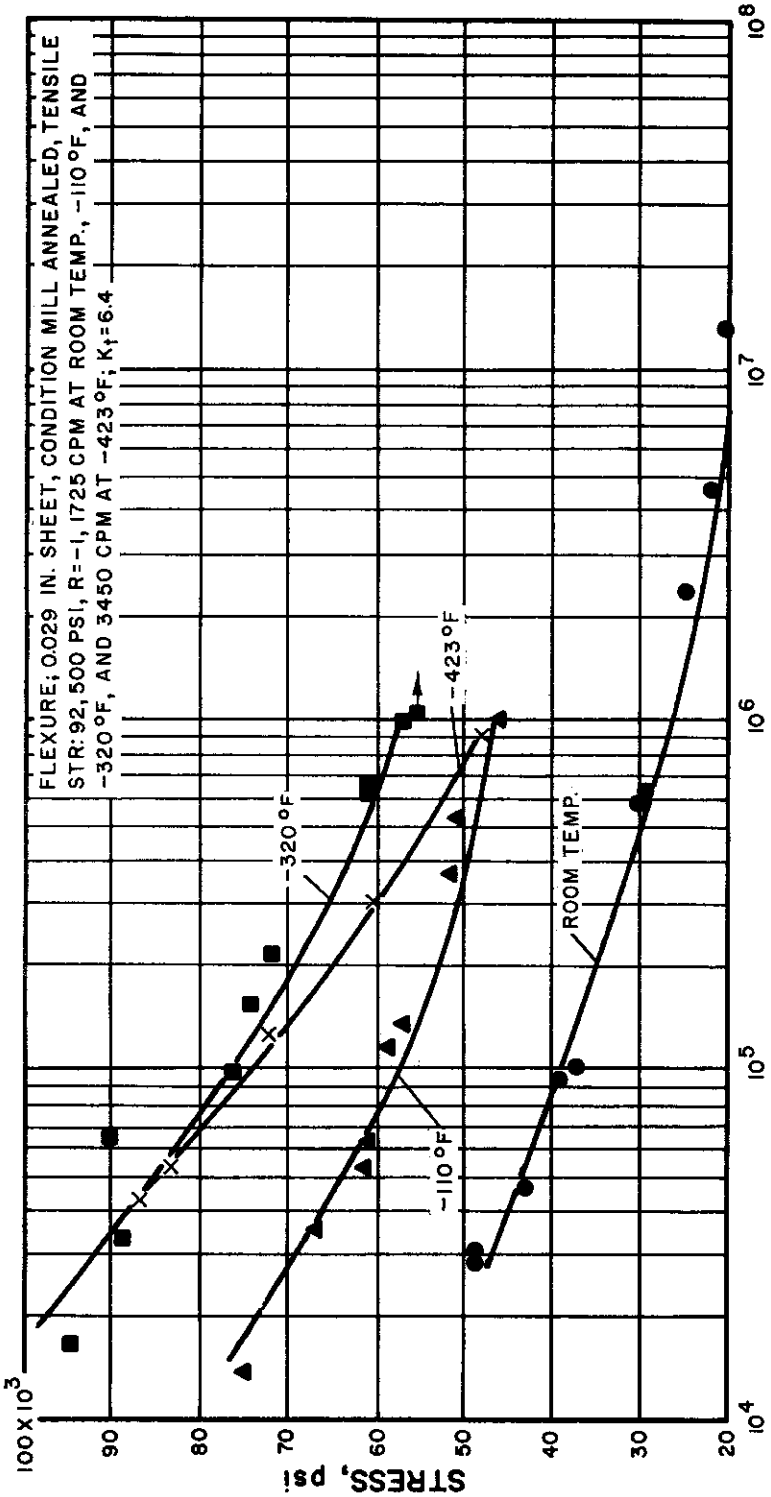

FIGURE 53. NOTCHED (K_T = 6.4) FATIGUE BEHAVIOR OF ANNEALED 347 STAINLESS STEEL

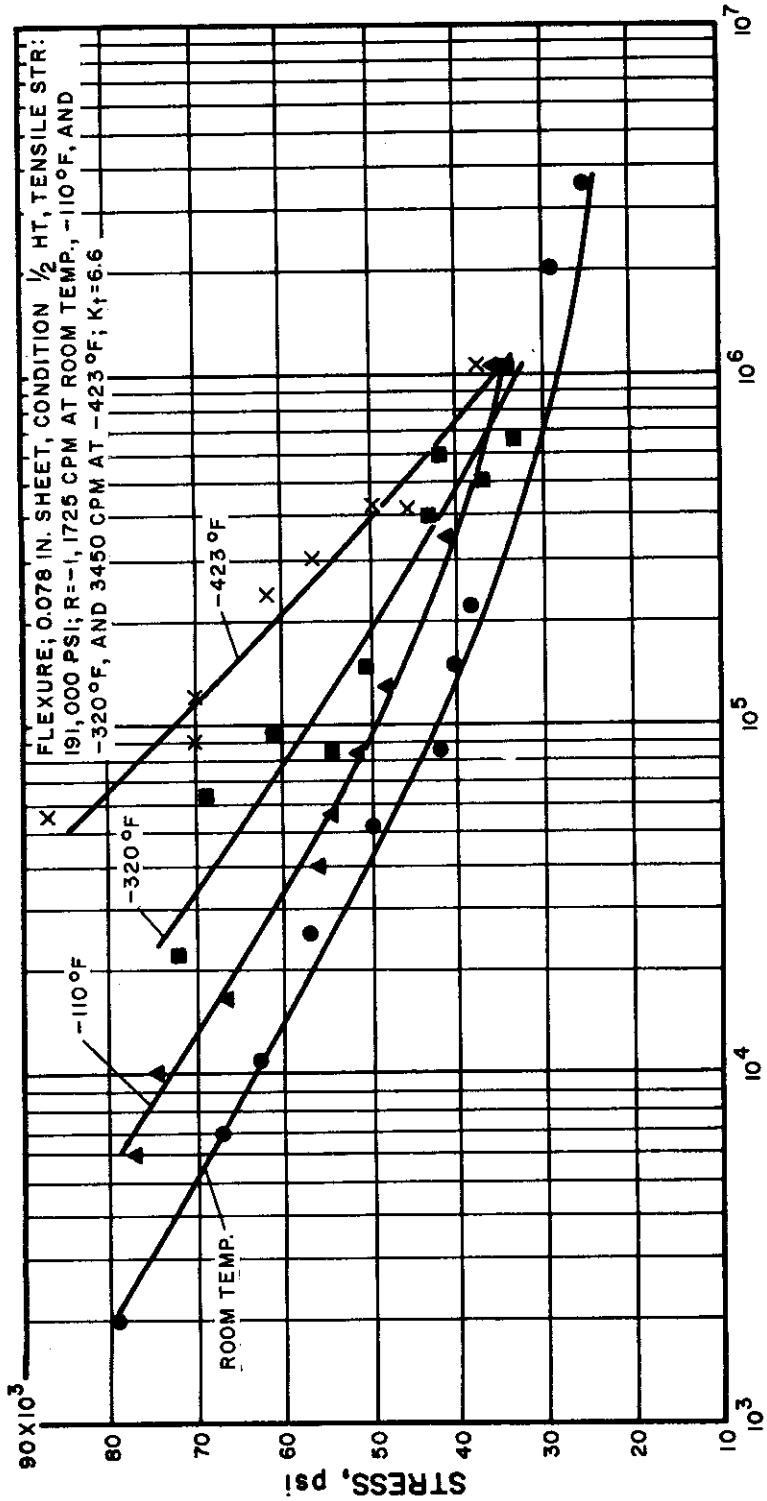

FIGURE 54. NOTCHED (K_T = 6.6) FATIGUE BEHAVIOR OF COLD-ROLLED AND AGE-HARDENED BERYLCO 25 BERYLLIUM-COPPER

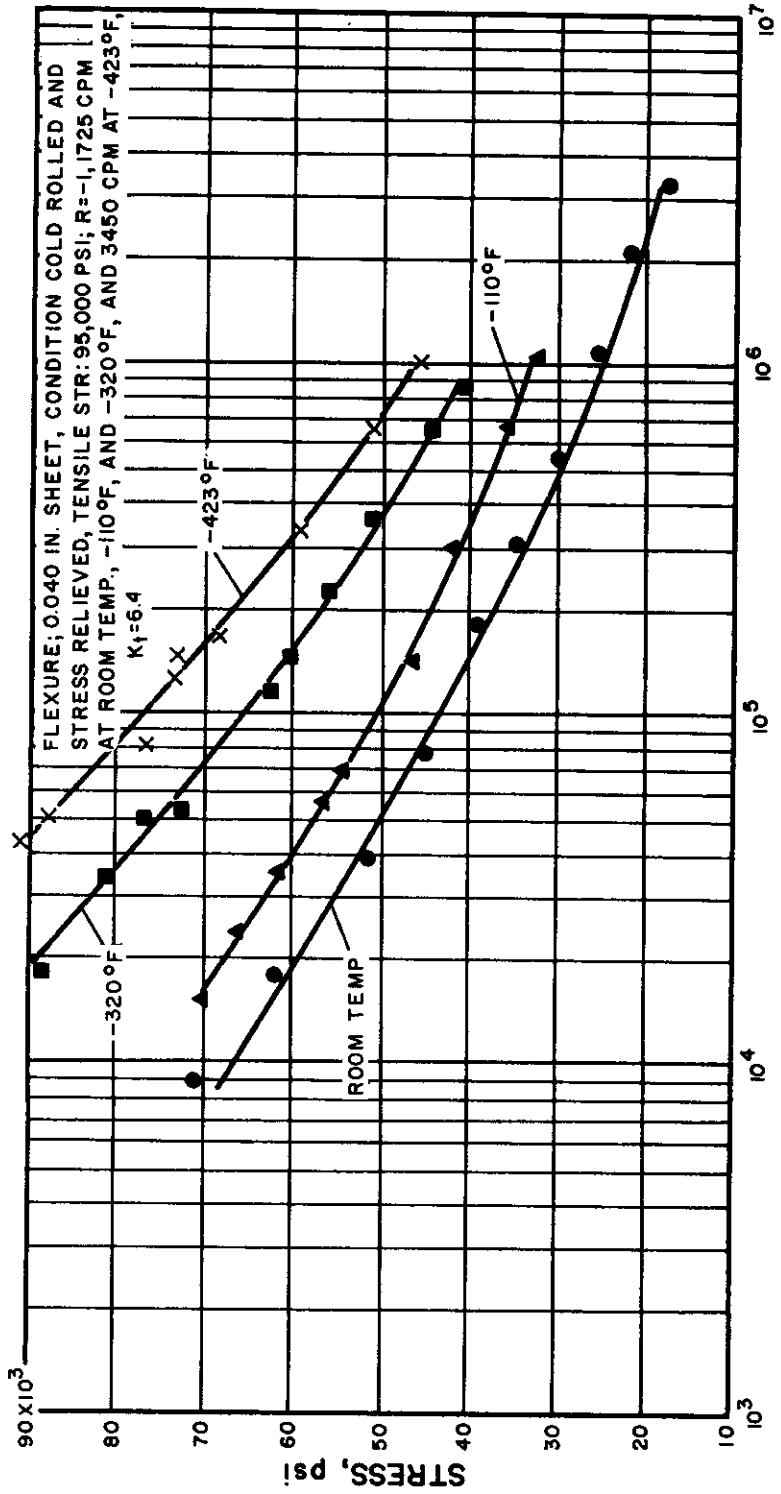

FIGURE 55. NOTCHED (K_T = 6.4) FATIGUE BEHAVIOR OF COLD-ROLLED AND STRESS-RELIEVED 70/30 BRASS

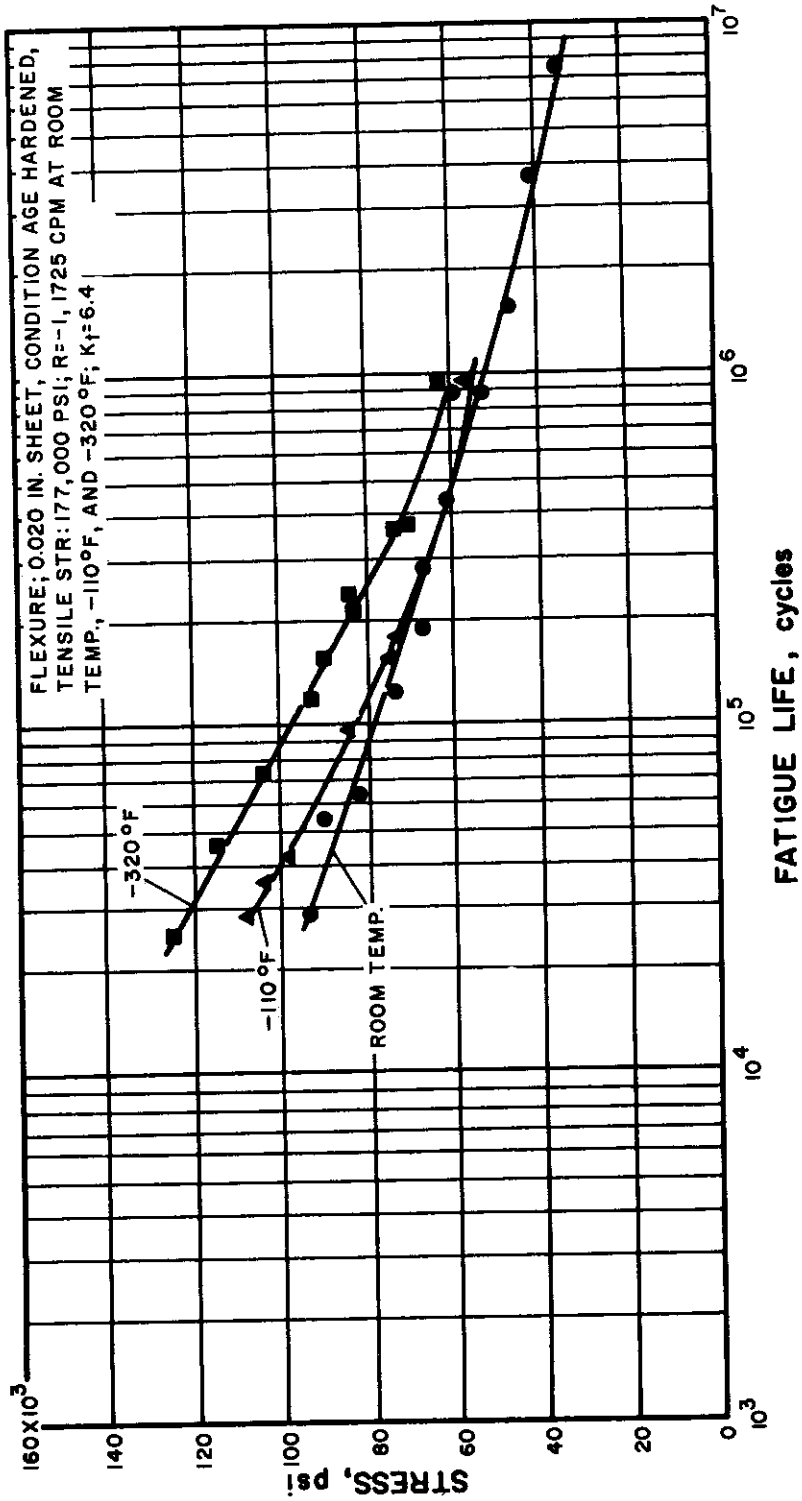

FIGURE 56. NOTCHED (K_T = 6.4) FATIGUE BEHAVIOR OF ANNEALED AND AGE-HARDENED INCONEL "X" NICKEL

The generalities, trends, and interpretations of research that have been conducted on materials at cryogenic temperatures should be a useful background in attempting to understand how a metal behaves under cyclic loading at these low temperatures.

In general, the ultimate tensile strength and tensile yield strength of metals increase with decreasing temperature. Along with the increased strength a reduction in ductility occurs. For some metals it has been found that below a certain temperature range (termed the brittle-ductile transition temperature range) little or no ductility remains.

This brittle-ductile transition-temperature range is dependent not only on the metal and its condition but also on the type of test and how it is conducted. For example, an increased strain rate or increased triaxiality of stress raises the transition temperature. Also, metallurgical structure affects fracture toughness and the factors of crystal structure, interstitial elements, impurities, grain size, and microstructure have been studied.

The transition from ductile-to-brittle behavior is very pronounced for body-centered cubic metals such as alpha iron and beta titanium. Other crystal structures which undergo transition are the hexagonal close-packed structure, which includes alpha titanium, zinc, and cadmium; the body-centered tetragonal structure (tin), and the body-centered rhombohedral structure (bismuth). Face-centered cubic metals such as gamma iron, nickel, copper, and aluminum do not exhibit transition behavior. The situation is complicated by the fact that engineering alloys may contain combinations of crystal structures, interstitial or impurity elements, and may undergo phase changes or phase rearrangements as a result of heat treatment or cold working. Consequently the chemistry and condition of an alloy may greatly affect its performance at cryogenic temperatures.

A fairly representative group of engineering alloys has been evaluated in this fatigue program and it will be shown that many of the factors mentioned above influence fatigue strength.

Effect of Notches and Low Temperatures on Fatigue Behavior

The unnotched fatigue strength of metals at room temperature generally increases with the tensile strength of the metal and, within a given alloy system and set of test conditions, the fatigue strength can be estimated to be some fraction of the tensile strength. While a notch often raises the tensile strength of a metal the fatigue strength is reduced. The effect of a notch on the fatigue strength of a metal is described by its notch sensitivity, q:

$$q = \frac{K_N - 1}{K_T - 1} ,$$

where K_N is the ratio of unnotched to notched fatigue strength, and K_T is the theoretical stress concentration factor for the notch. Numerical values of the notch sensitivity q of a material normally vary from zero for complete insensitivity to unity for a material whose fatigue strength reduction is equal to that predicted by the theoretical stress concentration factor. The few cases in which K_N appears slightly greater than K_T may be ascribed to experimental error.

As temperature is decreased the notch sensitivity, q, approaches 1.0 for a brittle material and rises slowly, if at all, for a ductile material. Table 5 lists the notch sensitivities at $K_T = 3.1$ for the metals studied in this program. It is noted that the body-centered cubic metal, plain carbon 1075 steel, has a q value approaching 1.0 at -320 F and below. At -110 F the 1075 alloy has such a low notch sensitivity that it bears further investigation. Low-temperature fatigue behavior is so poorly understood that apparent anomalies will have to be investigated by testing at intervening temperatures and with additional heats or lots of material. At -320 F and below brittle behavior can apparently be expected from 1075 steel.

The heavily cold-worked 301 austenitic stainless steel does not exhibit high notch sensitivity until the lower temperatures are reached. This pattern is in accord with published tensile data on cold-worked 301 in which investigators have attributed low-temperature brittleness to the formation of martensite from the unstable cold-worked austenite. The 347 austenitic stainless steel which was not cold worked did not exhibit high notch sensitivity.

An isolated case of high notch sensitivity was obtained for the alpha-beta titanium alloy at -320 F. Here again, as in the case of the 1075 steel, the data suggest that more research effort is needed to confirm or explain the results.

A comparison of the materials should not be based on notch sensitivity alone, however, as the fatigue strengths themselves present an interesting story. Tables 6 through 9 summarize the fatigue results at each of the four temperatures.

In the notched experiments the nickel alloys showed up well in comparison with the other alloys investigated. Inconel "X" was outstanding among the nickel alloys. At the lower test temperatures the notched annealed Type 347 stainless steel moved up in ranking until it matched the $K_T = 3$ notched strength of Inconel "X" at -423 F. In considering Type 347 for its high notch fatigue strength at -423 F, however, one must keep in mind its low static yield strength at room temperature.

It is interesting to note that for the two material conditions of beryllium copper evaluated (annealed and age hardened, and cold work and age hardened), there was little difference in the fatigue strengths, compared with the difference in their static tensile strengths.

The 70/30 brass alloy was not the highest nor the lowest strength material for any temperature or notch condition. However, the cryogenic fatigue behavior of this material appears remarkably regular in comparison with many of the other materials.

As might be suspected, the titanium alloy 6Al-4V compares well with the other materials on a strength/weight basis. The 6Al-4V alloy is compared on a strength/weight basis with outstanding alloys at each temperature and stress concentration condition in Table 10. It would be interesting to investigate an alpha titanium alloy such as 5Al-2.5Sn which has been shown to have good notched tensile strength at -423 F.

TABLE 5. NOTCH SENSITIVITIES WITH $K_T = 3.1$

Material	Notch Sensitivity Factor, q, at Indicated Numbers of Cycles							
	Room Temp		-110 F		-320 F		-423 F	
	10^5	10^6	10^5	10^6	10^5	10^6	10^5	10^6
301 SS	0.41	0.88	0.33	0.52	0.50	0.76	--	--
70/30 brass	0.21	0.11	0.29	0.23	0.42	0.38	0.53	0.52
1075 steel	0.35	0.30	--	--	--	--	--	--
2800 steel	0.17	0.43	--	--	--	--	--	--
Ti-6Al-4V	0.25	0.48	0.18	0.34	0.51	0.93	0.46	0.51
347 SS	0.03	0.15	--	--	--	--	--	0.02
"A" Nickel	--	--	--	--	--	--	--	--
"K" Monel	0.16	0.19	0.17	0.27	0.13	0.18	0.25	0.52
Inconel	0.27	0.20	--	--	--	--	--	--
Inconel "X"	0.11	0.08	--	--	--	--	--	--
Berylco 25, AT	0.42	0.48	0.28	0.53	0.36	0.44	0.45	0.77
Berylco 25, 1/2 HT	0.39	0.39	0.35	0.43	0.28	0.34	0.25	0.41
Ni-Span C	0.29	0.52	0.25	0.56	0.29	0.58	0.15	0.54
17-7PH (RH 950)	0.95	0.82	--	--	--	--	--	--

TABLE 6. SUMMARY OF FATIGUE RESULTS AT ROOM TEMPERATURE FOR $K_T = 1$, $K_T = 3.1$, AND $K_T = 6.4$

Material	Fatigue Strength, ksi, at Indicated Lifetimes					
	10^5 Cycles			10^6 Cycles		
	$K_T = 1$	$K_T = 3.1$	$K_T = 6.4$	$K_T = 1$	$K_T = 3.1$	$K_T = 6.4$
301	104	56	--	72	25	--
70/30	67	46	44	34	26	25
1075	91	51	--	50	30	--
2800	78[a]	59	--	70[a]	37	--
6Al-4V	63	41	41	50	25	25
347	38[a]	36	39	34[a]	26	26
"A" Nickel	(a)	18	--	(a)	16	--
"K" Monel	90	66	--	55	39	--
Inconel	96	61	--	56	39	--
Inconel "X"	108[a]	86	79	74	62	51
Berylco 25-AT	94	50	--	60	30	--
Berylco 25-1/2 HT	78	43	42	56	31	28
Ni-Span C	112	70	--	82	39	--
17-7PH (RH 950)	115[a]	39	--	85	32	--
17-7PH (TH 1050)	114	--	--	86	--	--

(a) Unnotched fatigue data for these materials are in the plastic range and reported in strain. These stress values are estimated from available uniaxial stress-strain data.

TABLE 7. SUMMARY OF FATIGUE RESULTS AT -110 F FOR $K_T = 1$, $K_T = 3.1$, AND $K_T = 6.4$

Material	Fatigue Strength, ksi, at Indicated Lifetimes					
	10^5 Cycles			10^6 Cycles		
	$K_T = 1$	$K_T = 3.1$	$K_T = 6.4$	$K_T = 1$	$K_T = 3.1$	$K_T = 6.4$
301	115	68	--	65	31	--
70/30	90	54	51	54	36	34
1075	(a)	62	--	(a)	44	--
2800	(a)	65	--	(a)	46	--
6Al-4V	72	52	43	55	32	27
347	(a)	58	58	(a)	47	46
"A" Nickel	(a)	22	--	(a)	18	--
"K" Monel	100	74	--	67	43	--
Inconel	(a)	70	--	(a)	40	--
Inconel "X"	(a)	92	83	(a)	60	54
Berylco 25-AT	100	63	--	70	33	--
Berylco 25-1/2 HT	87	50	49	67	35	35
Ni-Span C	119	78	--	100	46	--
17-7PH (RH 950)	--	47	--	--	32	--
17-7PH (TH 1050)	137	--	--	112	--	--

(a) Unnotched fatigue data for these materials are in the plastic range and reported in strain.

TABLE 8. SUMMARY OF FATIGUE RESULTS AT -320 F
FOR K_T = 1, K_T = 3.1, AND K_T = 6.4

Material	Fatigue Strength, ksi, at Indicated Lifetimes					
	10^5 Cycles			10^6 Cycles		
	K_T = 1	K_T = 3.1	K_T = 6.4	K_T = 1	K_T = 3.1	K_T = 6.4
301	137	66	--	115	44	--
70/30	125	64	66	72	39	41
1075	(a)	38	--	(a)	29	--
2800	(a)	65	--	(a)	37	--
6Al-4V	97	47	43	80	27	27
347	(a)	65	76	(a)	50	58
"A" Nickel	(a)	24	--	(a)	21	--
"K" Monel	105	82	--	69	48	--
Inconel	(a)	72	--	(a)	40	--
Inconel "X"	(a)	101	97	(a)	64	59
Berylco 25-AT	114	65	--	75	39	--
Berylco 25-1/2 HT	106	67	57	81	47	33
Ni-Span C	129	80	--	100	45	--
17-7PH (RH 950)	--	63	--	--	45	--
17-7PH (TH 1050)	160	--	--	140	--	--

(a) Unnotched fatigue data for these materials are in the plastic range and reported in strain.

TABLE 9. SUMMARY OF FATIGUE RESULTS AT -423 F FOR $K_T = 1$, $K_T = 3.1$, AND $K_T = 6.4$

Material	Fatigue Strength, ksi, at Indicated Lifetimes					
	10^5 Cycles			10^6 Cycles		
	$K_T = 1$	$K_T = 3.1$	$K_T = 6.4$	$K_T = 1$	$K_T = 3.1$	$K_T = 6.4$
301	107	50	--	97	--	--
70/30	172	79	77	102	49	47
1075	(a)	38	--	(a)	30	--
2800	(a)	58	--	(a)	37	--
6Al-4V	102	52	54	77	37	29
347	(a)	82	74	70[(a)]	67	48
"A" Nickel	(a)	41	--	(a)	37	--
"K" Monel	142	95	--	101	48	--
Inconel	(a)	98	--	(a)	47	--
Inconel "X"	(a)	101		(a)	67	
Berylco 25-AT	156	80	--	113	43	--
Berylco 25-1/2 HT	120	79	72	84	45	36
Ni-Span C	145	110	--	122	57	--
17-7PH (RH 950)	--	78	--	--	57	--
17-7PH (TH 1050)	129	--	--	112	--	--

(a) Unnotched fatigue data for these materials are in the plastic range and reported in strain. These stress values are estimated from available uniaxial stress-strain data.

TABLE 10. FATIGUE STRENGTH/DENSITY COMPARISON OF 6A1-4V TITANIUM WITH OTHER ALLOYS S

Material	Fatigue Strength at 10^6 Cycles/Density, 10^3 in., at Indicated Temperatures and Stress Concentrations									
	RT/1	RT/3	RT/6	-110 F/1	-110 F/3	-320 F/1	-320 F/3	-423 F/1	-423 F/3	-423 F/6
6A1-4V	312	156	156	344	200	500	169	481	233	181
Inconel "X"	246	207	--	--	200	--	213	--	223	--
70/30	110	084	081	175	117	234	127	332	159	153
347	117	090	090	--	162	--	172	241	231	165
Be 25 - 1/2 HT	188	104	094	226	118	273	158	282	151	121
Ni-Span C	278	132	--	340	156	340	153	415	194	--

CONCLUSIONS

This report has presented data describing the effects of notches and of low temperatures on the fatigue behavior of 13 alloys. In choosing materials for specific applications, many material factors other than fatigue behvaior must often be taken into account, such as thermal or electrical conductivity, corrosion resistance, density, fabricability, magnetic properties, mechanical hysteresis and related properties, static mechanical strength properties, etc. Since fatigue strength and notch sensitivity are only two among several factors which the designer must account for, attempts to order materials in some order of merit are practically of little value. When the principal requirements of a specific application have been determined, however, usually the choice of a material will be reduced to a few materials with a suitable combination of properties. In this light, the following conclusions pertain to the specific materials studied and are based only on data in this report:

(1) For most conditions of temperature and notch sharpness, the 6A1-4V titanium alloy is better than the other alloys on a fatigue strength/density basis.

(2) In the unnotched condition and at the three highest temperatures, the 17-7 alloy has the highest fatigue strength; at -423 F the Ni-Span C alloy has the highest fatigue strength.

(3) In the notched conditions, the nickel alloys compare favorably with the other alloys, Inconel X being outstanding among the nickel alloys.

(4) The notch sensitivities of the face-centered cubic metals increase only slightly with decreasing temperature; for Berylco 25, 1/2 HT, no significant change in notch sensitivity occurs.

(5) For the two conditions of Berylco 25 evaluated the differences in fatigue strengths are small compared with the difference in their static tensile strengths.

(6) The 301 stainless steel XFH apparently develops high notch sensitivity only below -320 F. In spite of its high-notch sensitivity at -423 F, however, it does have measurable fatigue strengths.

(7) The hardened 1075 steel also has a relatively high notch sensitivity at cryogenic temperatures, but its measurable fatigue strengths, plus its recognized spring qualities, would qualify this alloy for some cryogenic applications.

(8) The Type 347 stainless steel and the "A" Nickel exhibited very good fatigue behavior in relation to the very low static tensile strengths of these alloys in the annealed condition.

RECOMMENDATIONS FOR FUTURE WORK

This study has provided preliminary engineering data on the fatigue strengths of a variety of metals at cryogenic temperatures. Some trends and apparent anomalies were noted, and as a result of this work questions concerning the fundamental fatigue behavior of metals at cryogenic temperatures have appeared. In this section some possible directions of future fatigue work at room temperature and below are suggested:

(1) In considering the fatigue strength and tensile strengths of alloys in the same metals classification, particularly with respect to cold-worked versus heat-treated conditions, it is apparent that increased tensile strengths (and in some cases also increased notched tensile strengths) do not always result in corresponding increases in fatigue strength. This trend became more pronounced as the temperature decreased. A suggested approach for tackling this unexplained phenomenon is to include in future programs a study of the stress field around the notch, before, during, and after fatigue cycling.

(2) Although many cryogenic applications involve biaxial stress conditions, very little has been done on the effect of biaxiality on fatigue at room temperature. To Battelle's knowledge no data are available on the effect of biaxiality on cryogenic fatigue behavior.

(3) A slightly different picture of the relative fatigue behavior of the alloys is obtained by looking at the 10^5 rather than the 10^6 lifetime strengths. From the S-N plots it can be predicted that, if a low cycle (1000 cycles or less) fatigue investigation were carried out, a vastly different material rating might be obtained.

(4) A study correlating cryogenic fatigue behavior with basic structural elements should be made. Christian[12] is carrying out a program to evaluate the resistance of complex welded joints to repeated axial

loading at cryogenic temperatures. The emphasis in Christian's work is in the high stress, finite life range. Other possible areas of study would include structural elements other than welded joints and the low stress, long-lifetime portion of the S-N curve.

(5) In addition to establishing the basic fatigue behavior of a number of engineering metals some effort should go into an evaluation of such factors as the following:

- Effect of testing in contact with liquid cryogent
- Effect of melting practice (vacuum, air, etc.)
- Effect of higher notch factors than 6
- Effect of other factors such as surface finish oxides, coatings, etc., known to be important at higher temperatures.

(6) Understanding of fatigue behavior will probably be furthered most efficiently by careful choice of experimental materials and objectives. For example, a clearer picture of the role of crystal structure may be obtained by evaluating relatively pure metals. Other techniques for uncovering possible clues might include the measurement of microstresses by X-ray diffraction techniques and the observation of crack initiation and propagation using the electron microscope.

REFERENCES

(1) Favor, R. J., et al., "Investigation of Fatigue Behavior of Certain Alloys in the Temperature Range Room Temperature to -423 F", Battelle Institute, WADD TR 61-132 (March, 1961).

(2) Cryogenic Materials Data Handbook, Office of Technical Services, United States Department of Commerce, Washington, D. C.

(3) Memorandum from C. W. Bert to D. N. Gideon (March 10, 1961).

(4) Lee, G. H., "The Influence of Hyperbolic Notches on the Transverse Flexure of Elastic Plates", J. Appl. Mech., 7, p A53 (1940).

(5) Petersen, E. R., Stress Concentration Design Factors, John Wiley and Sons, Inc. (1953).

(6) Tamate, O., and Shroya, S., "On the Transverse Flexure of an Infinite Strip With Semicircular Notches on Both Edges", Bulletin of JSME, 2, p 264 (1959).

(7) Reissner, E., "The Effect of Transverse Shear Deformation on the Bending of Elastic Plates", J. Appl. Mech., 12, p A69 (1945).

(8) Naghdi, P. W., "The Effect of Elliptic Holes on the Bending of Thick Plates", J. Appl. Mech., 22, p 89 (1955).

(9) Scott, R. B., Cryogenic Engineering, D. Van Nostrand and Company, Inc., p 246 (1959).

(10) Espey, G. B., "Sheet Alloys Graded by Sharp-Notch Sensitivity", Metal Progress, 78 (2), pp 83-88 (August, 1960).

(11) Hardrath, H. F., and McEvily, A. J., Jr., "Engineering Aspects of Fatigue Crack Propagation", Langley Research Center, paper presented at a Symposium on Crack Propagation, Cranfield, England (September 26-28, 1961).

(12) Christian, J. L., "Physical and Mechanical Properties of Pressure Vessel Materials for Application in a Cryogenic Environment", Convair Astronautics Division, General Dynamics Corp., Contract AF 33(616)-7719, Task No. 73812.

* * * * * * *

The data presented in this report are recorded in Laboratory Record Books Numbers 16840, 17850, and 18080.